

ADDIS ABABA UNIVERSITY
ADDIS ABABA INSTITUTE OF TECHNOLOGY
AFRICAN RAILWAY CENTER OF EXCELLENCE



**EVALUATION OF REMAINING FATIGUE LIFE OF PRE -
STRESSED CONCRETE RAILWAY BRIDGE**

A Thesis in Railway Engineering (Civil Infrastructure)

By GEBREMEDHIN KIDUS

June 2023

Addis Ababa, Ethiopia

A Thesis

Submitted in Partial Fulfillment of the Requirements for the Degree of Master of Science
in Railway Engineering (Civil Infrastructure)

APPROVAL

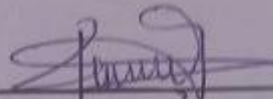
This is to certify that the thesis prepared by Gebremedhin Kidus, entitled: **Evaluation of Remaining Fatigue Life of Pre-stressed Concrete Railway Bridge** and submitted in partial fulfillment of the requirements for the degree of **Master of Science in Railway Engineering (Civil Infrastructure)** complies with the regulations of the University and meets the accepted standards concerning to originality and quality.

Dr. Abrham Gebre
Advisor's Name


Signature

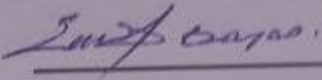
Date

Dr. Fiseha Nega
Internal Examiner


Signature

29/06/2023
Date

Dr. Esayas G/Yohannes
External Examiner


Signature

June 30, 2023
Date

Mr. Zewdie Moges
Chair Person


Signature

June-30-2023
Date



UNDERTAKING

I certify that research work titled “**Evaluation of Remaining Fatigue Life of Prestressed Concrete Railway Bridge**” is my own work. The work has not been presented elsewhere for assessment. Where material has been used from other sources it has been properly acknowledged / referred.

Gebremedhin Kidus

Name

Signature

June 23, 2023

Date

ABSTRACT

Nowadays reinforced bridges are being replaced by pre-stressed bridges because of their cost efficiency and serviceability. Pre-stressed concrete railway bridges are widely used in various parts of the world. Their main function is to transfer load coming from the track super structure to the sub-structure part like of that pier through bearing. The bridges are mostly failed by fatigue failure as a result of repeated cyclic load. Previously, the fatigue life of the railway bridges subjected to design and operational loading on these loading capacities, has not been well investigated on the Addis Ababa LRT. The general objective of this thesis is to estimate the remaining fatigue life of pre-stressed concrete railway bridge subjected to operational cyclic load. The study addresses the fatigue life of pre-stressed concrete railway bridge of Addis Ababa Light Rail Transit as a case study. Imperative issues like load application, bearing profile and arrangement of static analysis results to generate the data for fatigue evaluations have been studied. To implement this numerical approach, ANSYS 2020 was used. The minimum fatigue life obtained is $1e^8$ cycles. These number of cycles correspond to about 114.16 years which is 14 percent more than the design life of the railway bridge. The railway bridge serves more than the design life of 100 years (175,200,000 cycles). However, other parts of the railway bridge, especially the steel bearing section can attain life greater than $1e^{10}$ cycles (infinite life).

Keywords: - Fatigue, Fatigue life, Failure, Pre-stressed Concrete, Pre-stress Losses and Railway Bridge.

ACKNOWLEDGEMENTS

First of all, enormous thanks to almighty God for his priceless help to finish my thesis successfully.

Next, I particularly wish to acknowledge my advisor Abrham Gebre (PhD), for making this work possible. I am very grateful for his time, guidance, support and encouragement throughout this research study. In addition, I would like to thank Mr. Awel Mohammedaman (Phd candidate) for the guidance and support.

Thanks to my colleague: Awet Tekle and Biniyam Kidus for sharing experience, encouragement and support during my studies. Also, thanks to Ethiopian Railway Corporation Light Rail Transit Construction department staff's workers for their positive cooperation and providing me all the required data's. Furthermore, I would like to thank African Center of Railway Excellence (ARCE) for giving me this great scholarship opportunity to expand my knowledge on the Railway Engineering Civil Infrastructure Stream.

Unlimited thanks to my parents and friends for their prayers, encouragement and critical support.

Finally, I would like to thank everyone who supports me in my entire period of study.

Table of Contents	page
ABSTRACT	ii
ACKNOWLEDGEMENTS	iii
List of Figures	vii
List of Tables.....	ix
LIST OF NOTATION AND DEFINITIONS	x
ACRONYM AND ABBREVIATIONS	xi
CHAPTER ONE INTRODUCTION	1
1.1 Background.....	1
1.2 Statement of the Problem	2
1.3 Objectives.....	3
1.3.1 General Objective.....	3
1.3.2 Specific Objective	3
1.4 Scope and Limitation of the Study	3
1.5 Structure of the Thesis.....	4
CHAPTER TWO LITERATURE REVIEW	5
2.1 Introduction	5
2.2 Railway Bridge Components	8
2.3 Types of Railway Bridges	9
2.4 Loads for Design of Concrete Railway Bridge	9
2.4.1 Live Loads	9
2.4.2 Impact Load	10
2.4.3 Permit load.....	10
2.5 Basic Concept of Pre-stressing Concrete	11
2.5.1 Methods of Pre-Stressing.....	12

2.6	Overview of Current Fatigue Analysis.....	16
2.6.1	General Background on Fatigue	16
2.6.2	Types of Fatigue Damage.....	16
2.6.3	Fatigue Analysis Types	17
2.7	Fatigue Analysis.....	18
2.7.1	Fatigue Failure in Concrete Structures.....	22
2.7.2	Fatigue Loads	24
2.7.3	Fatigue Failure in Steel Reinforcement.....	24
2.7.4	Loading Type	26
2.8	Parameters that Affect Fatigue Strength	27
2.9	Fatigue Life Assessment of Complex Based on Strain Time Histories	29
A.	Uniaxial Fatigue Evaluation.....	29
B.	Multi Axial Fatigue Evaluation.....	30
2.10	Structural Model for Fatigue Stress Analysis of Railway Bridge.....	30
2.11	Fatigue Analysis of Railway Bridge.....	30
CHAPTER THREE RESEARCH METHODOLOGY.....		32
3.1	Introduction	32
3.2	Research Methodology	32
3.2	Study Area.....	36
3.2.1	Bridge Description	36
3.3	Simplifications/Assumptions	37
3.4	Finite Element Modelling.....	38
3.5	Validation and Modelling of Railway Bridge	38
3.5.1	Validationand Railway Bridge Modelling	38
3.5.2	Pre-stressed Sleeper Modelling and Validation.....	43

3.6 Numerical Modeling of Pre-stressed Railway Bridge	50
3.6.1 Railway Bridge Cross-Section.....	51
3.6.2 Material Properties for the Pre-stressed Railway Bridge	52
3.6.3 Railway Bridge Model Analysis with ANSYS 2020	56
3.6.4 Meshing	59
3.6.5 Boundary and Loading Conditions.....	61
3.6.6 Analysis Settings	62
3.6.7 Solution in ANSYS Static Structural.....	62
3.7 Pre-stress and Pre-strain	62
3.8 Pre-stress Loss Determination.....	63
3.9 Bridge Girder Loading	65
CHAPTER FOUR RESULT AND DISCUSSION.....	67
4.1 Pre-stress Loss Calculation	67
4.2 Static Analysis of Pre-stressed Concrete Railway Bridge	68
4.2.1 Deformation	69
4.2.2 Stress	72
4.2.3 General Fatigue Results	75
CHAPTER FIVE CONCLUSION AND RECOMMENDATION	79
5.1 Conclusions	79
5.2 Recommendation.....	80
REFERENCES.....	81
APPENDICES.....	84

List of Figures	Page
Figure 2. 1 Axle load and wheel load	11
Figure 2.2 cyclic stress curves for concrete in compression.....	14
Figure 2. 3 Typical crack width versus number of cycles	20
Figure 2. 4 Typical Paris-Erdogan equation graph	21
Figure 2. 5 Horizontal Cracking near the axle load.....	22
Figure 2. 6 The Stress-Life (S-N) Curve draw to logarithmic plot.....	25
Figure 2. 7 Horizontal fatigue life under biaxial Loading	28
Figure 3. 1 Fully reversed cyclic load (loading and unloading) applied on the bridge 33	
Figure 3. 2 Flow chart of the work	35
Figure 3. 3 Railway bridge cross-sectional Dimensions and pre-stress tendon (source Ethiopian Railway Corporation, drawing and technical specification)	36
Figure 3. 4 Pre-stressed concrete sleeper	40
Figure 3. 5 Dimensions and reinforcement detail of PCS used for validation	41
Figure 3. 6 Test set-up used in the test done by Rikard, 2000	42
Figure 3. 7 Static structural model with fixed support condition	42
Figure 3. 8 SOLID 65 Geometry	44
Figure 3. 9 LINK 180 Geometry.....	45
Figure 3. 10 Concrete body and pre-stressing wire with four supports	46
Figure 3. 11 Meshed sleeper model with the location of the area	47
Figure 3. 12 Applied load on the sleeper	47
Figure 3. 13 Compressive stress-strain graph for 52 MPa concrete	48
Figure 3. 14 Sleeper Directional Deformation.....	48
Figure 3. 15 Force vs Deformation graph with FEM results in blue and experimental test results in red color.....	49
Figure 3. 16 Existing Railway Bridge Cross Section	50
Figure 3. 17 Railway Bridge cross sectional dimensions model	51
Figure 3. 18 Geometric dimensions layout plan of pre-stressed tendons (unit: mm).	54
Figure 3. 19 geometric dimension of the Tendons elevations	55
Figure 3. 20 Railway Bridge reinforcement Model	56

Figure 3. 21 Finite Element Model based on Ansys (a) Reinforcement; (b) pre-stressed Tendon; (c) 1/2 bridge model.	58
Figure 3. 22 LINK 180 Elements used as Pre-stressing Tendons.....	58
Figure 3. 23 Equivalent Stress Convergence Plot.....	60
Figure 3. 24 Meshed Model of Railway Bridge	61
Figure 3. 25 Pre-stressed Boundary conditions and input data.....	61
Figure 3. 26 Operational Load Schematic Diagram for Passenger Coach	66
Figure 4. 1 Pre-stress loss of railway bridge deformed shape.....	68
Figure 4. 2 Maximum Total Deformation on the Railway bridge	70
Figure 4. 3 Directional Deformations in Concrete for 165 kN operational load	70
Figure 4. 4 Maximum Directional Deformation on the Railway bridge.....	71
Figure 4. 5 Equivalent Von-Mises Stress of the railway bridge.....	73
Figure 4. 6 Force Reaction versus Equivalent Stress of the pre-stressed railway bridge .	74
Figure 4. 7 Cyclic load Vs Equivalent Stress	74
Figure 4. 8 Available Life for operational load	76
Figure 4. 9 Fatigue Damage.....	76
Figure 4. 10 Safety Factor.....	77
Figure 4. 11 Equivalent Alternating Stress	78
Figure 4. 12 Fatigue Sensitivity Curve.	78

List of Tables	Page
Table 3. 1 General Information of pre-stressed concrete railway bridge model from ERC.	37
Table 3. 2 Pre-stressed concrete material properties	40
Table 3. 3 Typical property of pre-stressing wire material properties.....	41
Table 3.4 Total number of Nodes and Elements for the pre-stressed sleeper.....	47
Table 3. 5 Force Vs Deformation	49
Table 3. 6 Material properties of pre-stressed concrete railway bridge.....	52
Table 3. 7 Material properties of pre-stressing tendon	53
Table 3. 8 Reinforcement used for the modelling of the railway bride	56
Table 3. 9 Assembly and constituent parts of pre-stressed concrete railway bridge	58
Table 3. 10 Equivalent Stress Convergence	59
Table 3.11 Total number of elements for railway bridge	60
Table 3. 12 Allowable value of controlled stress for stretching	63
Table 4. 1 Centroid of the cross-section model along the 3-D	67
Table 4. 2 Cyclic load versus Deformation and Stress	69
Table 4. 3 Cyclic load versus Equivalent Stress	73
Table 4. 4 Maximum and Minimum Values	75

LIST OF NOTATION AND DEFINITIONS

Notation	Definitions
μ_c	Concrete Poisson's Ratio
μ_s	Steel Poisson's Ratio
ρ_c	Concrete Density
α_c	Concrete Thermal expansion
f_{plk}	Characteristic Strength of Steel
f_c	Characteristic Strength of concrete
F'_{ct}	Tensile Strength on concrete
A_{pw}	Pre-stressing Wires cross section area
A_p	Area of one Pre-stressing Wire
P_t	Pre-stressing Force
E_s	Steel Young's Modulus
E_c	Concrete Young's Modulus
B	Girder Width
P	Load
I	Impact Factor
S	Girder Spacing
δ	Deflection/Displacement of bridge
L	Span Length

ACRONYM AND ABBREVIATIONS

Term	Definition / Meaning
AA-LRT	Addis Ababa Light Rail Transit
AASHTO	American Association of State Highway and Transportation Officials
ARCE	African Railway Center of Excellence
AREMA	American Railway Engineering and Maintenance-of-Way Association
ASTM	American Society for Testing and Materials
CAD	Computer Aided Design
DNN	Deep Neural Network
ERC	Ethiopian Railway Corporation
E-W	East-West
FC	Fully Connected
FDRE	Federal Democratic Republic of Ethiopia
FEA	Finite Element Analysis
FEM	Finite Element Method
HTL	High Tonnage Loop
LRT	Light Rail Transit
LSTM	Long Short-Term Memory
N-S	North-South
PC	Pre-stressed Concrete
PCBGRB	Pre-stressed Concrete Box Girder Railway Bridge
Rd	Relative Deviation
TTCI	Transportation Technology Center Inc
WSS	Wireless smart sensor
UIC	International Union of Railway
USA	United States of America

CHAPTER ONE INTRODUCTION

1.1 Background

Bridges are structural elements used to provide a passage over a gap, or a barrier like a lake, valley, river, or trough in a railway line. A bridge contains a super-structure that includes all elements of the bridge above the bearing support like (i.e., slab deck, truss, arch, and different girder types) and structures below the bearing support called sub-structure such as (i.e., abutment wall, piers on middle span, and foundations) constructed to support the superstructure.

Pre-stressed concrete box girders are an integral part of the railway superstructure that helps to support and transfer the operational vertical loads. Railway bridges are one of the most important means of transportation in the world as they have high-capacity transportation, are environmentally friendly, and have efficient energy usage. Their occasional failures have often been the stimulus for research into the proper use of materials, better design, and appropriate maintenance methods [1].

Railway bridges are subjected to cyclic train loads, which can lead to fatigue collapse. Railway bridges are intended to last for a designated service life as key linkages in a transportation network; however, they can break sooner than predicted due to repetitive loading. To improve the target bridge's life, bridge maintenance activities like strengthen, and repair should be properly undertaken after local inspection. The fatigue life of a structure is dependent on realistic assumptions about loading cycles and the availability of strain time histories. A multi-axial non-proportional load rating history is used for the evaluation of fatigue life and structural condition of railway bridges. The load applied by the tram vehicle uses the railway bridge information found in the cross-section plans and material properties.

This thesis presents the remaining fatigue life of a box girder railroad bridge based on design and operational loads. It also estimates the fatigue failure with a combined operational and designed live load. The railway bridge is subjected to a concentration of stress from upper parts like rails, pads, sleepers, and ballast. Excessive stress caused by cyclic load may result in bridge failure, as well as wear and fatigue damage to bridge

components. As a result, knowing a pre-stressed railway bridge's remaining fatigue life is critical for improving railway bridge maintenance and safety. The Chinese design standard and operational live load causes are the main components examined in this study. For a railway bridge's life and structural condition, a multi-axial operational load history is used. In this paper, a simplified Ansys finite element model for a pre-stressed railway bridge subjected to train loading at the time of passing is developed for the application. The objective of this study is to estimate and identify characteristics of the fatigue life along with fatigue failure and fatigue cyclic load for a pre-stressed box girder railway bridge using numerical methods.

Thus, the backbone of the paper is to estimate the remaining fatigue life of box girder railroad bridge using the maximum operational live load before failure due to cyclic load.

1.2 Statement of the Problem

As transportation demand grows, numerous railway line projects are being built around the world, and feasibility studies are being conducted. In addition, the Ethiopian Railway Corporation in Ethiopia has also constructed the Addis Ababa Light Rail Transit. However, the performance of the railway bridge is not assessed yet. Pre-stressed concrete structures initially serve well and fail later due to fatigue or repeated cyclic loading during service life. This fatigue failure can lead to serious safety problems and accidents if it exceeds the limit and if remediation is not taken on time. So far, the fatigue life of the AA-LRT has not been analyzed, although an extensive study has been conducted to determine the phenomena of fatigue for reinforced concrete and sleepers basically at material level and structural level. In connection with this, estimating the remaining fatigue life and checking the fatigue failure due to cyclic repetition of the elevated concrete railway bridge of Adis Ababa is advisable; so that, the bridge management team can improve their railway bridge inspection techniques and maintenance methods to prolong their design or service life through the use of new or innovative equipment and by restricting traffic on the railway bridge.

1.3 Objectives

1.3.1 General Objective

The main objective of this paper is to estimate the remaining fatigue life of stated pre-stressed concrete box girder railway bridge. Non-linear finite element model ANSYS 2020 is used to carry out the fatigue life for the box girder railway bridges constructed along the AA-LRT line during its service life.

1.3.2 Specific Objective

The specific objectives of this study are:-

- To estimate the fatigue life and remaining fatigue life of pre-stressed concrete railway bridges based on numerical analysis of Ansys 2020 software.

1.4 Scope and Limitation of the Study

Due to time shortage and budget constraints, the research was focused on determining the remaining fatigue life of pre-stressed concrete girder railway bridges for AA-LRT under static analysis. Then the fatigue life will be evaluated using numerical simulation analysis using Ansys software. Further, the numerical analysis measure for fatigue failure due to cyclic axle load, considering the design and operational load, was only considered. To simplify fatigue life, the operational load used in this thesis includes a similar operational load with a value of 165 kN. Additionally, the Ethiopian Railway Corporation data source was used as input for checking pre-stressed concrete box girder railway bridge fatigue life analysis.

1.5 Structure of the Thesis

The overall content of this thesis is the Evaluation of the remaining fatigue life of a pre-stressed concrete railway bridges for Addis Ababa LRT. The paper starts with an introductory section that gives the relevant basis for the fatigue life of bridges and how it is accounted for in design by a factor. In general, the thesis is comprised of five chapters.

Chapter One of the thesis includes an introduction, a problem of statment, the general and specific objectives of the thesis, the scope and limitation of the thesis, and structure of the thesis.

Chapter Two includes different literature review about fatigue performance of railway bridges, the fatigue life of bridges, and an evaluation of pre-stressed railway bridges with the software procedures.

Chapter Three includes the methodology followed to determine the stated objectives the finite element modeling procedure utilized the finite element modeling of the railwaybridge, cross section of the existing structure, assumptions considered and material property of the railway bridge. The validation of FEM, using cross-sectional dimension pre-stressed sleepers is discussed for the validation of railway girder bridge. This chapter also presents the validated results by considering pre-stressed sleepers.

Chapter Four deals with result and analysis discussion based on the output of software and prestrss loss calculations in the model.

Finally, Chapter Five includes the conclusion and recommendation of the results of the analysis regarding modeling in Ansys and fatigue life of pre-stressed concrete railway bridges due to cyclic load trains.

CHAPTER TWO LITERATURE REVIEW

2.1 Introduction

The essence of fatigue was occurred when a material or a structure is subjected to repetitive load. The civil infrastructure structural elements of railway bridges fail statically because they are subjected to deterioration and damage, as well as deflection due to stress produced by the cyclic repetition of traffic or train loads. Most structures' static failures give warning signs, but fatigue failures may not be because they are sudden and dangerous. If no preventive mechanism is implemented, load damage eventually leads to cracking, large deformation, and delamination, lowering the performance level and resulting in an unsafe structure.

Bear in mind the need to construct a pre-stressed concrete railway bridge with satisfactory performance through its designed period or service life, which the structure must satisfy. Thus, it is mandatory to assess or estimate remaining life of structures to avoid such unexpected problems caused by shorter service life. With increased axle load, the carrying capacity of bridge has become different or altered. In real world, the existing bridge structures are expected to carry larger loads than what they are designed for. Therefore, after estimating the service life, the engineer can plan maintenance or replacement by their priority of remaining life. If the structure of railway bridges are integrated and meet their requirements, their design and service life are increased, becomes economical in terms of saving money and the environmental impact was decreased. The fatigue eventually leads to fracture criticality due to environmental loads and bridge loading conditions. According to AREMA, fracture-critical members are those tension components which can result in bridge failure and collapse and failure to perform its main purpose [2].

The fatigue characteristics failure evolve in three stages. The first stage I involves the production of more than one micro fractures due to repetitive plastic deformation followed by cyclic plastic deformation, followed by the crystallographic propagation from two up to five grains about the origin. It is impossible to see fractures with the naked eye. The second Stage II results in analogous, plateau like fracture surface but separated by

longitudinal ridges. When the remaining material cannot handle the stress during the final stress cycle, stage III occurs, resulting in an abrupt, quick fracture.

In the transportation industry, the essence of fatigue on materials was well investigated around the late 1850s by Ajibola [3]. Arthur Morin in France and J.O York and William Rankine in Britain investigated axle failure in horse drawn and carriage railway lines. The scholar Jean Victor Poncelet is credited with coining the term "fatigue". Various academics explored fatigue failure as a major issue in all transportation and other industries around the world [3].

Different researchers have carried out various theoretical and experimental studies to estimate the fatigue life and parameters that determine a pre-stressed concrete railway bridge. They have followed different approaches and methodologies to analyze such railroad bridge components. The following section briefly describes a few of the kinds of literature available related to research on fatigue life of structures.

Xia et al. [4] have presented a work that looked at the experimental examination of a high speed railway bridge. They have also considered a bridge built using continuous span supported by simple support girders by considering the articulated cars that run on the structure as trains. The study of the recorded data yielded useful insights regarding articulated trains, some of which are provided in the thesis. The Author from experimental test revealed that the vertical deflection was within allowable, with only minor changes between single and double train deflections. The bridge's greatest vertical acceleration was less than 1 m/s^2 , and its maximum lateral acceleration was significantly lower. However, the response of the vertical deflection caused by single and double train was not remarkable change.

Matias et al. [5] simulated the fatigue result using the ratio of 0.45–0.8, and the result follows the same trend. The performance of the railway bridge under cyclic load depends on the material fatigue performance or properties of concrete, reinforcing steel and pre-stressed tendon. The S-N curve is obtained from laboratory experimental test results, and currently, it has a limitation on estimation fatigue life of railway bridge based on the current AREMA manual. The propagation time is predicted based on the initial

crack. The Author has also studied the strain difference by comparing the result with a program using the Moving load (ML) model for moving spring mass damper (MSMD). The Author stated that and confirmed that there is no significant difference with the strain reader. Further, the Author looked into the impacts of irregularity of the track structure and operating speed of the train on fatigue crack initiation [5], [6].

Ibrahim Abdu, [7] conducted research on the economic importance of railroad girder bridge and deck bridges by considering the cross-sectional dimension of the Leghar Light Rail Transit pre-stressed concrete railway bridge. The bridge's name was LRT Leghar Bridge which crosses the Highway located around Leghar Station with a precast concrete bridge type. Pre-stressed simply support a post-tensioned box girder with length 20 meter, deck width 7.14 meter, deck thickness of 0.30 meter, girder depth of 1.60 meter, and the distance between centers of tracks of 4 meter. The Author found that Box Girder Bridge has significant importance in terms of cost and benefit. However, in his analysis, fatigue life is not considered.

Pipinato, et al. [8] in their study conducted a finite element model to determine the nominal stress for a 12.40 m span length by assuming a maximum annual daily traffic of 235 trains/day for the analysis as per the recommendation of the national railway line. The Author found that with an increase of 1%, 2%, or 3% percent of increase versus time of regression tendency and the UIC stated that it was possible to estimate the number of trains that pass on it. The Author in his study considers the past traffic as 50% of passenger and 50% freight trains in equal proportion. In addition, the Author has mentioned three parameters that affect the fatigue damage of railway bridge. These are: range of stress amplitude, the geometry of the structure and number of stress cycles of the past traffic which have influence on the fatigue life.

Gulgec et, al [9] use inexpensive sensor networks to get the stress and strain data used for fatigue analysis and estimating the remaining life for the structural element. In addition, the Author uses acceleration and strain sequence inputs from the selected location to the train as a deep neural network (DNN) model. This train model was used as input to check the strain and stress response from the acceleration data from the selected sample location. The proposed network exploits the temporal modeling of long

short-term memory (LSTM) and non-linear mapping of fully connected layers (FC layers) to be able to discover temporal dependencies and complex relationships between input and output sequences. Furthermore, the study presents a novel step-wise training methodology to deal with the computational expense of sequential learning and long-time histories generated as a result of fatigue life assessment. During the step-wise training strategy, the researcher addresses three challenges: (a) the difficulty of training large sequences, (b) the initialization of network parameters and convergence issues, and (c) the time dependency of the time series. The study's findings reveal that the stream of predicted values matches the testing samples. The network's performance has to be improved for load scenarios involving impact loading.

Rakoczy et al. [10] also studied the fatigue failure evaluation on riveted steel railway bridges based on a reliability based approach. The Author performed the evaluation randomly in nature and determined the failure probability based on the Transportation Technology center Inc (TTCI) for (5) five riveted railway bridge which is erected in 1997. The bridge has a two span with length of 55 ft., 6 in and 65 ft with carrying capacity of 150 MGT per year heavy axle traffic. The Author also stated that the bridge life is dependant on fatigue category and applied load. In addition, results are presented in statistics parameter bilinear S-N curve and probabilistic method. Finally, the researcher recommends using a probabilistic method to estimate the life of the steel bridge when it has high initial crack detection and the inspection shall be increased accordingly.

H. Li and G. Wu [11] investigated the fatigue of crucial features using a multi-scale dynamic analysis of the train-track-bridge system and linear elastic fracture mechanics. The analysis, which is based on a vehicle-bridge analysis model made up of a 3-D vehicle model, a multi-scale bridge finite element model including the track system, and a wheel-rail interaction model, allows for the correct and efficient computation of fatigue stresses produced by moving trains in structural details.

2.2 Railway Bridge Components

Bridges have several benefits and are constructed around the world. They are the main important elements in any railroad network. The prestressing of bridges currently have gaining popularity in bridge Engineering due to their better servicability, aesthetic

appearance and their stability. The pre-stressed concrete railway bridges can be classified based on the use and functions provided to the environment.

The pre-stressed concrete railway bridge is divided into two major parts based on their location:- the substructure and the superstructure.

- I. Bridge Sub-structure:** The sub-structures of a bridge consist of all components that support the superstructure bridge. This includes elements like, piers, abutments, foundations, etc.

Bearings are used transfer loads from the above superstructure to the lower boun of substructure with a relative movements or deflection in between them.

- II. Bridge Super-structure** consists of all the elements of the railway bridge above the bearing support like girders, decks, trusses, arches, etc.

2.3 Types of Railway Bridges

Railway bridges can be divided based on the following characteristics.

- 1) Classification according to construction material as Concrete, Steel, Masonry (brick, rock), Pre-stressed concrete, Timber, or a combination of any two or more.
- 2) Classification according to span length as Short, Medium, or Large.
 - ✓ Short Bridges: (6-30 m)
 - ✓ Medium Bridges: (30-100 m)
 - ✓ Long Bridges: > 100 m
- 3) Classification according to structural forms such as T-Girder, Box Girder, Arch, Suspension, etc.
- 4) Classification according to span type as Single or Multi-Span.

2.4 Loads for Design of Concrete Railway Bridge

2.4.1 Live Loads

The recommended train vehicle live load for modeling the railway bridge uses Cooper E 80- or 80-kip (EM 360 kN) axle load spacing and configurations. The single-track live

load was assumed to be uniform, but this single load cannot determine the accumulated cyclic load that affects the life of the bridge under fatigue. The AA-LRT is designed based on China's standards with only six axle loads. AREMA Bridge Design Manual, Section 2.2.3 Design Loads, Figure 8.2.1 demonstrates axle spacing and axle load of eighteen axle train loads for strength evaluation. However, the AREMA [12] manual is conservative but much safer for the repetition of train loads and the increase in train loads during the bridge service life.

2.4.2 Impact Load

The impact load is applied and happened at the rail top. The impact load is also added to the static load in the load rating. The AREMA manual proposed different percentage values of impact and dynamic allowances for pre-stressed railway bridges for rolling equipment without hammer blows, like electric locomotives. The manual also proposed different formulas based on the span length of the bridge. For the length less than 4 and greater than 39 meters the Impact considered are 60% and 20% respectively. If the Span length of the bridge is in between the four and 39 a formula stated in equation 2.1 was used.

$$\text{For } 4 \text{ meters} < L < 39 \text{ meters, } I = \frac{125}{(L)^{1/2}} \dots\dots\dots (2.1)$$

Where,

L = Span Length

I = Impact

2.4.3 Permit load

Permit loads are loads that are beyond the capacity or range of standard legal tram-train. The trains that needs a permit are the trains that carry higher higher operational load beyond the capacity of the bridge. The construction of the AA-LRT line was a major project in Addis Ababa, Ethiopia. The China Railway Group Limited is responsible for design and construction of the project based on the condition assessment from the Ethiopian Railway Corporation and for designing a live load for the bridge along the railway line [13].

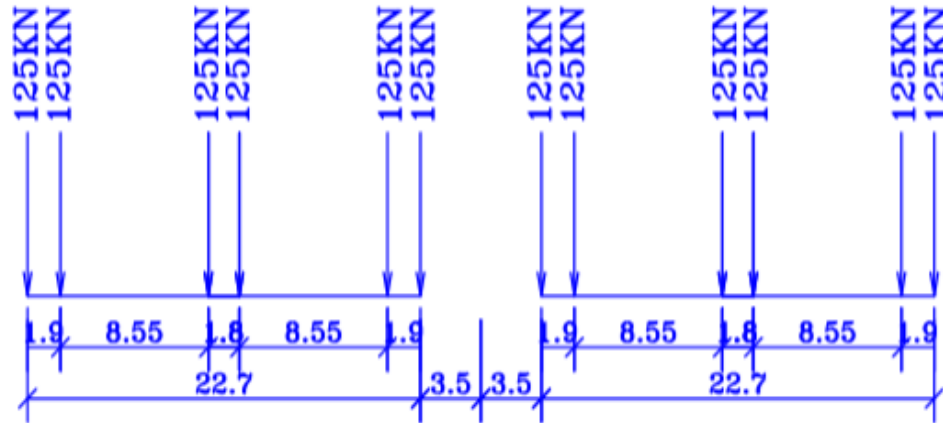


Figure 2. 1 Axle load and wheel load

As it is shown in the above Figure 2.1, a train axle load of 125 kN expressed in force was used with a simplified real geometry of a railway bridge. This axle load is being applied in the specified spacing of the bridge deck. According to an AA-LRT passenger transport survey, the passenger flow of Line E-W is expected to be 734.4 thousand and Line N-S is expected to be 536.9 thousand per day.

2.5 Basic Concept of Pre-stressing Concrete

Pre-stressing is the the application of a pre-compression load on the a structure to resist the stress coming from the combination of loads at design life. Pre-stressed concrete girder railroad bridges and the design of pre-stressed concrete, on the other hand, are created when the appropriate magnitude of internal forces is spread across the area to resist the counterforce. In addition, the structural components must be built/designed for both initial and final pre-stressing forces to fulfill the service and strength limit states, which regulate the design. Many of the important bridges that were destroyed during wartime had to be rebuilt quickly. Different countirs in Western and Central Europe like Belgium, Paris and France extensilvly practiced on the concept of prestressing for the construction and design bridges.

There are several studies conducted on static structural and dynamic moving load problems by considering pre-stressed concrete bridges and a tram vehicle model. The static and impact responses of previous investigation on moving load is presented in the

following section. The fatigue strength of railway bridges was performed based on some experimental data that correlate with stress range and used to determine the live load induced stress range through field strain measurement as specified in the AREMA manual [14].

In Ethiopia, the construction of long span pre-stressed concrete girder bridges has been established for a few years. According to the information obtained from the Ethiopian Railway Corporation Construction Management Team, there are several pre-stressed railway bridges along the AA-LRT and the Ethio-Djibouti National Railway Line.

2.5.1 Methods of Pre-Stressing

There are two methods of prestressing concrete based on the pre-stressing tendon with respect to the concrete and exact location. These prestressing methods are:-

Pre-tensioning: It is the process of applying pre-stress to prestress tendon or steel strand before concrete is casted.

Post-tensioning: It is the method of applying pre-stress force to pre-stress tendon strands after concrete is casted [15], [16].

2.5.1.1 Pre-Tensioning

This is a type of prefabrication in which the concrete element is prepared away from the final structure location and then transferred to the site once it has cured. It necessitates the use of robust, solid end anchorage sites where the tendons are stashed. In post tensioning after the concrete has gained its required pre-stressing strength the pre-stressed tendon must be cut from the anchorage end.

2.5.1.2 Post-Tensioning

This is a method used to pre-stress a reinforced concrete after the casting of the concrete. It provides an immediate and active load carrying capacity. The process have two stages. Stage 1 the pre-stress tendons are inserted to the concrete and stage 2 is tensioned the inserted tendon and then anchored to the concrete. This method is also used to reduce

the displacements in the structure and it turns the discontinuous member to the continuous member [15], [17]. The duct in the in post tensioning is prevent bonding on the concrete and pre-stress tendon during tensioning operation. The post tensioning member is either bound or unbound.

Advantages of Pre-Stressing Concrete

- Preferable for cast in situ members of the railway bridge
- Used to construct large span structure, so saving the weight and it is economically viable.
- Less time is required on the casting bed.
- A pre-stressed concrete deflects within allowable limit and gives warning sign before collapse.

Disadvantages of Pre-Stressed Concrete

- It has transportation risk by equipment.
- The construction system needs highly experienced professionals.
- Initially, the cost of the equipment is very expensive.
- The obtainability of experienced professional is limited.
- They are less fire-resistant.

2.5.1.3 Pre-stressing Wire and Strand

Pre-stressing tendons have long transmission length features with of pre-tensioned railway bridge. They are available in diameter of 15.24 mm of wire to 21.8 mm of the seven-wire strand. There are also small diameter wire less than 9.3 mm for a seven-wire strand down to 6.3 mm which are used in certain countries. For the end of the railway bridge, 15.2 mm wire is mainly used. The choice of strands or individual wire was depend on the manufacturer decision and the material efficiency [17], [18].

2.5.1.4 Concrete

Concrete will behave linear elastic behavior when initially subjected to a small load. When the load is increasing, defects like macro-cracks are formed in the material structure, which makes the strain increase rapidly and results in a non-linear, non-elastic

relationship. If the section is unloaded when it reaches a large portion of ultimate strength, the residual strain will remain due to defects in the microstructure [18].

The stress-strain curve failed rapidly after reaching the ultimate strength by creating a small area under the curve. Pre-stressing concrete used high strength concrete. The AREMA manual recommended a minimum comprehensive strength of 48 MPa (7,000psi) at 28 days. While other manufactureres achieve the strength above 69 MPa (10,000 psi).

2.5.1.5 Deformations in Concrete

The stress strain response evolves from concave towards the strain axis to straight line and then to convex dependent on the number of load cycles. The degree of convexity reflects how close to failure the concrete is. During fatigue loading, the overall strain gradually increases as the number of cycles increases. According to Holemen, strain growth is classified into three stages, the first of which is a rapid increase in stresses from 0 to 10% of the fatigue life. This stage is distinguished by fracture initiation and deterioration of the aggregate-mortar connection. The second stage is the increase in strain from 10% to 80% of the fatigue life owing to crack propagation. Finally, the third stage is the rise from 80% until the strain failue occurs as shown in the Figure 2.2 below [19].

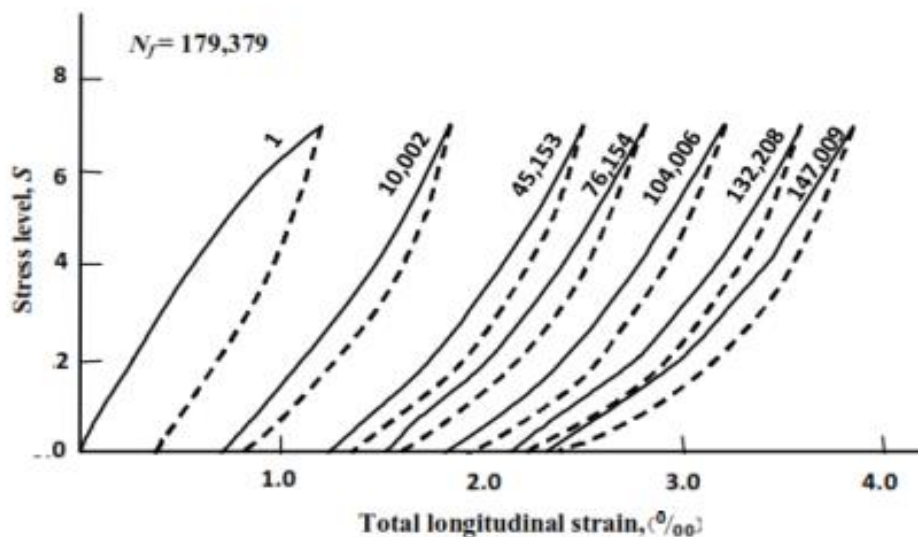


Figure 2.2 cyclic strss curves for for concrete in compression

2.5.1.6 Pre-stress Losses on Concrete

Pre-stress losses are the reduction of the induced stress or strain due to various reasons. The reduction in pre-stress force is because of this loss of pre-stressing as it happens at decreasing rate until it gains its strength. This reduction of pre-stressing force happens immediately which corresponds to elastic loss during construction or fabrication or time dependent causes like (Creep, shrinkage steel relaxation etc). The total pre-stressing loss is the sum of all losses in combination of fabrication process and material characteristics loss is a combination the fabrication process and material characteristics such as the following [20], [21]:-

- ❖ **Elastic Shortening:** It is encountered mainly in pre-tension member. In this loss the pre-stressing force is transferred to concrete member and the concrete undergoes fastly shortening as the result of pre-stress. Simultaneously pre-stressing steel shortens by the same amount.
- ❖ **Relaxation:** It is a reduction in stress in long term time under a constant tension. It is also defined as the loss of prestressing force in long time at constant length and temperature. In addition, the pressure in the prestress tendon is decreased with time by steel relaxation. The relaxation process is equivalent to creep. The stress loss depends on the steel type, initial pressure and temperature.
- ❖ **Shrinkage:** It happens over time as the free water within the concrete is utilized during hydration and evaporates, allowing the concrete to shorten.
- ❖ **Creep:** It is the minimum deformation that occurs over time as a result of applied compressive stress in long term. It occurs in both pre-tension and post-tension member. The concrete deformation behavior is affected by applied load, the duration of load, the properties of concrete like mix ratios, curing time and environmental condition [22].
- ❖ **Anchorage Set:** When mechanical losses set in during pre-stressed fabrication, chucks put around pre-stressing steel to maintain tension suffer mechanical losses. The losses from the sources described above are added together to yield the total pre-stressing loss. Some occur instantly (elastic shortening and anchoring) whereas others occur during the life of a pre-stressed member (creep,

shrinkage, etc.). Losses are computed separately and then summed to produce the most accurate result, or a lump sum estimate of the losses might be obtained.

2.6 Overview of Current Fatigue Analysis

2.6.1 General Background on Fatigue

Fatigue is defined as the lowering in the material strength and is structural damage as a result of repeated load. Several studies have been made on the determination of fatigue failure. Fatigue was first studied for iron. Sursh (1998) conducted study on metal fatigue for the first time in the late 1820s by the German engineer Julius Wilhelm Albert. Pre-stressed concrete railway bridge materials undergo fatigue due to repetitive stresses that are repeated a large number of times and cause fatigue failure. The increase repetitive stress leads to the crack growth and fracture of the material.

2.6.2 Types of Fatigue Damage

Fatigue damage of the structures can be classified into four types based on loading conditions and environmental conditions.

- **High - Cycle Fatigue:** This high cycle is occurred is due to low stress or large number of cycles. If the material requires more cycles starting from 10^3 to 10^4 cycles to fail then we call the material have high cycle fatigue.
- **Low - Cycle Fatigue:** It is formed due to high stress or low number of cycles. If the material requires a low cycle to failure, starting from less than 10^3 to 10^4 . It is associated with high load amplitude which yields in loss of material stiffness.
- **Thermal Fatigue** occurs due to temperature variation (rapid heating and cooling) over time and produces cyclic stress in the sample of material. crack propagation has started due to expansion and extension as a result fatigue process was increased by rise in variation of temperature.
- **Corrosion Fatigue:** It is formed when the material is exposed to cyclic load and a corrosive environment. The environment has a significant effect on the fatigue process [23].

2.6.3 Fatigue Analysis Types

There are three types fatigue analysis which are available in the Ansys software. These are stress life, strain life and fracture mechanics. S-N approach is the basis of current design codes such as Euro Code 3, Parts 1-9. The fatigue strength expressed in S-N curve and it is constructed by plotting the number of load cycles (N) versus the maximum stress (S). Fatigue curves are drawn based on failure load versus log of the wheel load passage of the selected panel. If the structure or materials reaches its design life, it fails due to fatigue loading.

a) Strain Life

Strain life can be measured for classifying low cycle fatigue and it naturally deals with crack initiation. The majority of the time, strain life deals with or addresses a small number of cycles, but it works well with a large number of cycles.

b) Stress Life

Stress life is concerned with the total life of the structure based on stress- number of cycles curve (S-N). The stress life does not differentiate between initiation and propagation crack.

c) Fracture Mechanics

Fracture mechanics begins with a known flaw size to determine the crack growth and some times it is called crack life. It also used to determine the interval of inspection. To establish the inspection technique, first identify the detectable flaw size, and then calculate the time required for the crack to expand to a critical size using the detectable flaw size. We can then set our inspection interval to be less than the time it takes for the crack to grow. Strain life techniques are sometimes employed to assess crack initiation, and fracture mechanics are used to predict crack life; thus:-

Crack initiation+Crack propagation = Total life

2.7 Fatigue Analysis

During the last decade, different researches (theoretical and experimental) methods have been proposed to determine the fatigue analysis of pre-stressed concrete beams with respect to their material properties like pre-stressing force, longitudinal reinforcement ratio, and concrete strength. A scholar named Wollmann [24] conducted an tentative experimental investigation to fatigue strength of a concrete girder. The Author found that the fatigue failure happens in areas of cracks. The paper also shows that the simulated curve was extended with the same slope and seems to have no fatigue limit as it is subjected to low load ratio which is caused by cracking in concrete.

Materials undergo fatigue due to the progressive internal structural change and they undergo due to repetitive stresses. This leads to crack growth and material fracture when the stress repetition is high. The performance of railway bridges due to cyclic load depends on the fatigue property of concrete, steel and pre-stressed tendon [25]. The S-N curve is determined from laboratory test results, and currently, it has a limitation in the estimation of railroad bridge life based on the current AREMA manual. The propagation time is predicted based on the initial crack. MacDougall et al. [6] calculated the difference between the fatigue lives of short-span and medium-span bridges under successive passage. After determining the fatigue life of the structure in terms of cycles and years can be estimated based on traffic volume of the railway bridge site.

Palmgren-Miner [26] used a formulation rule for the fatigue design. The Author assumes a linear relationship between damage and number of cycles. In addition, in his design, the paper concludes that for a given number of cycles at stress level S_1 and corresponding fatigue life endurance N_1 , it is assumed that the degree of fatigue resistance consumed is n_1/N_1 . If the individual's level of stress continues at level 2, they may experience failure. This depends on how much of their fatigue resistance is consumed.

$$\frac{n_1}{N_1} + \frac{n_2}{N_2} + \dots = 1 \dots \dots \dots (2.2)$$

For different or multiple stress level of block loading, the system fatigue can be generalized in the following equation stated below as follows:

practice, crack growth is slow to start but as it propagates the crack accelerates exponentially, eventually leading to a failure (Figure 2.3).

As shown in Figure 2.3, which depicts a typical graph of fatigue crack length as a function of the number of fatigue cycles, for a simple sinusoidal loading condition, the crack grows slowly at first, then gradually accelerates, eventually leading to rapid crack growth and ultimate failure. Even under constant sinusoidal cycle loading circumstances, the cyclic stress intensity amplitude, K , increases as the fracture length increases. The rate of crack growth is clearly increasing as well, and Paul Paris was the first to detect the relationship between these two parameters (i.e., stress and loading condition) by plotting them against each other on a log-log scale (Paris and Erdogan, 1963) [26]. This resulted, in general, in a linear relationship over the central portion (Figure 2.4) that could be characterized by the so-called Paris-Erdogan equation, as related in Figure 2.3 below.

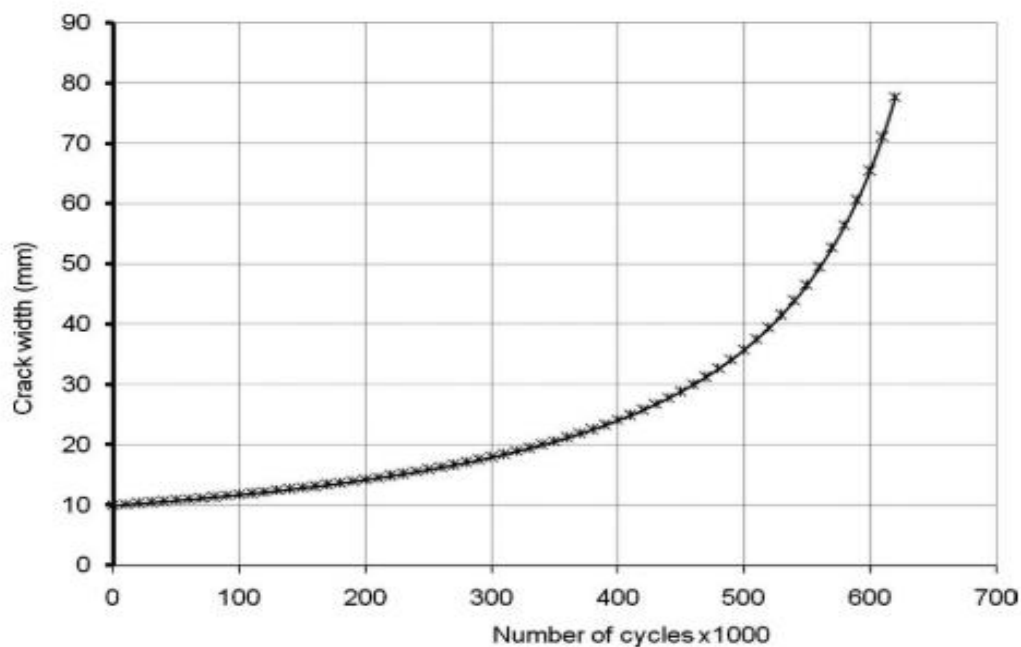


Figure 2. 3 Typical crack width versus number of cycles

The initial crack length depends on the stress intensity exposure. This intensity factor ΔK is main main source of crack growth rate, da/dN to the cyclic stress intensity amplitude ΔK :

$\frac{da}{dN} = C\Delta K^m$, Where C and M are experimentally obtained constants for material characteristics, N is number of cycles and a depth of crack, M is the slope curve, which is close to 3 (ranges from 2-4), and C is the characteristics where the material data is located on the da/dN versus ΔK graph and it is mostly affected by frequency and environmental.

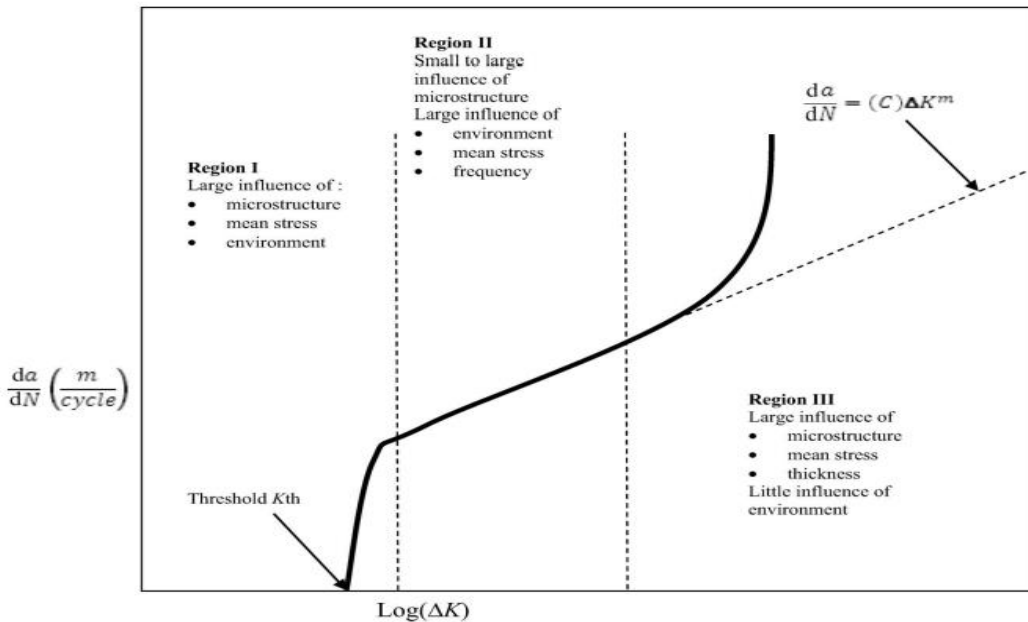


Figure 2. 4 Typical Paris-Erdogan equation graph [26] .

The strength of fracture mechanics based on the Paris-Erdogan equation for fatigue development resides in the ease with which fatigue life prediction calculations may be performed. We can obtain the following by rearranging the above Paris-Erdogan equation to make dN the subject, substituting in for K, and integrating the equation:

$$N = \int \frac{da}{C(Y\Delta\sigma\sqrt{\pi a})^m} \dots\dots\dots (2.5)$$

The integration limit ranges from the initial defect or crack size, which could be the detection limit of non-destructive testing (NDT) methods, to the top limit of the critical flaw size under stress as determined by fracture mechanics methods (Equation 2.5). This strategy is limited to applications where the linear section of the Paris curve applies and is not influenced by the environment when it is away from the threshold and is not overly influenced by the environment. In the cause, fracture propagation is governed by one fatigue crack increment (or pattern) each cycle, which is typically relevant to the Paris

curve's center linear area II. Accurate fatigue life estimations are easily determined by applying the integration technique, which is based on the values of cycle stress and material property inputs, C and m , as well as starting and final fault sizes. These qualities, in turn, lead to functional recommendations for inspections to check the structural integrity of the construction using non-destructive testing (NDT). This damage tolerance can easily be expanded to allow for the use of numerical integration as needed and the refinement of the life-prediction procedure for safe fatigue operation [26].

2.7.1 Fatigue Failure in Concrete Structures

Fatigue of concrete is defined as larger strain micro-cracking as compared to static loading. Concrete is a heterogeneous material and its resistance is affected by different factors like the maximum load, load frequency, moisture content, and properties of the concrete material. Fatigue failure evaluation is performed by taking the maximum and minimum stress, as well as the design strength, into account (f_{cd} , f_{at} , and f_{ctd}) [27].

Different researchers use different hypotheses regarding crack initiation and propagation. Murdock and Kessler (1960) in his study concluded that failure was caused by the bond between the aggregate and binding matrix. Another scholar called Antrim (1967) stated that concrete failure is caused by the small crack formed in the cement paste, which results in decreasing the strength of the section and it cannot sustain the applied load [23], [28]. Concrete structure studies began at the turn of the 19th century. Following this, numerous countries conducted extensive research on fatigue in concrete structures [29].



Figure 2. 5 Horizontal Cracking near the axle load

We can see from Figure 2.5 that the main concerns with concrete bridges are degradation, abrasion, and cracking. Abrasion and chemical deterioration is not purely structural processes and cracking is commonly used as a failure criterion in the design process to determine the fatigue state of concrete sleepers. Figure 2.5 above depicts the most common types of concrete bridge cracks.

Fatigue failure also occurs below a material's stress limit after it has been subjected to cyclic loadings. The effect of fatigue are based on the following concepts [29], [30]:-

- ✓ The Stress Range Magnitude.
- ✓ The quality of structural detail and its type type.
- ✓ The number of cycles of the stress range.

According to RILEM technical committee 90 FEM and Elfgren, failure in concrete can be modeled in three separate ways, as described by Wittmann in 1980. The method is known as the 3-L method.

- At the micro-level, calcium silicate hydrate crystals with primary and secondary connections are studied. This level is uninteresting in terms of fracture mechanics, according to RILEM technical committee 90 FMA and Elfgren (1989). Physical and chemical processes that can be active in a given situation influence behavior at the micro-level. The models in this level are material science models.
- On a meso-level, study the cement paste, aggregate, and their interaction. The strength of some of the following failure modes surrounding an aggregate particle is commonly found to be the source of failure: Bond failure due to tension, shear failure, matrix failure due to tension or shear, and aggregate particle failure [23].
- For practical applications at the macro level the concrete is modeled as a homogeneous, isotropic material containing flaws. The average strain-stress characteristics as well as the non-linearity of mechanical properties are fascinating to study. This level's engineering models should be provided in a way that allows them to be employed immediately in numerical analysis.

2.7.2 Fatigue Loads

For concrete railway bridges, cracking in the structure may be appear due to excessive flexural, shear stress. Fatigue load of the railway bridge is the vertical wheel load distributed on the box sleeper over the slab part of the railway bridge, which may be divided in to dynamic load and impact load.

2.7.2.1 Dynamic Load

Dynamic load is widely recognized to be employed frequently in the design of railway tracks and railway applications. The dynamic load takes into account the dynamic load track interaction under normal circumstances; it does not take into account the extreme impact factor (IF) in railways. The acceptable stress design approach employs dynamic load, which is typically connected to train speed.

2.7.2.2 Impact Load

It is not uncommon for railroad tracks to experience impact loads as a result of train vehicle repetition linked with abnormalities in the track wheel, sleepers and bridges. Impact loads on the contact region of a box sleeper railway bridge far outnumber static wheel loads. The impact load value was shown to be not only related to train speed, but also to the causes of such loads (e.g., sleeper spacing flatness, span length, wave length of rail). Wakui and Okuda studied the characteristics of impact loads by measuring the axle-box acceleration of a wheel axle box. The Author discovered it is possible to reduce the impact load to a shock pulse that occurs after the wheel load is removed.

2.7.3 Fatigue Failure in Steel Reinforcement

Steel constructions were the first to exhibit the fatigue phenomenon. Albert conducted fatigue testing on welded mine hoist chains in 1830. Cracks in steel often require high-stress levels. The geometry of the element subjected to cyclic loadings, such as a crack due to local restrictions, influences the behavior and velocity of crack propagation. The reinforcement bars have plain and rib surfaces. The ribs in the reinforcement help to increase the stress concentration and reduce fatigue, and their shape gives importance to the transition between the rib and bars.

Reinforcing steel has the same elastic reaction as concrete at early loading, and as the load increases, the yield surface is achieved. This causes elastic and plastic deformation, such as the dislocation of steel crystals. Because steel hardens, it can withstand more force before failing. Failure occurs if the loading continues until the static strength is attained. The fatigue of reinforcement is affected by several distinct criteria. Some parameters that influence fatigue life include stress variation, bar surface, and area of reinforcement [23].

When we utilize Ansys software, the fatigue findings are based on the linear static. Even if the model has non-linearity, the program expects linear behavior. Young's modulus, mass, and density are the inputs to fatigue analysis. Thermal loads, thermal expansion coefficients, and thermal conductivity are also considered. The mean stress effects in fatigue are typically represented on the material property as a stress amplitude versus mean stress plot. For a given cyclic life, the load amplitude of the endurance limits typically decreases with increasing mean stress or static load. Figure 2.6 depicts a typical stress-life curve, or S-N curve, that displays the link of stress amplitude to failure.

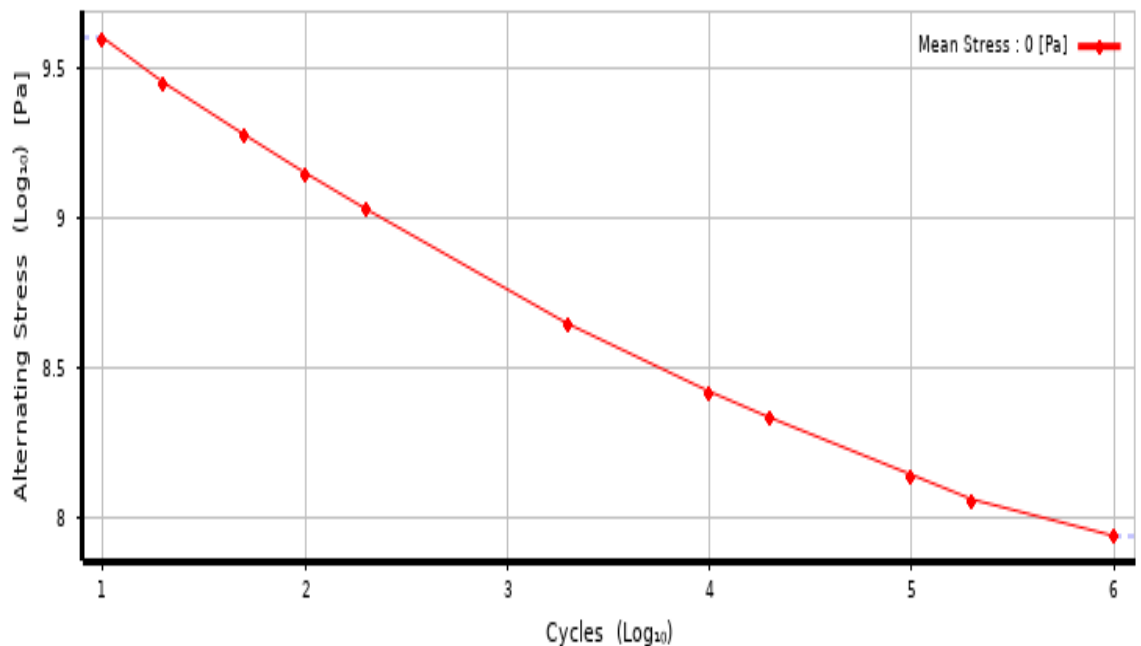


Figure 2. 6 The Stress-Life (S-N) Curve draw to logarithmic plot

2.7.4 Loading Type

A. Constant Amplitude, Proportional Loading

Constant amplitude, proportionate loading is the basic "back of the envelope" calculation that describes whether the load has a set maximum value or fluctuates over time. The loading has constant amplitude because only one set of FE stress measurements and a loading ratio are required to determine the alternating and mean values. The loading ratio (LR) is defined as the ratio of second load to first load ($LR = L2 / L1$). The two most frequent types of constant amplitude loading are fully reversed (add a load, then apply an equal and opposite load; a load ratio of -1) and zero-based (provide a weight, then remove it; a load ratio of 0). Due to the proportionality of loads, a single set of FE measurements can detect critical fatigue. [31].

B. Constant Amplitude, Non-Proportional Loading

Constant Amplitude, non-proportional loading investigates two load instances that are not linked by a scaling factor. The loading is of constant amplitude but non-proportional since the principal stress or strain axes are allowed to fluctuate between the two load sets. There is no need to keep track of the cycles. However, due to the non-proportional loading, the critical fatigue position may occur in a spatial location that is difficult to identify by observing either of the base loading stress states [31].

C. Non-Constant Amplitude, Proportional Loading

A single set of FE findings is also required for non-constant amplitude, proportional loading. The load ratio, however, varies throughout time rather than employing a single load ratio to calculate alternate and mean values. Consider this as combining a FE analysis with strain-gauge data acquired over a specified time interval. Because loading is proportionate, a single set of FE findings can be used to determine the critical fatigue position. However, the fatigue loading that causes the most damage is not clearly visible. Cumulative damage (including cycle counting such as Rain-flow and damage summation such as Miner's rule) must be conducted to determine the total amount of fatigue damage and which cycle combinations cause that damage. Cycle counting is a technique for

breaking down a complex load history into a series of occurrences that can then be compared to accessible constant amplitude test data. [31].

D. Non Constant Amplitude, Non Proportional Loading

The most general example is non-constant amplitude, non-proportional loading, which is identical to constant amplitude, non-proportional loading except that there are more than two different stress situations involved in this loading class that have no relation to one another. The spatial location of critical fatigue life, as well as the combination of loads that causes the most damage, are unknown. The ANSYS Fatigue Module does not yet support this type of fatigue loading.

2.8 Parameters that Affect Fatigue Strength

The fatigue strength of concrete is affected by several parameters in compression loading. Most experiments conducted on fatigue and try to find the relation between fatigue strength and the effects of different loading condition. Among the influencing factors are those discussed in detail below: -

a) Stress Gradient

The first are the applied cycles' maximum and minimum stress levels. The failure cycle grows in lockstep with the increase in S_{min} . To determine the S-N curve, different specimens must be tested at each level of S_{max} . The fatigue strength is unaffected by cement content, water-to-cement ratio, concrete age, or curing conditions [23].

Second, at high stress levels S_{max} , fatigue strength became more sensitive to time-dependent effects. According to the authors, 80% of static strength did not demonstrate a significant variation in the effect of the number of stress cycles to failure with time. Time-dependent effects were taken into consideration for the calculation over 80% of static strength.

b) Rest Periods, Effects of Stress Rate and Loading Frequencies

Atypical loading sequences, periods without loading, and static loading at low-stress levels all increase concrete fatigue life. Rest intervals of up to 5 minutes can improve

fatigue life; however, rest intervals of more than 5 minutes do not appear to improve fatigue life. Ameen et al. [23] provide evidence that the duration of a rest period must be dependent on when it occurs in the loading history and the loading levels it is working with.

Furthermore, one of the elements influencing fatigue strength in tests is the frequency of loading. According to some researchers, the number of cycles to failure increases as the frequency of repetition increases under steady stress. However, the frequency range is from 1 to 15 HZ and $S_{max} < 0.75$ do not affect the fatigue life of the concrete.

c) Lateral Confining Pressure

Lower stress levels are suggested to benefit from lateral pressure on tiredness. This is especially true for stressed-out individuals. The relationship between mean stress S_m , stress range R , and fatigue life N is depicted in Figure 2.7. According to P. Ameen, [23] the beneficial effect of lateral confining pressure on fatigue performance is typically lost when the specimen has been loaded more than 50 times at any ratio of lateral stress to longitudinal stress compared to static biaxial strength.

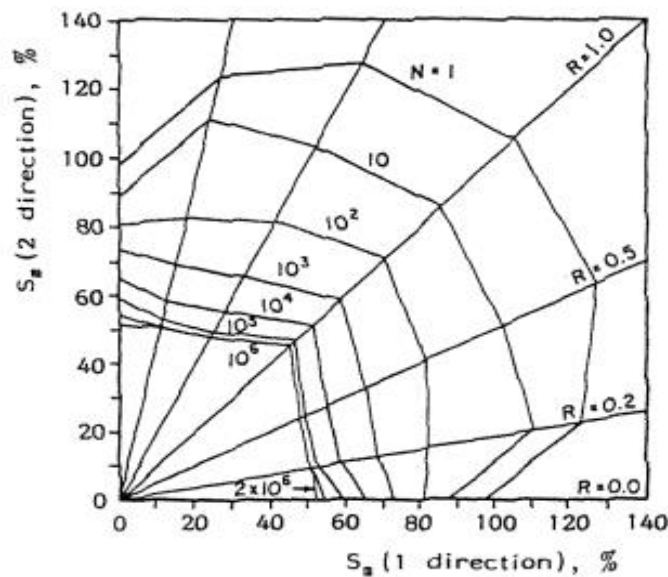


Figure 2. 7 Horizontal fatigue life under biaxial Loading [23]

2.9 Fatigue Life Assessment of Complex Based on Strain Time Histories

The nominal stress method is used for the evaluation of remaining fatigue life in most design and evaluation codes around the world, including Eurocode, AASHTO, and AREMA manuals. Based on the plastic strength of materials theory, nominal stresses should be calculated adjacent to potential crack locations, excluding stress concentration effects. Additionally, strain time histories derived from field tests or finite element models can be used to estimate nominal stresses. Alternative analysis techniques, such as fracture mechanics models, energy-based models, the local notch stress approach, and the hot-spot stress method are also suggested for predicting the fatigue life of railway bridge.

A. Uniaxial Fatigue Evaluation

Field strain measurements, according to AASHTO's bridge evaluation guideline, are the most accurate approach to evaluate effective stress ranges at fatigue-prone details. Three key elements influence the fatigue life of a pre-stressed railway bridge. These are the number of loading cycles applied to a detail or member, the range of these cycles, and the detail type. Standard structural details are classified based on their projected fatigue life. S-N curves for each category relate the number of cycles to failure at various stress levels [27], [32]. Fatigue curves for each detail are representative of experimental tests and take geometry-induced local stress concentrations, weld defects with constant, normal fabrication standards, and high residual stresses into account. The stated curves are represented by log log scale and are expressed as:-

$$N = AS^{-m} S_r^m \dots\dots\dots (2.6)$$

Where,

N = Number of stress cycle to failure;

A= Category Constant;

Sr= Nominal stress range at fatigue detail and

M=Slope assumed to be 3 in AASHTO.

B. Multi Axial Fatigue Evaluation

Multiracial or multi-axial is the general term for loading and geometry conditions in addition to loading, which causes complex stress and strain as they are heterogeneous and vary with time. The concept of multi-axial loading study was started since 1950s and the first fatigue estimation subjected to the kind load were published. This study mainly focused for high cycle fatigue materials or for materials with negligible plastic strain..

2.10 Structural Model for Fatigue Stress Analysis of Railway Bridge

The pre-stressed concrete railway bridge model was imported from AutoCAD to Ansys or other appropriate commercial software. The FEM Ansys software is a mathematical modeling technique involving discretization performed by applying static structural analysis. The static structural analysis is used to include the effects of static analysis and is also used to determine the stress and fatigue failure response under the design and operational live loads. The finite element is generated by the space claim or design modular obtained from the CAD drawing in the IGES file extension. Bridge members usually react to service stress far below design critical stress by way of elastic deformation. Fatigue crack in a bridge appear at the connection and girder of the bridge. Therefore, the bridge connection and girder sections shall be the main parts of the fatigue analysis for bridge. The crack initiation and growth should be modeled properly modeled and coupled in to the structural model of the bridge [33].

2.11 Fatigue Analysis of Railway Bridge

Bridge members typically respond to service stress much below the design critical stress through elastic deformation. Local failures, usually brittle, can nevertheless occur in the presence of notches or other sort of geometric discontinuity, such as holes, grooves, and welded connections, when stresses are locally raised. Bridge-deck sections are built by welding, riveting, or other means several plates, beams, and bars together. Bridge fatigue cracks are particularly common at connection points. As a result, the bridge deck section should be one of the primary components of a bridge's fatigue analysis [33].

Bridge fatigue is a high-cycle fatigue problem in which stress variations are mild, allowing the structure to flex elastically except at notches and welds where local stresses are concentrated. Crack initiation and growth in the area of welds should be accurately represented and connected into the structural model of a bridge-deck section for appropriate measurement of fatigue stress. In Ethiopia, few studies have been done on the railway area. Especially, when it comes to the fatigue life of pre-stressed railway bridges due to cyclic loads, there has been no research conducted in the area of pre-stressed concrete railway bridges. Therefore, this study is used to start on the pre-stressed concrete railroad bridge.

Finally, in this thesis, the researcher identifies the fatigue life of a railway bridge in ANSYS 2020 and validates it with experimental results obtained from Rikard. The main purposes here are estimating fatigue life and recommending maintenance for the remaining life. As the railway transport sector, ERC shall give priority for maintenance based on its remaining fatigue life.

CHAPTER THREE RESEARCH METHODOLOGY

3.1 Introduction

This thesis investigates the remaining fatigue life of a girder railway bridge using finite element Ansys workbench 2020, Modelling of pre-stressed concrete railway bridge geometries and validation of A9 type pre-stressed concrete sleeper for the AA-LRT.

The study area considered is an existing common pre-stressed concrete box girder railway bridge on E-W (from Ayat to Torhayloch) and N-S (from Kality to Menelik II) of the LRT route. This railway bridge is slab track or non balasted with block concrete sleeper on a slab track of the deck girder. This case study was limited to an elevated, simply supported box girder concrete bridge with spanlength of 25 m and a width of 4.5 m. This pre-stressed concrete railway bridge is selected to determine fatigue failure due to the repetition of cyclic load. Measuring the crack failure of the bridge during inspection can be taken as an input for verifying the finite element model prepared in Ansys can determine the failure that represents the actual design life or not.

3.2 Research Methodology

In this thesis work, a static analysis of the Addis Ababa Light Rail Transit railway bridge is performed using a numerical methodology, based on the moving loads model.

To assess the fatigue life of the pre-stressed concrete railway bridge, the load or stress state should be determined. The loads used for checking fatigue life are the design and operational loads. The operational load value is taken from Addis Ababa-Djibouti and AA-LRT data. The structure of the pre-stressed concrete railway bridge is loaded with applied load of 165 kN. This maximum load is applied repeatedly /cyclic to the railway bridge structure gradually with loading step of 500 N to investigate the the fatigue life and remaining life of the structure. This mechanism or the load step helps to avoid inertia effect and the damage on the structure. If the maximum load is applied once on the structure it will damage. Therefore, the load is applied in load step to avoid such sudden failure of the structure. To account for the scenario the loading type is considered as fully reversed cyclic loading in the Ansys simulation Software as shown in the figure below. For this case study a pre-stressed concrete railway bridge with maximum span length is

selected because the bridges were expected to carry more cyclic loads. In addition, if the maximum span is designed so that the minimum span is safe. The deflection obtained from Ansys can be used as one of the permit loads or the number of cycles that passes through the pre-stressed concrete sleeper is used as an input to verify the finite element model prepared in Ansys Workbench 2020 represents the actual life of the pre-stressed railway bridge. The selected railway bridge is modeled using the finite element analysis (FEA) Ansys simulation software package. Finally, the estimation of the fatigue life and determination of the deformation and Equivalent Stress is performed for the section of the railway bridge by considering cyclic load applied obtained from the maximum operational load. This cyclic load is applied as shown in the Figure 3.1 below.

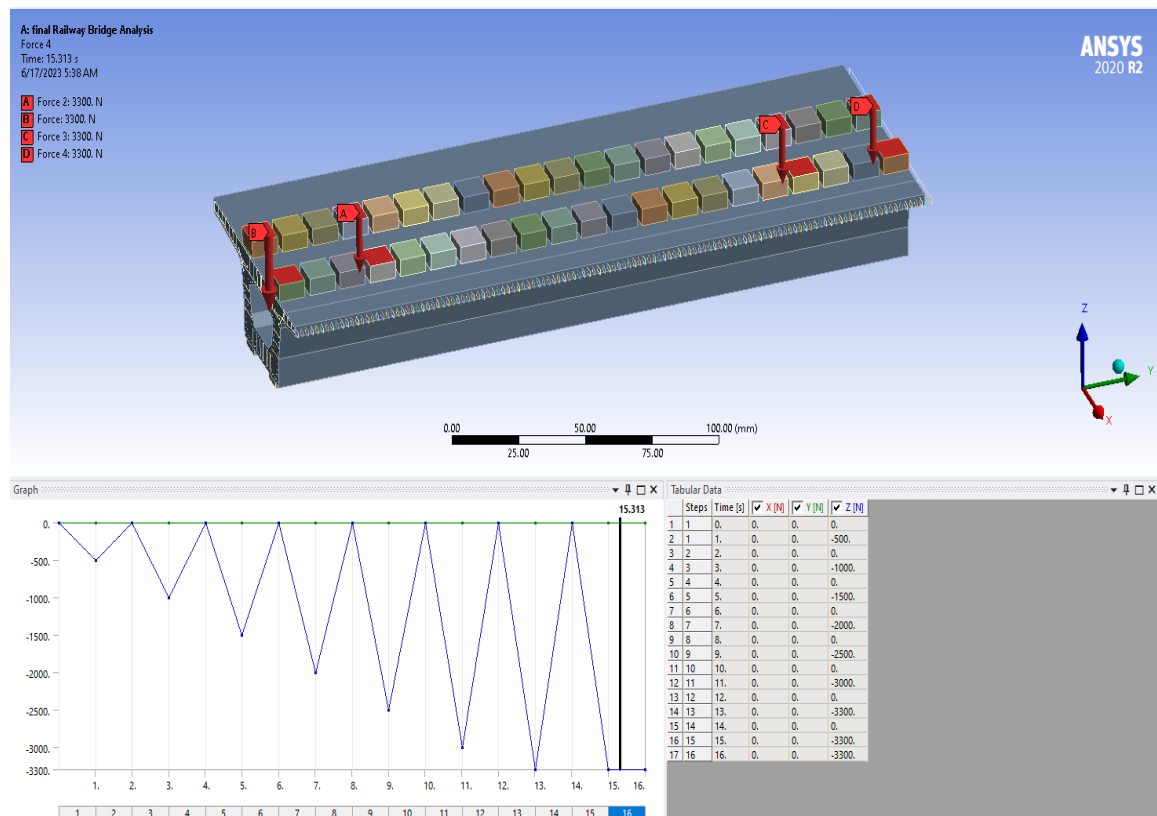


Figure 3. 1 Fully reversed cyclic load (loading and unloading) applied on the bridge

The detailed information, like cross section dimensions, material properties, design data, and as-built drawings of the railway bridge is taken from Ethiopian Railway Corporation. The numerical result is used to determine and check the bridge performance under cyclic load using the design live load and operational live load (maximum live load) with the

proposed Cooper E 80 load model adopted from the Chinese standard. The railway bridge of this study is modeled using 3-D AutoCAD and then simulated using ANSYS 2020 commercial software's finite element analysis to determine deflection and estimate the fatigue life. The following procedures are followed to estimate the remaining fatigue life of a pre-stressed concrete box girder railway bridge.

1. Reviewing different literatures, journals on fatigue life of pre-stressed concrete railway bridges, material properties, and crack initiation, propagation, and damage under high repetition loads.
2. Relevant data is collected from concerned staff members of the railway project. Ethiopian Railway Corporation (ERC), Chinese Standard, AREMA, and from acknowledged publications. During this stage, two types of data were gathered.
 - a. The primary data, like field inspection and reading documents on test results on the selected bridge like railway bridges design specifications, cross section and material property.
 - b. Site visits are conducted to inspect the different conditions of a pre-stressed railway bridge.
3. Static structural analysis and modeling using Ansys 2020 software is conducted to study the stress and deformation of the box girder railway bridge.
4. Validation of the material models used in modelling the railway bridge in the Ansys software by known experimental test results of a pre-stressed sleeper in finite element model and identify the response of load versus load deformation.
5. The load application of the railway bridge is as per the Chinese Standard specification design manual, and finally recommendations and conclusions based on data analysis and remaining fatigue life are analyzed based on the output of the Ansys software. The detailed methodology flow chart steps were shown in the Figure 3.2 below.

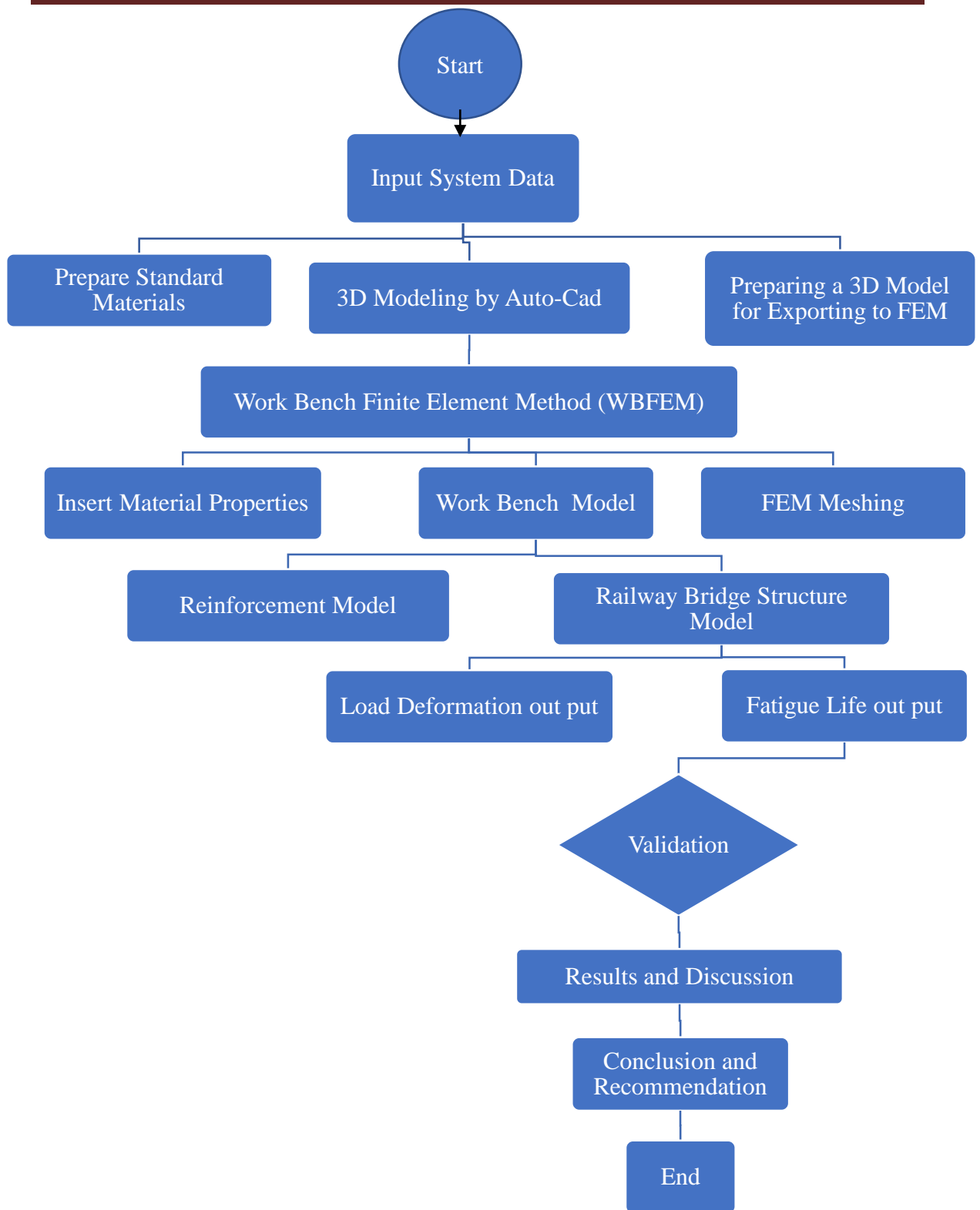


Figure 3. 2 Flow chart of the work

Table 3. 1 General Information of pre-stressed concrete railway bridge model from ERC.

Bridge Name	Addis Ababa Light Rail Transit ETAA400-S-GJ-400-QJQC2-15
Bridge Type	Simply Supported PCBGRB
Year of Construction	August 2015
Length X	90 mm
Width Y	250 mm double track
Length Z	31.6 mm
Volume	$2.895 \text{ e}^5 \text{ mm}^3$
Mass	$7.2377 \text{ e}^{-004} \text{ t}$
Centroid X	-45 mm
Centroid Y	125. mm
Centroid Z	15.8 mm
Support type	Steel bearings

(Source: Ethiopian Railway Corporation, Drawing and Technical Specification) [35]

3.3 Simplifications/Assumptions

In the modeling of the pre-stressed concrete railway bridge the following assumptions are adopted. These are:-

- i. Linear behavior of the pre-stressed concrete railroad bridge.
- ii. When considering a pre-stressed concrete box girder railway bridge, the bridge structure behaves as a linear system adequate as the bridge are expected to suffer minor elastic deformations and geometric non linear is absent.
- iii. The Railway bridge is considered as elastic. In this study, conventional static value of modulus of elasticity is employed.
- iv. The slab ballast and rails contribute only mass for for design and operational load but no contribution on the stiffness.

3.4 Finite Element Modelling

The FEM is used to determine an approximated solution for structures or other field variables which are difficult to obtain analytically. Models were established using the finite element package Ansys 2020 workbench, which is being used to simulate the behavior and response of railway bridge in terms of deflections, stresses, crack pattern, and fatigue.

Generally, the finite element analysis was carried out in the following ways;

- Validation of the Finite Element results with previously conducted experimental tests
- Modeling of a 3-Dimension pre-stressed concrete girder railway bridge with detailed features as obtained from Ethiopian Railway Corporation (ERC) As-built drawing.
- Determination of design and operational load or taken from the center
- Static structural analysis is used to study the response of railway bridge to the applied loading (Fatigue life, damage, deflections, strains and crack pattern, etc.).

In this research, a stress life type based on S-N curves (stress-cycle curves) is selected for the checking of fatigue analysis. Stress life is concerned with total life and does not distinguish between initiation and propagation.

3.5 Validation and Modelling of Railway Bridge

This section deals about the methods for the determination of the fatigue life of pre-stressed concrete railway bridges. The technique used in this research combines field inspection, data from the Ethiopian Railway Corporation (ERC), and 3-D non linear finite element analysis using Ansys 2020 commercial software package.

3.5.1 Validation and Railway Bridge Modelling

Validation is the process of ensuring that the simulation model represents reality. The finite element package Ansys 2020 is used in the present work for non-linear analysis of pre-stressed railway bridge simulation. Different methods of analysis, from simply forwarding to more complicated finite element analysis procedures like Ansys software,

are implemented. Because experimental work is both expensive and time-consuming, it is critical to apply advanced mathematical answers and methodologies for the virtual analysis of vast and complicated elements or structures. As a result, finite element analysis (FEA) has become a very valuable method in recent years for numerically answering complex stress concerns utilizing FEA software.

The experimental data on a full-scale pre-stressed sleeper model subjected to incremental cyclic loads versus vertical deformation was compared with a finite element model or analytical estimate, and thus the program was evaluated behavior sleeper under the horizontally repeated loads. To address this, a pre-stressed concrete sleeper verification example was presented in this sub-topic to verify the analysis results of the Ansys software. In the analysis of a pre-stressed concrete sleeper results obtained from Ansys have been verified against the results of experimental physical testing data of pre-stressed concrete sleepers carried out by Rikard [36].

3.5.1.1 Validation Data

The geometric detail of a pre-stressed sleeper is 2,535 mm by 280 mm by 222 mm in length, width, and height, respectively. The materials used for the casting of sleepers are coarse aggregate, fine aggregate (sand), 52-grade cement, and strand wire. The model was composed of a concrete body, pre-stressing wires, and four fixed supports as shown in Figure 3.4 below [36].

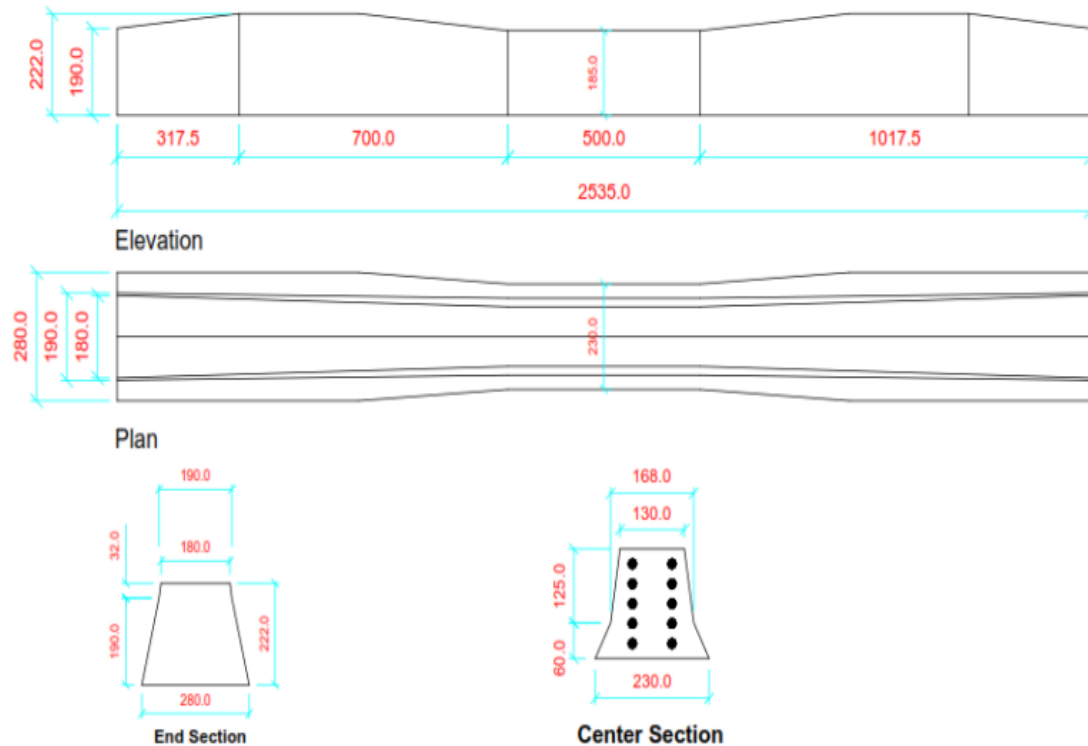


Figure 3. 4 Pre-stressed concrete sleeper [36]

3.5.1.2 Concrete and Pre-stressing Wires Materials

The pre-stressed sleeper has used the following typical concrete material as input data. The strength of concrete used in the validation of the sleeper was 52 MPa and the pre-stressed tendons have a diameter of 7 mm. Table 3.2 and Table 3.3 shows the detail properties aconcrete and tendon respectively.

Table 3. 2 Pre-stressed concrete material properties

Material Property of Concrete	Value
Density (kg /m ³)	2,400
Fc, cube (MPa)	67
Young of Elasticity Ec (MPa)	34,400
Poisson's Ratio (<i>νc</i>)	0.2
Comprehensive Strength, σ_{cc} (MPa)	52
Tensile Strength, σ_{ct} (MPa)	2.85
Fracture Energy G_F (N/m)	154

Table 3. 3 Typical property of pre-stressing wire material properties

Property	Value
Diameter Ø (mm)	7
Density (g /cm ³)	7.8
Young’s Modulus (GPa)	200
Poisson’s Ratio (μ)	0.3
Thermal Expansion (°c /)	1.1*10 ⁻⁵
Tensile strength (MPa)	1750
Tangent modulus, Est (MPa)	20,000
Initial strain, ε ₀ (mm/m)	5

The overall dimension and structural configuration can be seen in Figure 3.5 below.

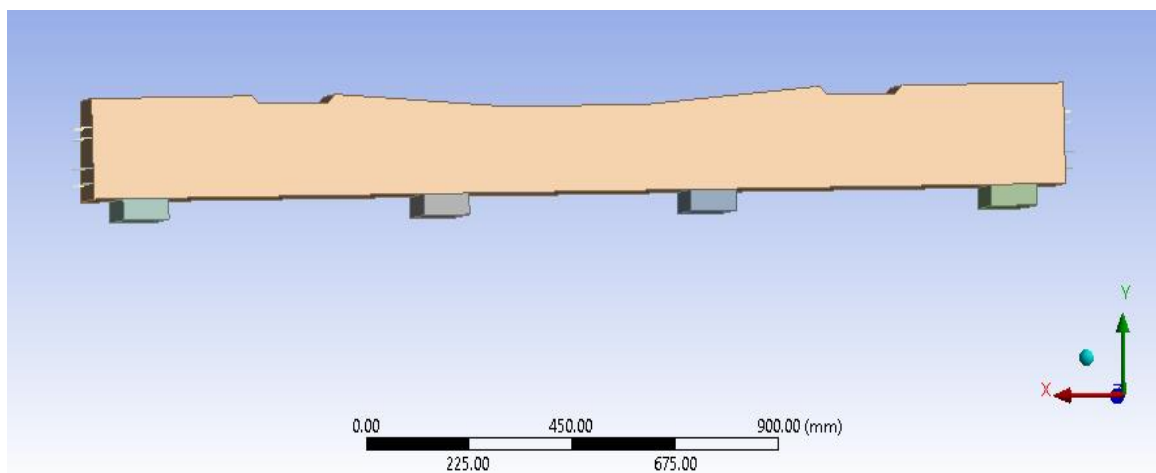


Figure 3. 5 Dimensions and reinforcement detail of PCS used for validation [36]

3.5.1.3 Static Full-Scale Test Done by Rikard

Firstly, a static pre-stressed model fixed support condition at four locations is modeled, analyzed, and compared with Rikard. The static test is performed using a hydrolic jack, which means the displacement at the rail seat increases at constant rate. A research study conducted by Rikard for a simple pre-stressed sleeper model is used for verification, as shown in Figure 3.6 below [36].

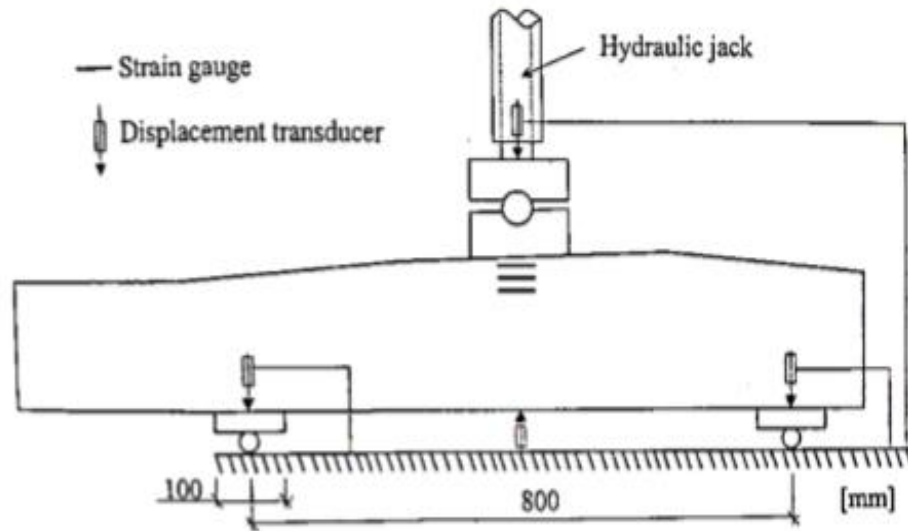


Figure 3. 6 Test set-up used in the test done by Rikard, 2000 [36]

According to the above Figure 3.6, the sleeper model has been supported. A sleeper type of A9P, which is manufactured by Abetong Teknik AB, was taken as symmetric as it has the same geometry and produces the same deflection and stress. According to Rikard, the pre-stressed sleeper was loaded with an applied rail seat load of 0 to 237.5 kN. In this case, the sleeper was first modeled with simple static structural equations and then compared with Rikard's results. A fixed support condition at four locations was considered for this cause, as shown in Figure 3.7 below.

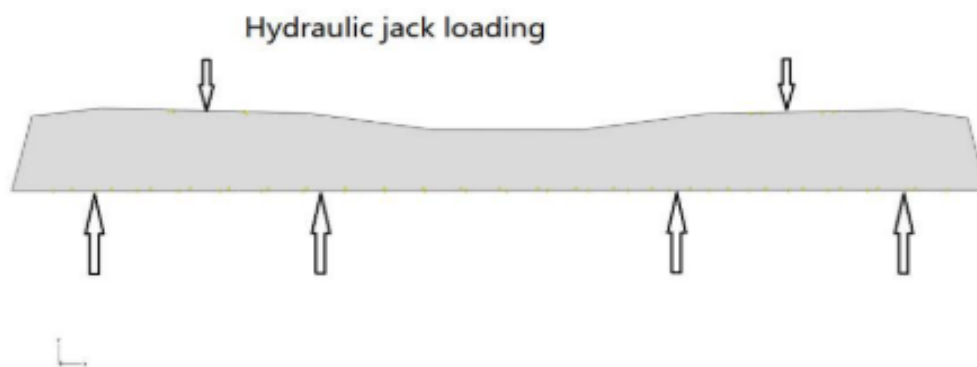


Figure 3. 7 Static structural model with fixed support condition [36]

3.5.2 Pre-stressed Sleeper Modelling and Validation

3.5.2.1 Modeling Elements Types

There are three common methods for finite element analysis of externally pre-stressed concrete railway bridges. These are 2-D plane beam element method, 3-D beam element method and 3-D solid element method.

When the 3-D beam element method is used, the concrete girder is simulated by a 3-D beam element with two nodes and six degrees of freedom at each node (translations in the nodal x, y, and z directions and rotations about the nodal x, y, and z axis), and the externally pre-stressed tendon is simulated by a 3-D spar element, which is a uniaxial tension-compression element with three degrees of freedom (translations in the nodal x, y and z directions). Node coupling of spar elements and beam elements is processed at the location where concrete and tendons are connected, and displacement in translations in the nodal x, y, and z directions is interactively limited. Although the 3-D plane element method can be used to calculate coupled bending and torsional effects, errors may occur for wide girders because of the plane section hypothesis. Furthermore, beam elements are unable to count in transversal mechanical effect; this is because girder section is simplified as a point [37].

When using the 3-D solid element method, the concrete girder is simulated using tetrahedral or hexahedral solid elements, with each node having three degrees of freedom (translations in the nodal x, y, and z directions). The externally pre-stressed tendon is simulated using a 3-D spar element, similar to the 3-D beam element method. Node coupling of spar elements and solid elements is processed at the location where concrete and tendons are connected, and displacement in translations in the nodal x, y, and z directions is interactively limited. Any random structure, such as curved, skew, or super wide bridges, can be accurately simulated using the 3-D solid element method. It can also be used to accurately simulate anchorage positions, pre-stressing deviating positions, and pre-stressing space effects. In addition, local stress at any random position could be analyzed by the 3-D solid method as well. Calculation precision is related to the element meshing plan, the smaller the element size, the bigger the data scale, and the longer the time it takes [37].

3.5.2.1.1 Solid 65

The concrete part of the pre-stressed railway bridges is modeled using a three-dimensional solid element, SOLID 65. This element is for 3-D modeling with and without reinforcement (rebar). The solid part of the railway bridge can crack in tension and crush in compression. In concrete applications, for example, the element's solid capacity is used to represent the concrete, while the reinforcement capacity can be utilized to model reinforcing behavior. The element is defined by eight nodes, each of which has three degrees of freedom: Translations in the nodal x, y, and z directions. It is possible to declare up to three different rebar requirements. The concrete element is analogous to a 3-D structural solid, but it also has particular cracking and crushing properties. Handling is the most significant feature of this element. The important aspect of this element is the treatment of nonlinear material properties. It is capable of simulating concrete cracking (in three orthogonal directions), crushing, plastic deformation, creep, and also capable of simulating reinforcement steel bar tension, compression, plastic deformation, and creep, but not shear performance [37].

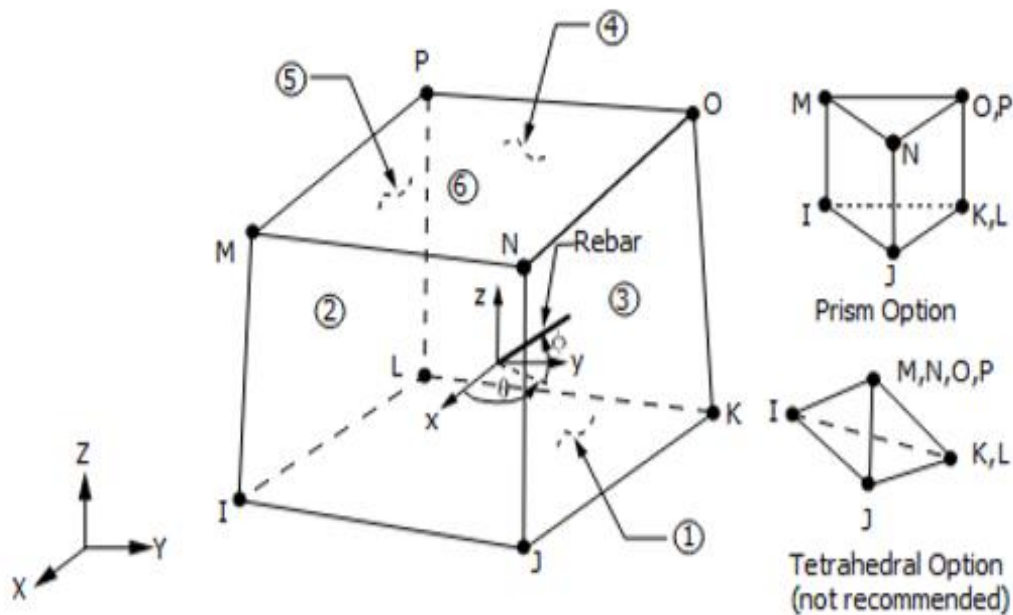


Figure 3. 8 SOLID 65 Geometry [37]

3.5.2.1.2 LINK 180

LINK 180 is a 3-D spar (truss) that is useful in a range of engineering applications for modeling pre-stressed tendons. The element can be used to simulate trusses, sagging cables, linkages, springs, and other structures. At each node, the link element has three degrees of freedom of translation in the nodal x, y, and z directions with uniaxial tension compression. There are tension-only (cable) and compression-only (gap) alternatives available. No bending of the element is considered, as in a pin-jointed structure. Plasticity, creep, rotation, significant deflection, and large strain are all supported. Users must enter "real constants" into LINK 180 to define reinforcement geometry, material behavior, and pre-stressing strain. However, the assumption of perfect bonding between concrete and pre-stressing wires must be made. One advantage of using LINK 180 is that the element's initial strain can be specified. This can be used to calculate the initial pre-stressing force as shown in section 3.7. LINK 180 also supports changing the cross-sectional area as a function of axial elongation. The cross-sectional area is changed by default so that the volume of the element is preserved even after deformation. The default setting is appropriate for elasto-plastic applications. LINK 180 is available in compression, tension compression only and tension only configurations.

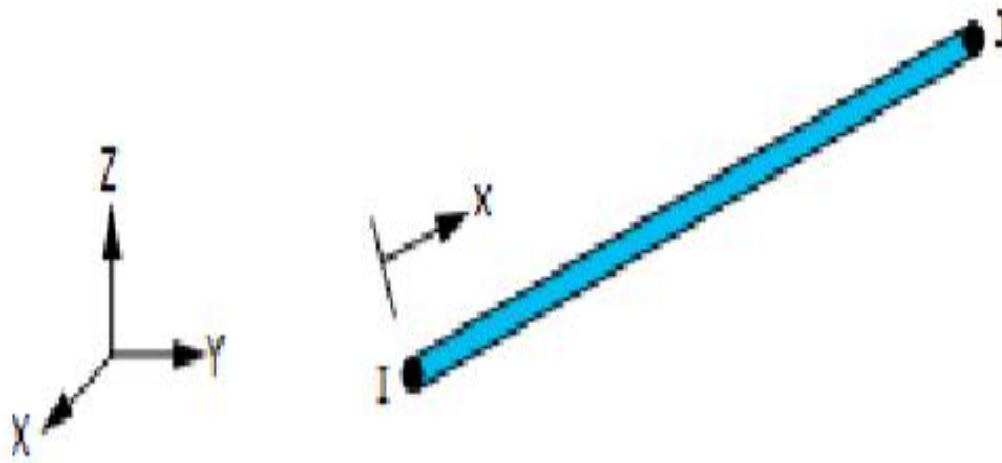


Figure 3. 9 LINK 180 Geometry

3.5.2.2 Static Modeling of Pre-stressed Sleeper

This section discusses a sleeper finite element model. The model is built with the ANSYS 2020 work bench, which is used to model and simulate a sleeper's response. In this thesis, concrete is modeled or represented as a 3-D solid element, Solid 65, and pre-stressed tendon as truss embedded element, LINK 180, with an initial pre-strain of 5 mm/m. Bond slip between concrete and reinforcement is not taken into account. The sleeper's cross section is simplified to be rectangular. The non-linear material inputs were discussed in previous sections.

The pre-stressed sleeper are modeled as a solid part and the tendon wires are embedded in concrete sleeper as mesh parts. The section properties of concrete and tendon wire are assigned according to the experimental test result. According to the Rikard study, the pre-stressed sleeper was loaded with an applied rail seat load of 0 to 237.5 kN. In this case, the sleeper was first modeled with simple static structural and then compared with Rikard's results [36].

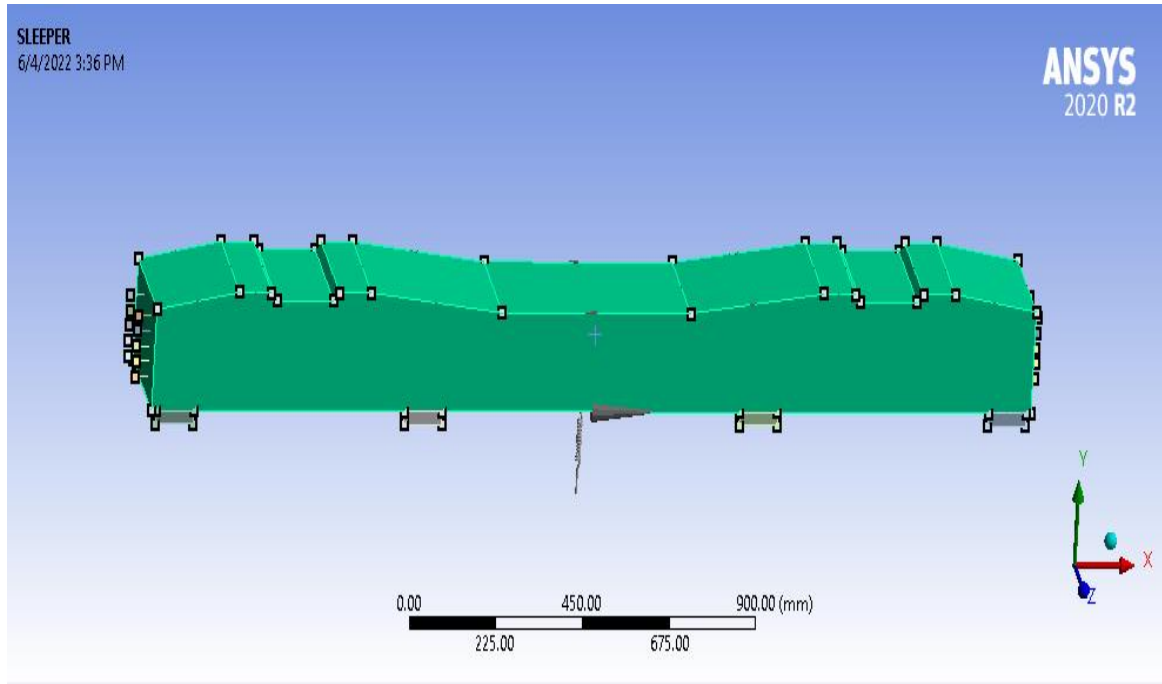


Figure 3. 10 Concrete body and pre-stressing wire with four supports

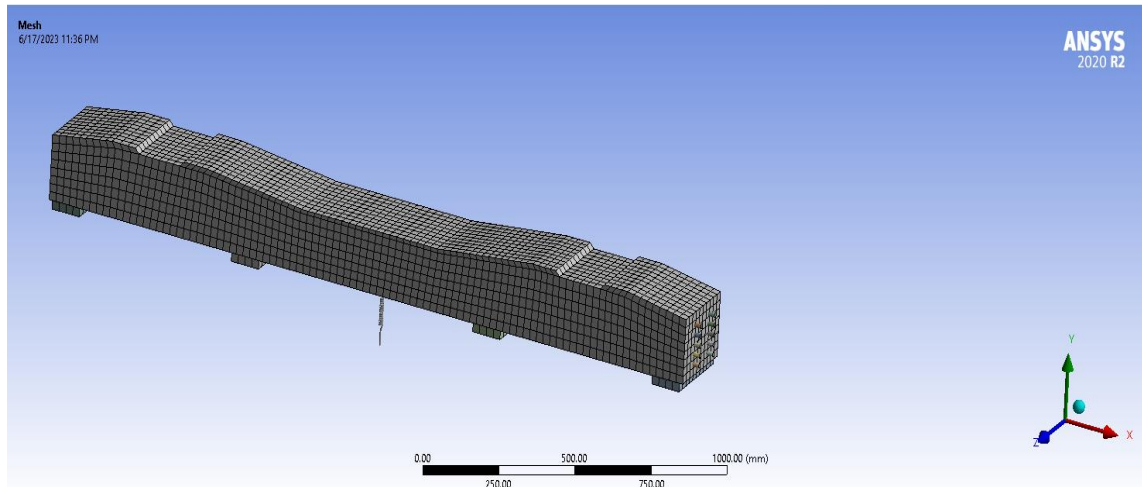


Figure 3. 11 Meshed sleeper model with the location of the area

Table 3.4 Total number of Nodes and Elements for the pre-stressed sleeper.

Mesh Size Statics		
Material Type	Nodes	Element
Concrete Sleeper	5,316	950
Impactor	432	40
Pre-stressed tendon	970	480
Total Number of Nodes and Elements	6,718	1,470

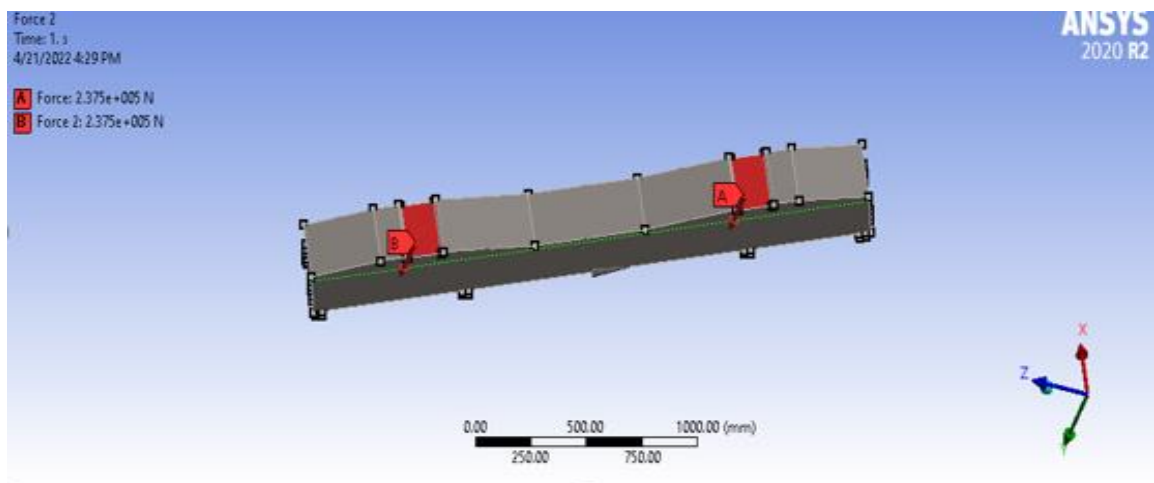


Figure 3. 12 Applied load on the sleeper

3.5.2.3 Numerical Results

The structural response in the experimental tests and the software analysis results were compared to validate the FE model. The finite element method is employed to analyze the load-vertical displacement relationship and is used to investigate the structural response of the concrete sleeper. The concrete was modeled as an elasto-plastic material in this FEM model but as an elasto-plastic and brittle cracking material in Rikard's model. The Ansys 2020 software package is used to perform the numerical analysis. Figure 3.13 depicts the stress-strain relationship of Rikard's concrete [36].

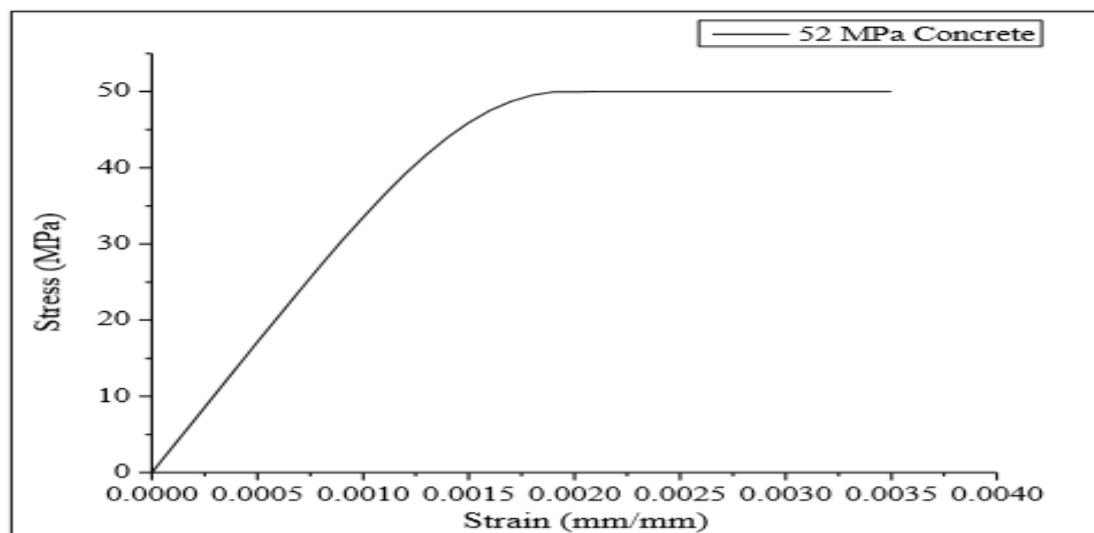


Figure 3. 13 Compressive stress-strain graph for 52 MPa concrete [36]

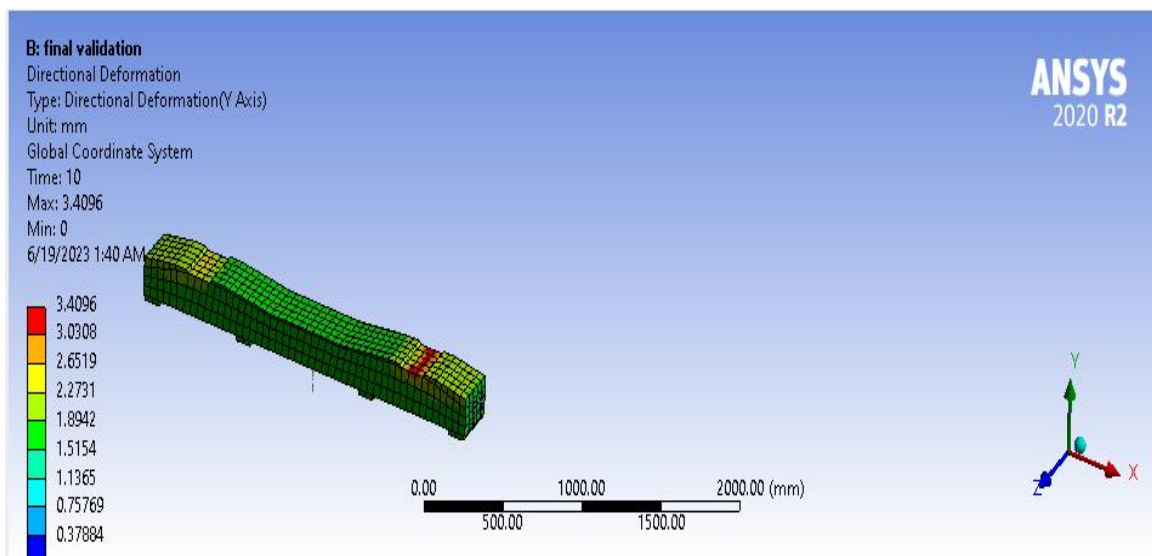


Figure 3. 14 Sleeper Directional Deformation

The maximum directional deformation (y-axis) of the sleeper was obtained at 237.5 kN. The ANSYS software gave the deformation in Table 3.5 below, with the corresponding applied force varying from 0 to 237.5 kN. The force-deformation graph is shown in Figure 3.15.

Table 3. 5 Force Vs Deformation

Force	Deformation FEM	Deformation Experiment	Rd%
0	0	0	0.00
50	0.36	0.357	0.84
100	0.77	0.76	1.49
150	1.157	1.087	6.30
200	1.92	2.089	8.43
237.5	3.4096	3.740	9.52

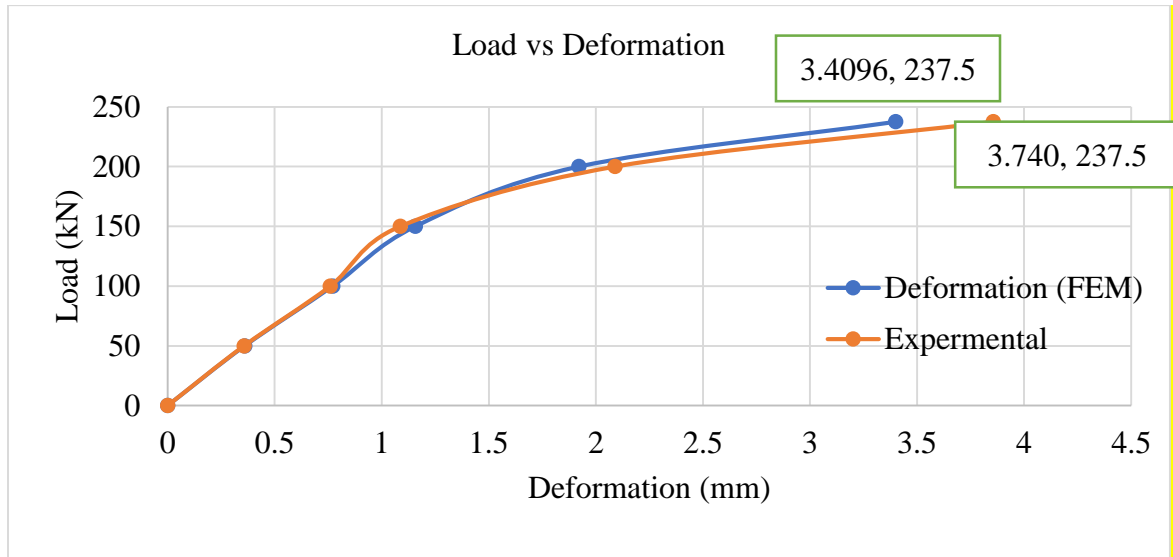


Figure 3. 15 Force vs Deformation graph with FEM results in blue and experimental test results in red color.

The load-deformation graph clearly shows that the force and deformation diagram matches the Rikard [36] model very well, indicating that the Finite Element results are high quality. As a result, now that the model has been validated in terms of laboratory

results, further modeling, and analysis using FEM for railway bridge with box girder type is discussed in the following sections of the report.

3.6 Numerical Modeling of Pre-stressed Railway Bridge

The 3-D finite element model Ansys work bench is used to model the selected railway bridge. The bridge is modeled from the data obtained from AA-LRT as built drawing. The concrete is simulated by a 3-D eight node solid element called SOLID 65. Later the output of the finite element is used in estimation of fatigue and validation of the railway bridge. As stated in above section an existing pre-stressed concrete railway bridge is used as a case study to demonstrate how to implement Finite element simulation in fatigue analysis of the railway bridge. The coordinate system employed in the software model are: -

- X-axis in lateral direction
- Y-axis in the longitudinal direction
- Z-axis in the vertical direction as convention

The study results from the above-mentioned program output have been validated on selected pre-stressed concrete sleepers with known length as indicated in section 3.5.1.1 and the remaining life curve in the logarithmic scale shall be identified or compared accordingly. In cases where significant differences are shown between the software output and the actual site condition, differences shall be considered as a deviation of the trial method from the software representation.

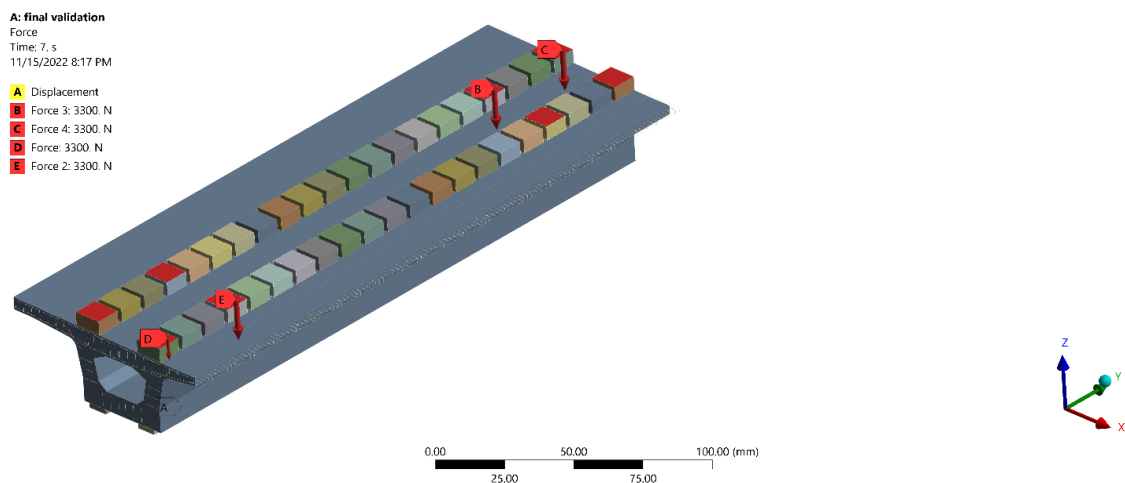


Figure 3. 16 Existing Railway Bridge Cross Section

3.6.1 Railway Bridge Cross-Section

The vertical loads or axle loads are subject to a cyclic load and the bending moment are dependent upon the stiffness of the bridge and its cross dimension. The performance of a pre-stressed railway bridge to endure the combined load (lateral and longitudinal loading) depends on the bridge size, shape and geometry and weight. The railway bridge used for modeling is the pre-stressed concrete railway bridge with a double track box girder used for passengers built in 2015, which is currently in use on the AA-LRT lines. In this thesis, the design track load and operational live load that was used are expressed in terms of force as per China's standard. This operational live load is being applied in the railway bridge model.

The AA-LRT physical properties as listed in Table 3.6 below and the pre-stressed concrete box girder railway bridge is used for modeling. Ansys and space claim software is used to analyze the data collected at AA-LRT. For simulation, the model was composed of a box girder with a length of 25 meters with a 50*50 cm sleeper and the spacing of reinforcement is specified in Appendix D figure D-13.

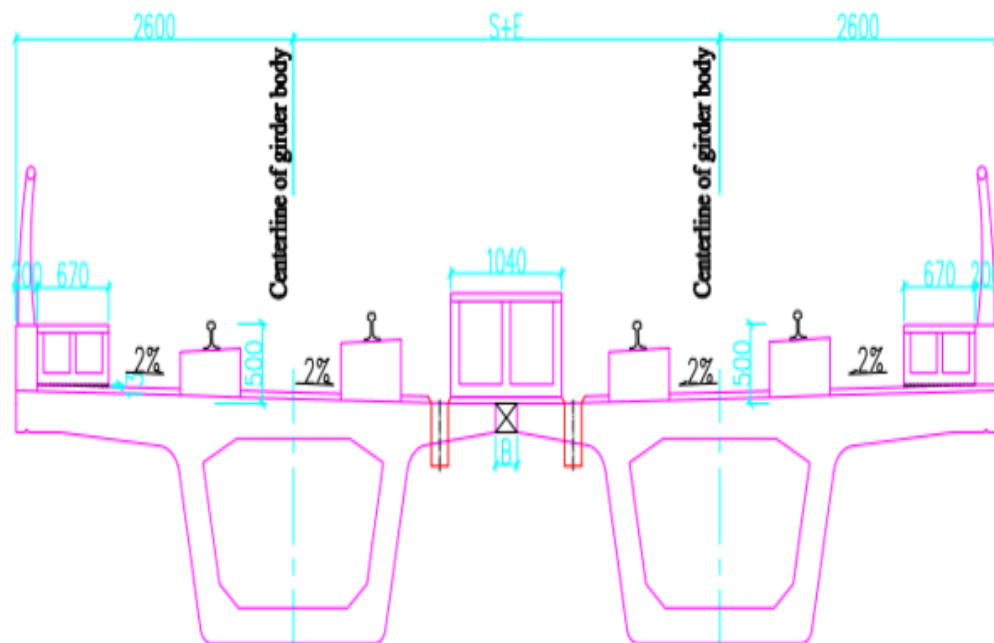


Figure 3. 17 Railway Bridge cross sectional dimensions model

3.6.2 Material Properties for the Pre-stressed Railway Bridge

To determine the crushing and cracking of railway bridges, critical parameters must be analyzed like maximum tensile stress and strain which can determine the crack propagation in static condition. The stress and strain are relevant property of materials and the material properties of concrete, reinforcement and pre-stress tendon for modeling of pre-stressed railway bridge is described in the Table 3.6 below. For this thesis the AA-LRT material property is used from the feasibility study. The concrete mixture used is designed by Ordinary Portland Cement with a comprehensive strength measured in cube of C-50 or 50 MPa as minimum strength at age of 28 days. This is equivalent to a comprehensive cylinder strength $f_{ck, cyl} = 40$ MPa. The materials which are commonly used for pre-stressing a railway bridge is the design strength for Ultimate Limit State for Concrete, Steel and pre-stressing Tendons are discussed below in detail. The material properties like Young's Modulus, Poisson's ratio and Mass Density, Strain, Tensile and Comprehensive strength are the required input in Ansys software. All other material properties can be specified but are not used in a static [38].

3.6.2.1 Concrete Characteristics

Concrete is strong in compression but weak in tension after the ultimate strength is reached. The stress-strain curve falls rapidly creating a very small area under the curve. Concrete with high strength is used in railway lines on the girder and bearing support to secure the deck slab, ballast, Girder and rail gauge, providing safe passage for the train vehicle.

Table 3. 6 Material properties of pre-stressed concrete railway bridge

Parameters	Values
Density (ρ_c)	2500 kg/m ³
Young's Modulus, (E_c)	29,725.41 MPa
Poisson ratio (ν_c)	0.2
Comprehensive Strength, (σ_{cc})	50 MPa
Tensile Strength, (σ_{ct})	2.85 MPa
Concrete strength at transfer (fck)	40 MPa

Parameters	Values
Strain Value	3%

- Stress limit for Pre-stressed concretes

$$F_{cd} = (0.85 * f_{ck}) / 1.5 = (0.85 * 40) / 1.5 = 22.66 \text{ MPa}$$

$$f_{ctd} = \frac{f_{ctk}}{\gamma_c}$$

$$f_{ctk} = 0.21 * f_{ck}^{2/3} = 0.21 * 40^{2/3} = 2.46 \text{ MPa}$$

$$f_{ctd} = \frac{f_{ctk}}{\gamma_c} = f_{ctd} = \frac{2.46}{1.5} = 1.64 \text{ MPa}$$

3.6.2.2 Pre-stressed Tendon

The prestressed tendon with high tensile wire and strands commonly used for pre-stressed concrete railway bridge have an acceptably low level of susceptibility to stress corrosion. The pre-stressing tendons are provided in structures for relaxation purposes. The actual value for modulus of elasticity, E_p can range from 195 to 210 GPa, as per the manufacturing process [39].

Table 3. 7 Material properties of pre-stressing tendon

Density steel (ρ_s)	7850 kg/m ³
Poissin's Ratio (ν_s)	0.3
Elastic Modulus (E_s)	210 GPa
Yield Strength	235 MPa
Tensile strength	455 MPa
Standard Strength (F_{pk})	1860 MPa
Yield Strength of tendon $f_{pi} = 0.75 f_{pk}$	1395 MPa
Pre-stresses steel Nominal diameter	15.2 mm
Elastic Modular of pre-stressed steel= E_p	$1.95 * 10^5$ MPa
Elongation	3.5%
Pre-stress Loss	12.2%
Nominal Cross-sectional area =A	139 mm ²

Pre-stressing Tendons, f_{pk} 1860 MPa

Yield Strength of Tendon, $f_{pi} = 0.75 * f_{pk} = 0.75 * 1860 = 1395$ MPa

Stress limit for Pre-stressing Tendons (F_{pe}): $F_{pe} = 0.82 * 1395 = 1143.9$ MPa

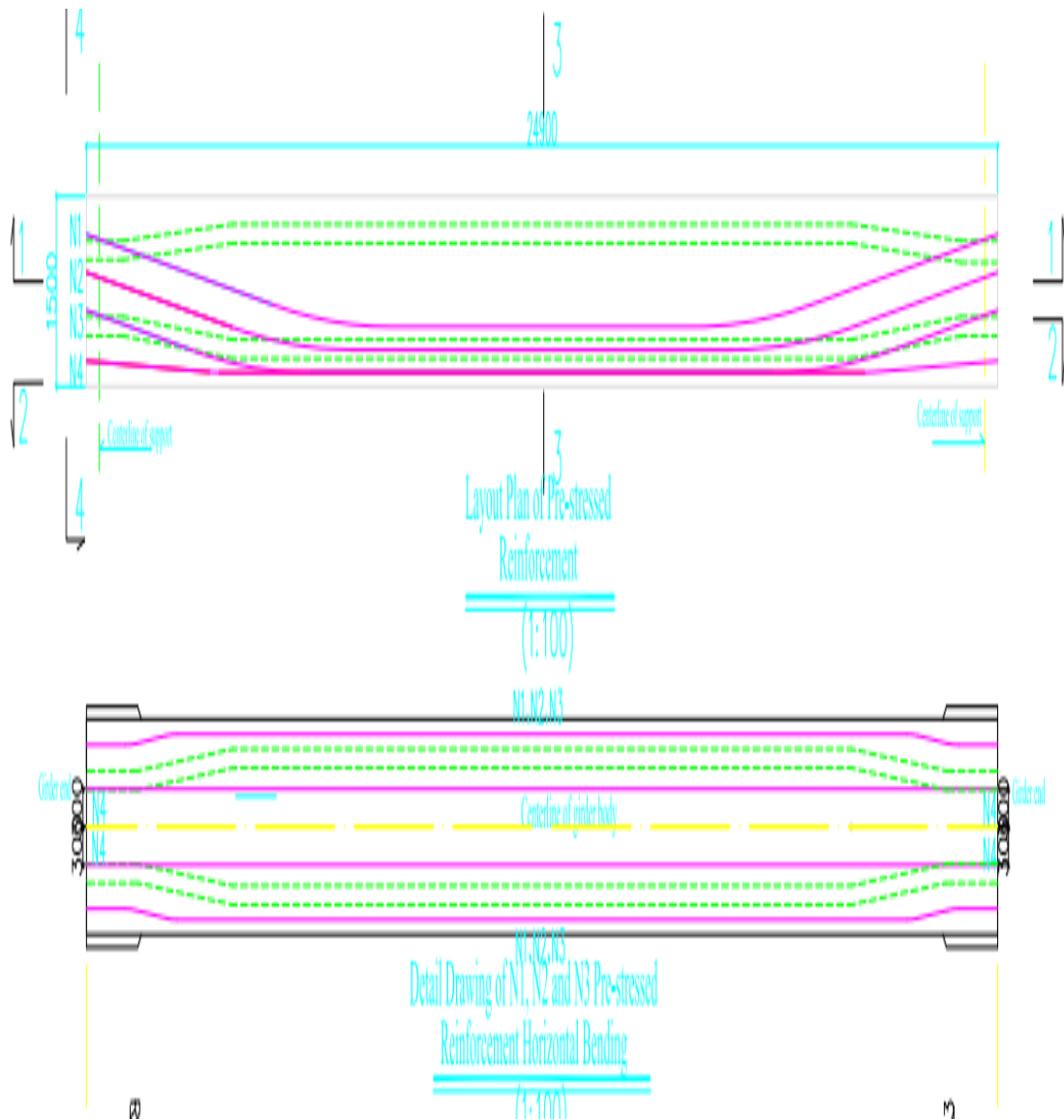


Figure 3. 18 Geometric dimensions layout plan of pre-stressed tendons (unit: mm).

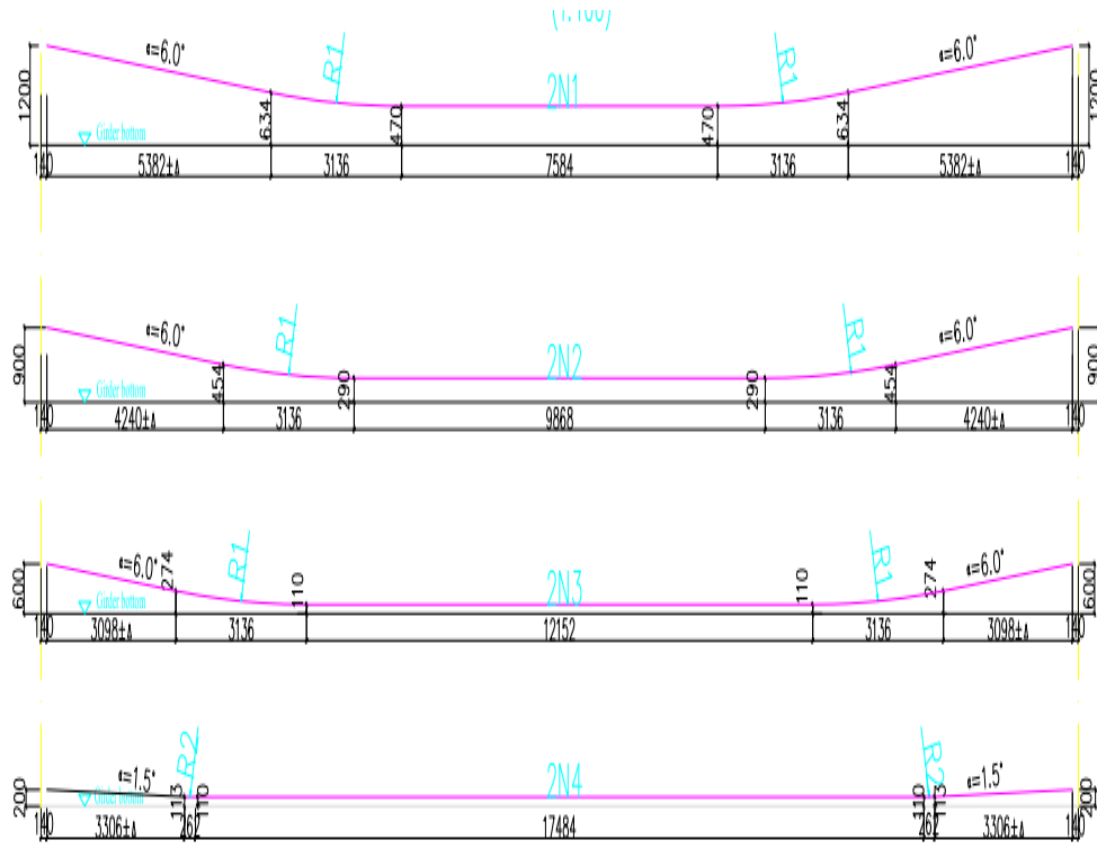


Figure 3. 19 geometric dimension of the Tendons elevations

Permissible stress at transfer

$$f_{ct} = 0.6 * f_{ck} = 0.6 * 40 = 24 \text{ MPa}$$

$$F_{tt} = 0.21 * f_{ck}^{2/3} = 0.21 * 40^{2/3} = 2.46 \text{ MPa}$$

Permissible stresses under working condition (after all losses)

$$f_{cw} = 0.5 * f_{ck} = 0.5 * 40 = 20 \text{ MPa}$$

$$F_{tw} = 0.75 * 0.21 * f_{ck}^{2/3} = 0.75 * 0.21 * 40^{2/3} = 1.84 \text{ MPa}$$

3.6.2.3 Reinforcing Steel

A structure without any form of reinforcement will be crack and fail when subjected to a relatively small tensile load. The failure occurs in most cases suddenly and in a brittle manner. To increase a structural load-carrying capacity and ductility it needs to be reinforced. Non-pre-stressed reinforcement generally consists of deformed bars or welded wire reinforcement. The yield strength f_y more than 270 MPa is used in pre-stressed low relaxation seven-wire strands steel with a minimum ultimate strength of 455 MPa.

Table 3. 8 Reinforcement used for the modelling of the railway bride

Reinforcement	Diameter (mm)	Density (kg/m ³)	Modulus of Elasticity (GPa)	Poisson's ratio	Ultimate Strength (MPa)	Applicable for
φ 10	10	7850	210	0.3	455	Main rebar
φ 12	12	7850	210	0.3	455	Traverse rebar
φ 16	16	7850	210	0.3	455	Traverse rebar

The model for reinforcement model for all is shown below in the Ansys Space claim with different colours.

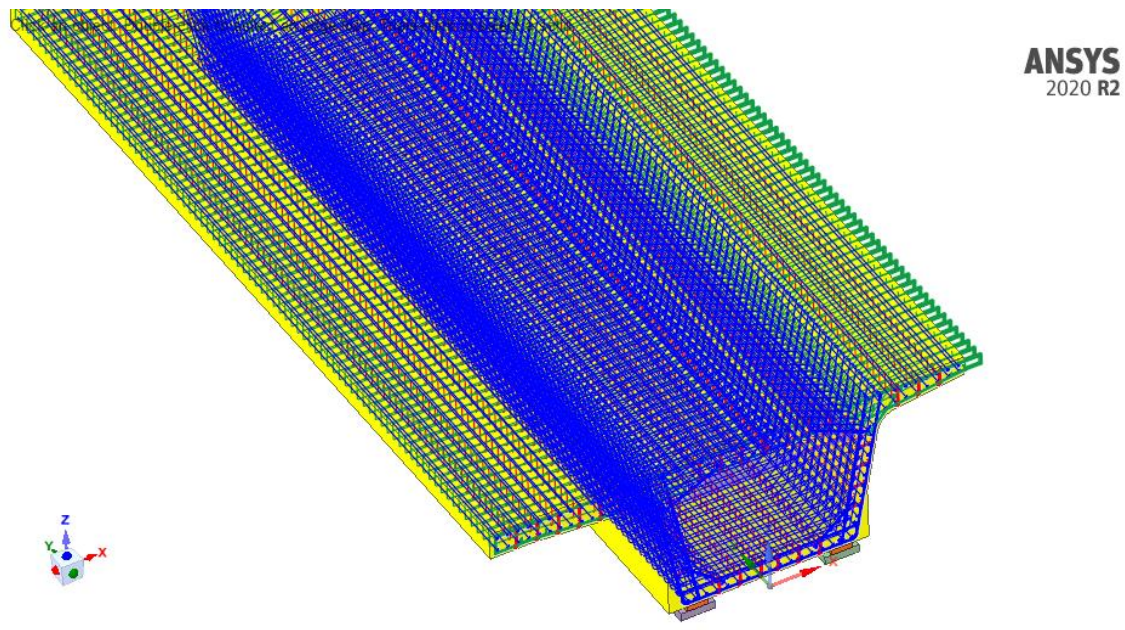


Figure 3. 20 Railway Bridge reinforcement Model

3.6.3 Railway Bridge Model Analysis with ANSYS 2020

The actual existing actual railway bridge is modeled and analyzed to estimate the fatigue life using finite element program called Ansys 2020 work bench. To prepare a realistic model of pre-stressed concrete girder railway bridge, a 3-D elasioplastic finite element model is needed. The whole bridge drawing was carried out first using AutoCAD (software and then imported to Ansys workbench in Ansys mechanical APDL. The pre-stressed railway geometry models are constructed by AutoCAD 2018 software, exported

as an IGES/SAT extension or compatible with ANSYS, and imported to the ANSYS 2020 workbench. After importing the pre-stressed concrete railway bridge geometries, line bodies were created with a minimum concrete cover of 40 mm at the soffit area, and the spacing between pre-stressing wires was taken as 30 mm for the total height/depth of 1500 mm of box girder as indicated in the drawing. The pre-tensioning process was next executed by applying an initial strain corresponding to the pre-stress. For analysis purposes, as the railway bridge was symmetric, half of the bridge length can be considered to reduce computational time.

The FEM should be able to accurately calculate the fatigue life and damage in the geometry. It also includes both material and geometric non-linearity. A pre-stressed concrete girder railway bridge 3-D non linear FEM is developed using the general-purpose finite element analysis Ansys 2020 Space Claim in Workbench, static structural. After giving the fixed boundary condition on one side and simply supporting it on the other end side of the girder, meshing of both parts follows. Then a live load force is applied on the block sleeper of the box girder railway bridge as per their spacing space provided in the standard. The model geometry of the girder railway bridge with detail dimensions was imported to the software based on the drawings.

The concrete part of the bridge is modeled by Ansys workbench simulation with a 3-D solid element, SOLID 65, which has the material model to predict the fatigue life of bridge materials. A solid 65-element is defined as an eight-node solid element that has three degrees of freedom at each node (translations in the nodal x, y, and z directions). The element has plasticity, creep, shrinkage, stress stiffening, large deflection, and large strain capabilities. The reinforcement and pre-stressed tendons were simulated using a 3-D two node link element, link 180, as it is shown in Figure 3.21 below (a, b, and c). In this paper, the modulus of elasticity was considered a constant. There is no slippage between the concrete, reinforcement, and pre-stressed tendons. The forces on the pre-stressed tendons were applied by considering the initial strain. Tendons had been united with the concrete by establishing a reasonable constraint equation between the tendon node and the concrete node.

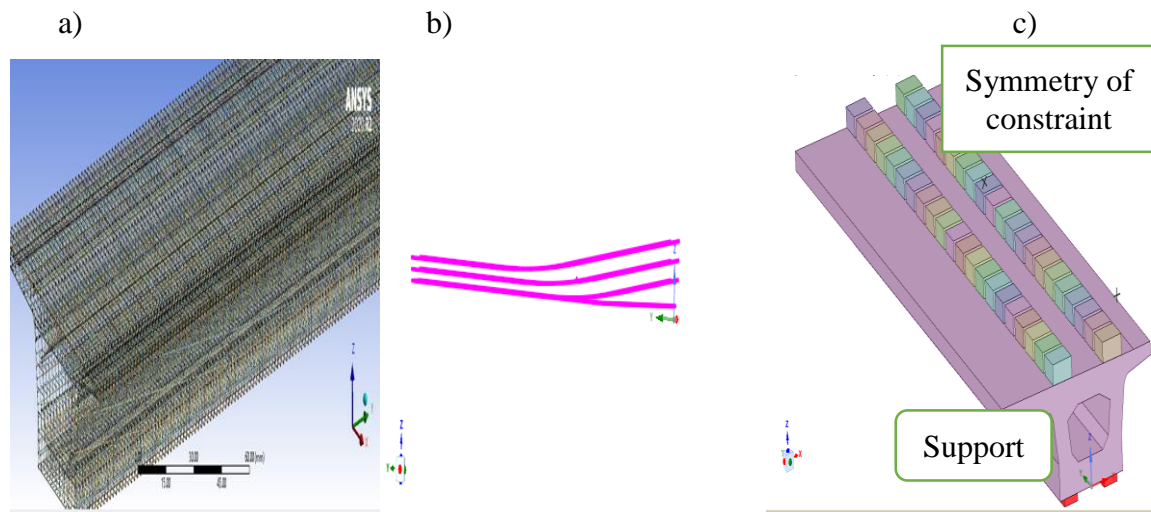


Figure 3. 21 Finite Element Model based on Ansys (a) Reinforcement; (b) pre-stressed Tendon; (c) 1/2 bridge model.

The railway bridge or the spacemen is symmetrix and due to symmetry half of the bridge structure is modeled, with symmetric constraint on the mid-section, as shown in the above Figure 3.21 c.

Table 3. 9 Assembly and constituent parts of pre-stressed concrete railway bridge

S. No	Basic Part	Type	Section Type
1	Bridge, Bearing and Box girder	Concrete	Solid
2	Longitudinal, Transverse and Stirrup reinforcement	Reinforcement	Lines
3	Pre-stressed tendon/steel wire	Steel	Lines

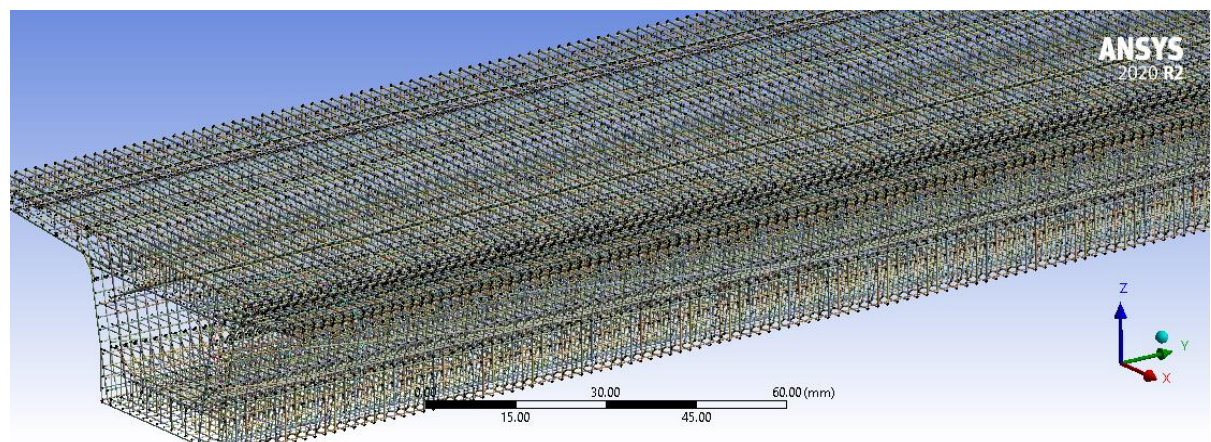


Figure 3. 22 LINK 180 Elements used as Pre-stressing Tendons

3.6.4 Meshing

Meshing is the discretizing of the model section into separate solid parts. Every model must be meshed before running. The mesh size shows the accuracy of the results. The smaller size of mesh gives accurate result, but it takes too long to compute. The use of fine meshes in finite element discretization produces more accurate results. The mesh sensitivity analyses are frequently used to select an satisfactory and reseanable mesh level of refinement in predicting the static and dynamic response parameter like Force, deformation and frequencyies with acceptable margin error. The concrete component is meshing with the hex dominant meshing method and is modeled with element order set to linear to force the use of an 8-node Solid 65 element. The reinforcement is meshed by Link 180. For the mechanical performance of a railway bridge in the ultimate limit state, a bridge model with a span length of 25 meters is used. The concrete girder is made up of Solid 65 element. Ththerefore, it is important to determine the optimum number of element that gives accurate result.

Table 3. 10 Equivalent Stress Convergence

	Equivalent Stress (MPa)	Change (%)	Nodes	Element
1	62.034	13.9%	452,342	226,898
2	122.25	49.3%	604,340	303,889
3	181.33	32.6%	675,120	351,778

The equivalent stress convergence plot shows that at about 351,778 elements, the solution converges to a mesh independent solution. The change in equivalent stress between 303,889 and 351,778 elements is small as compared the remaining. Therefore, the optimum number of elements that gives reasonably accurate results ranges from 351,778 elements. This number strikes the balance between accuracy of the results and reduced computational time.

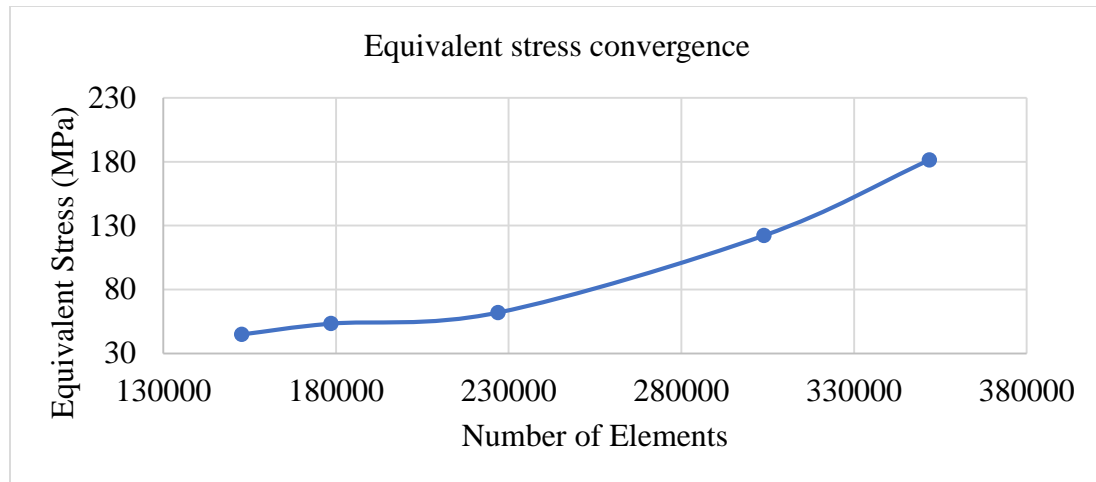


Figure 3. 23 Equivalent Stress Convergence Plot

To choose the appropriate mesh size the convergence studies was done in on finite element analysis of the railway bridge were reviewed. The approximate mesh size of 2 mm was chosen. After meshing the pre-stressed box girder railway bridge the model has to be do a data check to see if there is no error, then we have to create a job the run the model if there is error cross check of the model must be done.

Table 3.11 Total number of elements for railway bridge

Statistics		
Material Type	Nodes	Element
Steel Bearing	300	112
Concrete with Box Sleeper	61,326	47,138
Rebar Diameter 10	38,9628	192,939
Rebar Diameter 12	40,160	20,000
Rebar Diameter 16	181,062	90,275
Tendon	2,644	1,314
Total Number of Nodes and Elements	675,120	351,778

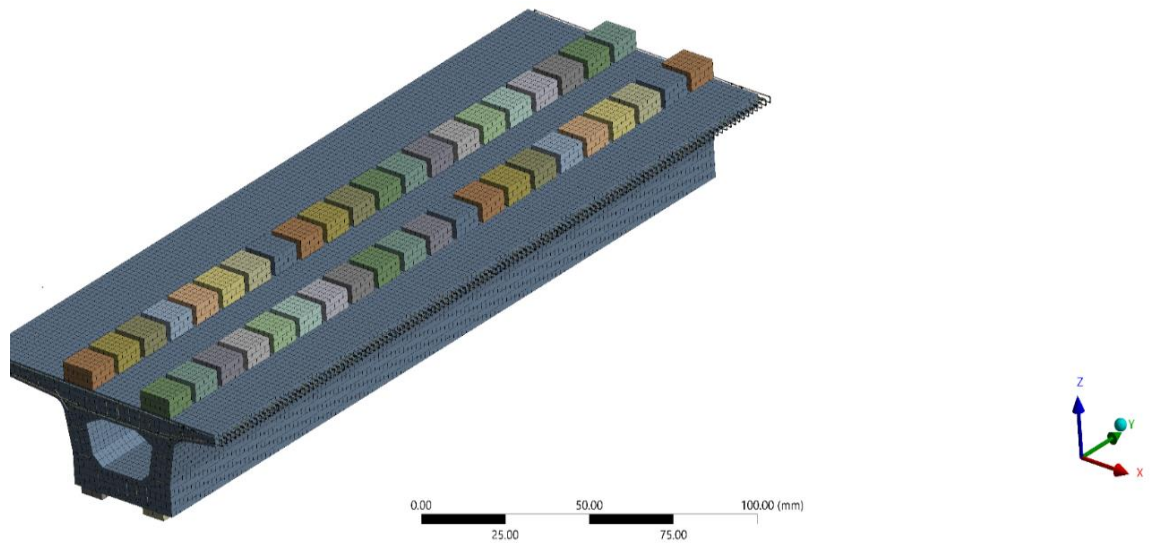


Figure 3. 24 Meshed Model of Railway Bridge

3.6.5 Boundary and Loading Conditions

The boundary, initial and loading conditions played a main role in solving the simulation and are applied to the bodies to restrict undesired displacements of the bodies. There are three sets of point's two supports and one loading cylinder. The end base of the girder railway bridge is constrained, which is not translated or rotated to any direction (x, y, z), and roller support is in one end. The boulder condition of the railway bridge is fixed fixed in one end and simple supported at two ends of the southbound and northbound in the railway bridge model.

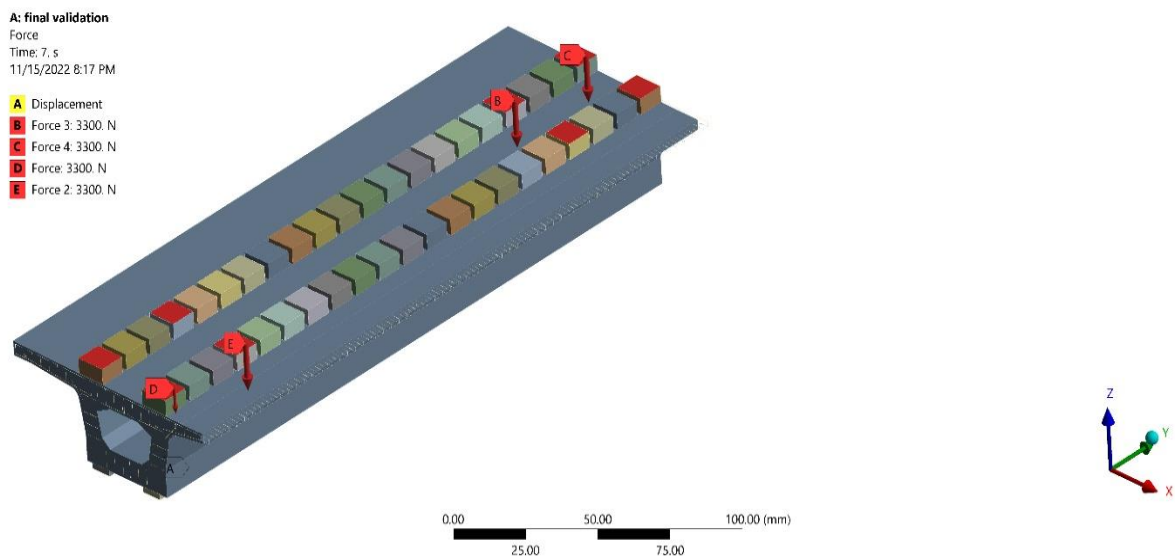


Figure 3. 25 Pre-stressed Boundary conditions and input data

3.6.6 Analysis Settings

1. Maximum number of cycles

The total number of cycles indicates at the top when the simulation model will stop. In all models, the total number of cycles used was 175,200,000 cycles. Detailed calculation of the maximum number of cycles is discussed in table B-1 Appendix B.

2. Ending time

The ending time specifies the maximum length of time to be used by the static analysis. An end time of 0.1 sec (10 m sec) was selected and thus used in the analysis.

3.6.7 Solution in ANSYS Static Structural

After solving the model, the total deformation, directional deformation, equivalent stresses, fatigue life, damage, and safety factor were recorded at support and mid-span.

3.7 Pre-stress and Pre-strain

The given maximum applied stress during the tensioning was taken as 1860 MPa. The value is taken from the specification of AALRT. The pre-stress force is calculated by subtracting the pre-stress losses value from initial stress. The losses like elastic concrete deformation, long term loss, creep, shrinkage and steel relaxation were automatically determined from the Finite element calculation [40]. The value of controlled stress for stretching pre-stressed reinforcement may not exceed the allowable value of controlled stress for stretching as stipulated in Table 3.12 and shall not less than $0.4 f_{ptk}$. When there conforms to one of the following conditions, the allowable value of the controlled stress may be increased to $0.05 f_{ptk}$.

- I. To increase the crack resistance in the construction stage for the members, it's required that the tendon or reinforcement will be provided in the compression zone at service stage.
- II. It is required to offset part of the loss of pre-stress caused by factors of stress relaxation, friction, batch stretching of steel reinforcement, or the difference in temperature between pre-stressed reinforcement and the stretching bed, etc.

Table 3. 12 Allowable value of controlled stress for stretching

Types of steel reinforcement	Method of stretching	
	Pre-tension	Post-tension
Stress-relief steel wire, strand	0.75 <i>f_{ptk}</i> .	0.75 <i>f_{ptk}</i>
Heat-treated steel bar	0.7 <i>f_{ptk}</i> .	0.7 <i>f_{ptk}</i> .

The value of stress for stretching the pre-stressing reinforcement is computed as shown below;

$$Prestress = 0.75 f_{ptk} = 0.75 * 1860 = 1395 MPa \dots\dots\dots (3.1)$$

The initial strain of tendons can be obtained from the formula

$$\epsilon = \frac{\sigma}{E_s} = \frac{1395}{210,000} = 0.006643 \text{ m/m} \dots\dots\dots (3.2)$$

The pre-stressing wire diameter was 15.2 mm with 8 total number of wires (8@15.2 mm diameter). The initial strain applied on pre-stressing wire corresponding to force was 6.643 mm/m.

The area of pre stressing wire strand for the railway bridge is computed as the equation 3.3 below,

$$A_{pw} = \frac{\pi \phi^2}{4} = \frac{3.14 * 15.2 * 15.2}{4} = 181.3664 mm^2 \dots\dots\dots (3.3)$$

3.8 Pre-stress Loss Determination

The total pre-stressed concrete loss is the sum of the loss due to elastic shorting/deformation (ES), creep loss (CR), shrinkage loss (SH), and loss due to relaxation of tendon (RE). The pre-stress loss enable designers to estimate various types of pre-stress loss rather than lump sum value. Given the uncertainties inherent in predicting creep and shirinkage and other pre-stess loss, it is imposible for design engineers to use creep and shirinkage formula to determine and predict the actual loss losses due to no control on the consitituent of concrete and loading history of thhe designed and the environment in which it is designed. This point should never be forgotten by the design engineer [21], [41].

The pre-stress loss calculation procedure depends on the initial stress level, the type of strand, exposure condition and type of construction. Creep is formed after the application of load the deflection of railway bridge with time. The process of creep in concrete is affected by the rheological property of the material like the physical and chemical ageing, the process of hydration and drying. A scholar called Katarina, et al. the immediate creep and deflection can be obtained from the computer program finite element method. Theoretical calculations shall be in good accuracy or good agreement with the data obtained from software calculation [42].

The pre-stress loss due to various losses such as the deformation, creep, shrinkage and relaxation of steel values with versus the year of bridge construction, as specified in PCI designmethod part 5.7 has been utilized in for the computation. The seventh edition of the PCI Design method for precast and pre-stress concrete, adopted by the American railway Engineering and maintenance of Way Association (AREMA), is referred to in the equations used to estimate the amount of railway bridge pre-stress losses [21].

1. Loss due to elastic deformation can be calculated as:

$$E_s \text{ Loss} = \text{Modular ratio} \times f_{ci}$$

$$ES = K_{es} * E_{ps} * f_{cir} / E_{ci}$$

Where,

$K_{es} = 1$ for pre-tensioned components

E_{ps} = modular elasticity of pre-stressed tendon

E_c = modular elasticity of concrete

$f_{ci} = P_o =$ comprehensive stress at the bottom of concrete level of tendon

$$\mathbf{Modular (m) = E_s/E_c,}$$

Where,

E_s = modular elasticity of steel and

E_c = elasticity of concrete

$$f_{co} = P_o/A + P_o * e^2/I \dots \dots \dots (3.4)$$

Where,

$P_o =$ initial stress, $A =$ area of concrete, $e =$ eccentricity and $I =$ moment of inertia.

2. Loss due to Creep of Concrete is calculated as follow:

$$\mathbf{Loss = \emptyset \times m \times f_{co}, \dots \dots \dots (3.5)}$$

Where, $\phi = 1.4$ for transfer after 28 days

3. Loss due to shrinkage of concrete

$$Loss = E_s \times \epsilon \dots\dots\dots (3.6)$$

Where, $\epsilon_{cr} = 300 \times 10^{-6}$ shrinkage strain for pre-tensioning

4. Loss due to relaxation of Steel

Loss = 5% of initial stress Thus, the total loss is the sum of the four losses.

3.9 Bridge Girder Loading

For railway bridge simulation, all load types recommended by China's standard manual for railway bridge evaluation are taken into account. The load condition on the railway track can be classified as vertical load, lateral load or longitudinal load. The vertical load is the most common vertical, lateral, or longitudinal, though vertical loading is the most common which consists of weight of vehicle plus additional dynamic increase in (Quasi static, Dynamic ride and Impact loads) which is super imposed on the static load. The general method used to estimate the vertical design load is expressed empirically as a function of wheel static load.

$$P_d = I \times P_s \dots\dots\dots (3.7)$$

Where,

P_d is the wheel designed load in kN,

P_s is the static wheel load in kN, and

I is the impact factor, that is always greater than one (> 1). The impact factor is calculated as discussed earlier in the previous section as; $I = \frac{125}{(L)^{1/2}}$

The static wheel load, $P_s = Q \times 0.5g$. $Q = 125$ kN and $I = 1.25$

Therefore, $P_d = 156.25$ kN.

As stated, earlier loads are taken from the China's standard manual for design and operational loads. In the numerical analysis a concentrated axle operational load of 165 kN, is applied to the pre-stressed box girder railway bridge.

- The successive distance between the nose and tail of the combined trains shall not less than 7 meter.
- A distance between the axle load configurations is shown below.

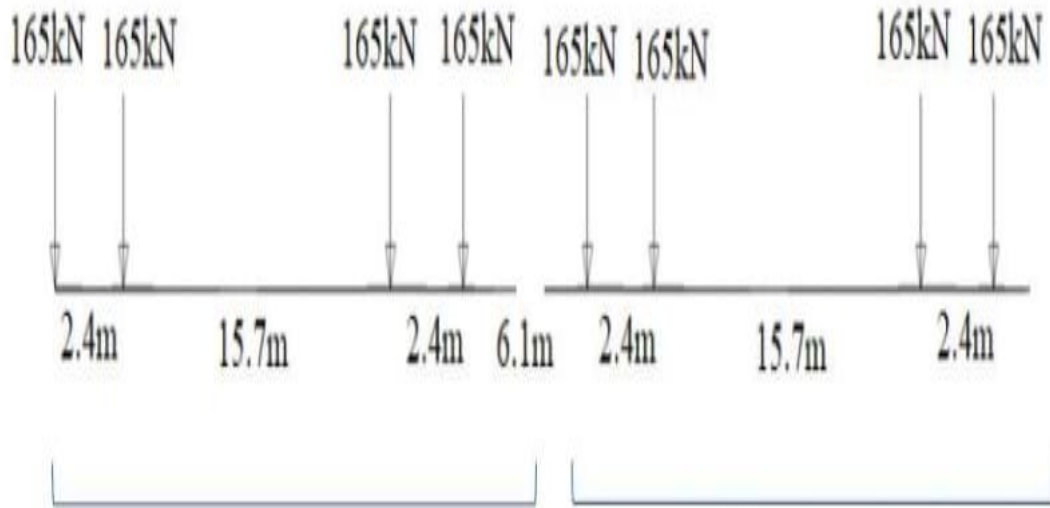


Figure 3. 26 Operational Load Schematic Diagram for Passenger Coach

CHAPTER FOUR RESULT AND DISCUSSION

This section develops a systematic way for determining of fatigue life of pre-stressed railway lines. For this thesis a 3-D non-linear finite element analysis using Ansys workbench 2020 is used. The geometry, material property, elements, and parameters used in modeling are highlighted in chapter three. The pre-stressed concrete box girder railway bridge was analyzed using Ansys Workbench through static structural analysis. In this section, the known pre-stressed concrete railway bridge with a known cross section was considered for Ansys software. Static analysis is employed obtain the equivalent stresses, deformation and fatigue life under cyclic operational loading. In addition, the result of the stress analysis, damage analysis, fatigue life, and safety factor from the FEM analysis was discussed below in detail.

4.1 Pre-stress Loss Calculation

The pre-stress loss in pre-stressed concrete railway ridge is calculated based on the formulas in analytical form as shown below. Pre-stress loss at mid span of girder bridge is considered the following given parameters from the model.

Table 4. 1 Centroid of the cross-section model along the 3-D

	X-direction	Y- direction	Z- direction
Centroid of concrete	45 mm	125 mm	15.8 mm

$$\text{Mass} = 0.7583 \text{ kg}$$

$$\text{Volume} = 2.895 \times 10^5 \text{ mm}^3$$

$$E_s = 195,000 \text{ MPa},$$

$$\xi_s = 3.5\%$$

1. Loss due to elastic deformation

$$\sigma_0 = \xi_s \times E_s = 0.035 \times 195,000 \text{ MPa} = 6,825 \text{ MPa}$$

$$\text{Loss} = \text{modular ratio} \times f_{co}$$

$$\text{Loss} = 180.79 \text{ MPa}$$

2. Loss due to Creep of concrete

$$\text{Loss} = \emptyset \times m \times f_{co} = 1.4 \times 6.56 \times 27.57 = 253.106 \text{ MPa}$$

3. Loss due to shrinkage of the concrete

$$Loss = E_s \times \epsilon_{cr} = 195,000 \text{ MPa} \times 300 \times 10^{-6} = 58.5 \text{ MPa}$$

4. Loss due to relaxation of the steel

$$Loss = 5\% \times \text{initial stress} = 5/100 \times 3.5\% = 0.175 \times 195,000 \text{ MPa} = 341.25 \text{ MPa}$$

Thus, total pre-stressed loss at Z=200 mm will be 12.2%

Pre-stresses loss from FEM output Result

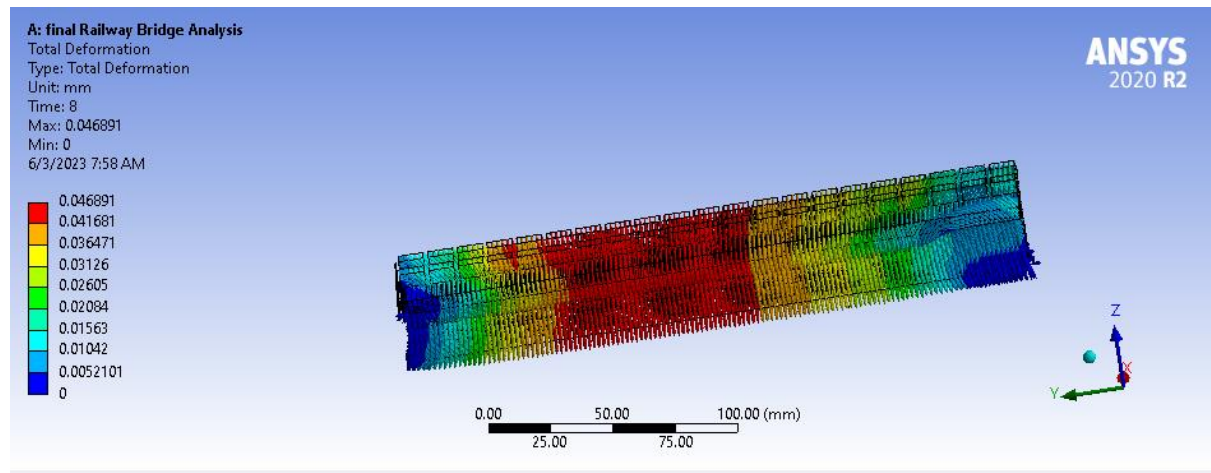


Figure 4. 1 Pre-stress loss of railway bridge deformed shape

The software output of the deformed shape along Y direction is 0.61 mm at Y=250 mm, thus the strain: $\epsilon_o = \Delta L/L = (0.61)/(250) = 2.44 \times 10^{-3}$

$$\text{Stress loss} = \text{strain} \times E_s = 2.44 \times 10^{-3} \times 1.95 \times 10^5 = 475.8 \text{ MPa}$$

$$\text{Stress loss in \%} = 475.8/6825 \times 100 = 6.97\%$$

Note: The pre-stress loss at the bottom level of the tendon using hand calculation and FEM is 12.2% and 6.97%, respectively. The low pre-stress loss result of the FEM is because it analyzed only the instantaneous pre-stress loss.

4.2 Static Analysis of Pre-stressed Concrete Railway Bridge

The static analysis assumes that the loads are applied instantaneously. It also determines the deflection, stresses, strains, safety factors, and fatigue life of structures caused by loads that do not induce significant inertia and damping effects. The load and structure response are assumed to vary slowly with respect to time which means steady loading and response condition are assumed. The type of loading that can be applied in static analysis is vertical wheel load (force).

4.2.1 Deformation

The deformation result can be obtained as total or directional deformation. The exact location of the maximum deformation of the railway bridge occurs at the mid span on the pre-stressing wires (line bodies) while the minimum deformation occurs on the concrete part. In this thesis, the critical sections such as the box sleeper, center, and end sections have been emphasized and maximum deformation in concrete is located at the mid span of the box girder section. Figure 4.2 shows the calculated maximum and minimum deformation for a 165 kN operational train load traveling at a speed of 70 km/h. According to AREMA manual, permissible limit value for the maximum allowed displacement is $\delta = L/640$ where L is span length. In relation to this, the allowable maximum displacement for the given railway bridge is 39.065 mm which corresponds to $25/640 \approx 39.0625$ mm. The total deformations at critical sections have been recorded using a probe tool in the ANSYS workbench as shown in Figure 4.2. The railway bridge satisfies the allowable limits for 165 kN operational cyclic load with allowable error 10% allowed for the allowable displacement of $39.0625+3.2$ mm between the modeling and the measurement. The plot is conducted by taking the maximum points at each cyclic load.

Table 4. 2 Cyclic load versus Deformation and Stress

Force/cyclic load (N) in -Z direction	Force Reaction (N)	Directional Deformation (mm)	Equivalent Stress (MPa)	Shear Stress (MPa)	Maximum Shear Strain (MPa)
0	2.63E-07	0	0	0	0
500	2000	7.10E-03	27.475	14.866	3.00E-04
0	2.63E-07	0	0	0	0
1000	4000	2.61E-03	54.95	29.732	6.00E-04
0	2.63E-07	0	0	0	0
1500	6000	3.92E-03	82.424	44.598	8.99E-04
0	2.63E-07	0	0	0	0
2000	8000	5.22E-03	109.9	59.464	1.20E-03
0	2.63E-07	0	0	0	0
2500	10000	6.53E-03	137.37	74.33	1.50E-03
0	2.63E-07	0	0	0	0
3000	12000	7.84E-03	164.85	89.196	1.80E-03
0	2.63E-07	0	0	0	0
3300	13200	8.62E-03	181.33	98.115	1.98E-03

Force/cyclic load (N) in -Z direction	Force Reaction (N)	Directional Deformation (mm)	Equivalent Stress (MPa)	Shear Stress (MPa)	Maximum Shear Strain (MPa)
0	2.63E-07	0	0	0	0

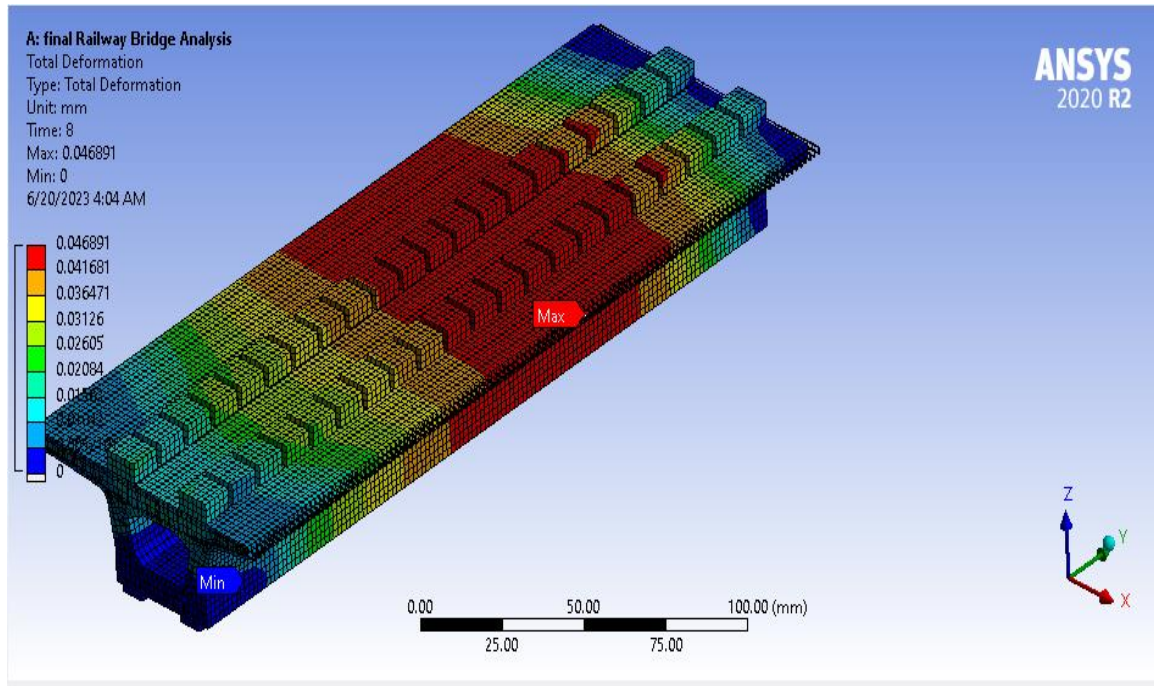


Figure 4. 2 Maximum Total Deformation on the Railway bridge

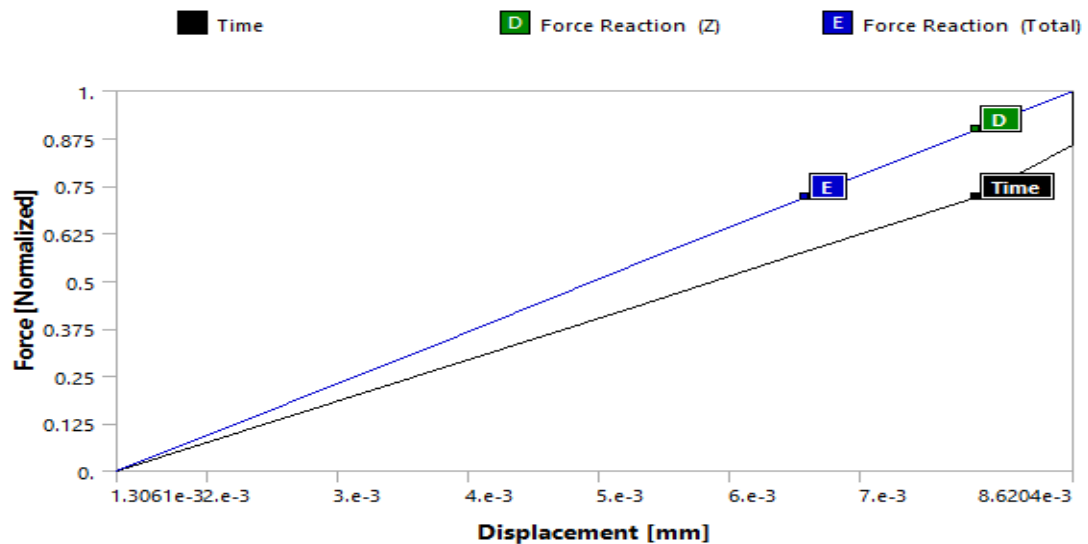


Figure 4. 3 Directional Deformations in Concrete for 165 kN operational load

The maximum static total deflection for is observed at the center of the span is 0.04689 mm for the operational load. The values are much less than the allowable deflection as it is 2.3445 mm based on the scale. In addition, the maximum directional deformation is recorded 0.0086204 mm with the allowed deflection of 0.43 mm. It is seen that the deflection is negative i.e., hogging due to pre-stressing force. This negative deflection will help to overcome the moving loads on the bridge during its service life. The Directional Deformation is shown in the Figure 4.4 below.

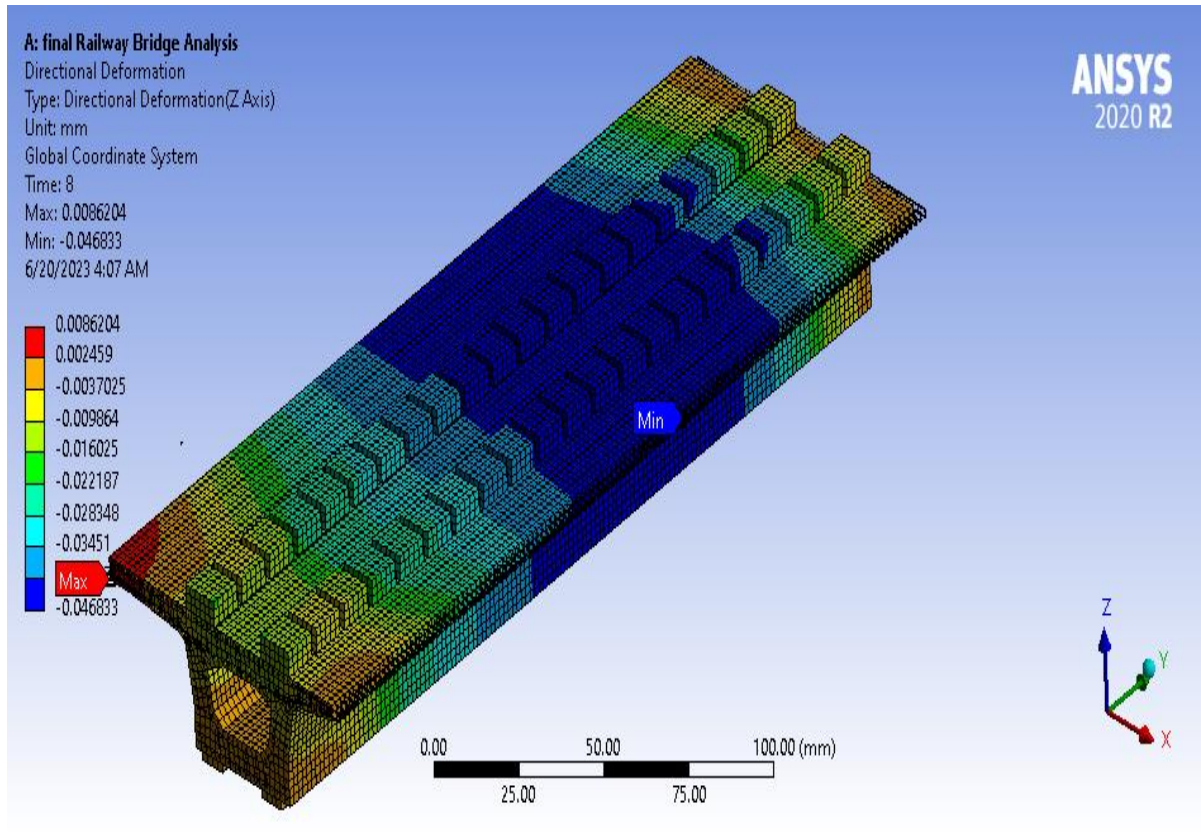
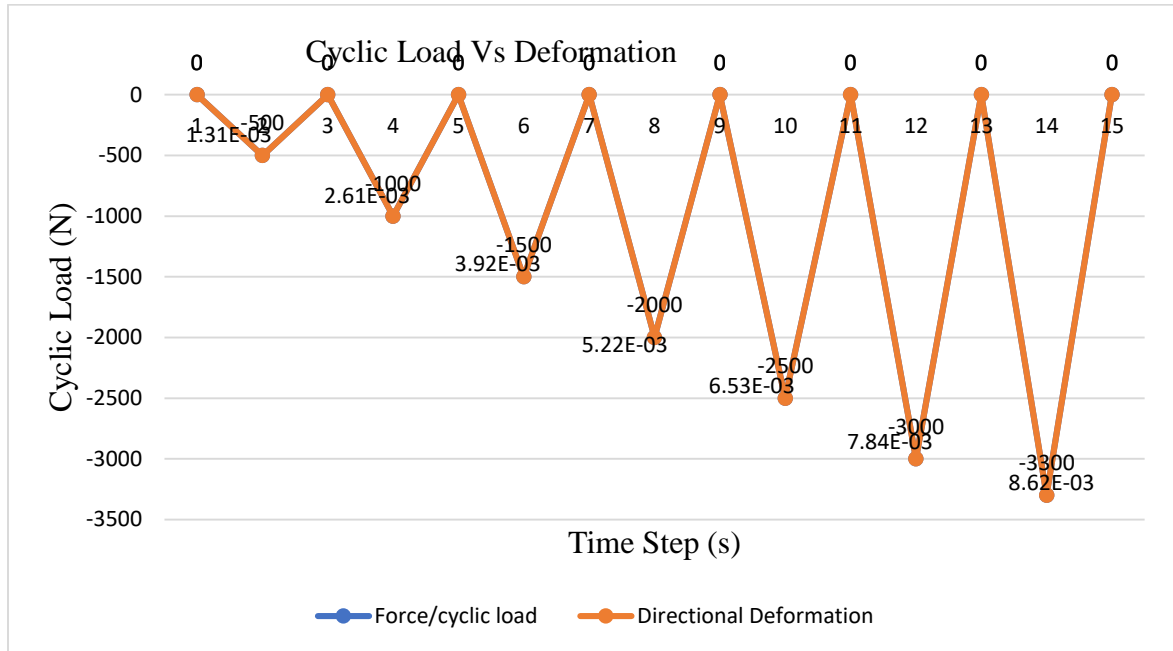


Figure 4. 4 Maximum Directional Deformation on the Railway bridge



4.2.2 Stress

The stress value can be defined as the average force divided by unit area. The particles of the body exerts an adjacent particle across an imaginary surface that separates them.

4.2.2.1 Equivalent (Von- Mises) Stress

Equivalent stress (Von Mises Stress) is often used in design work because it allows any arbitrary three dimensional stress state to be represented as single positive stress value. Equivalent stress is part of the maximum equivalent stress failure theory, which is used to predict yield strength of ductile material. On concrete, the maximum equivalent stress acting on the pre-stressed railway bridge is experienced, with the maximum being experienced at the ends of the bridge and the center sections experiencing almost different stresses as shown in Table 4.3 and Figure 4.5 below.

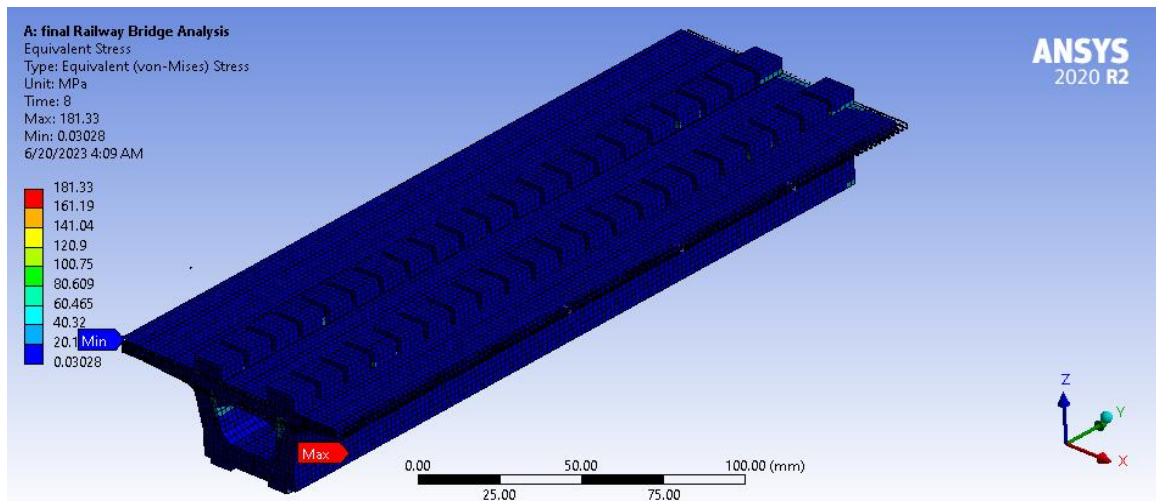


Figure 4. 5 Equivalent Von-Mises Stress of the railway bridge

The maximum Von mises stress at the top of the box railway bridge girder is 181.33 MPa and the minimum Von-Mises stress at the bottom is 0.0 MPa as shown in the Figure 4.5 above.

Table 4. 3 Cyclic load versus Equivalent Stress

Force/cyclic load (N) to -Z direction	Force Reaction (N)	Equivalent Stress (MPa)
0	2.63E-07	0
-500	2000	27.475
0	2.63E-07	0
-1000	4000	54.95
0	2.63E-07	0
-1500	6000	82.424
0	2.63E-07	0
-2000	8000	109.9
0	2.63E-07	0
-2500	10000	137.37
0	2.63E-07	0
-3000	12000	164.85
0	2.63E-07	0
-3300	13200	181.33
0	2.63E-07	0

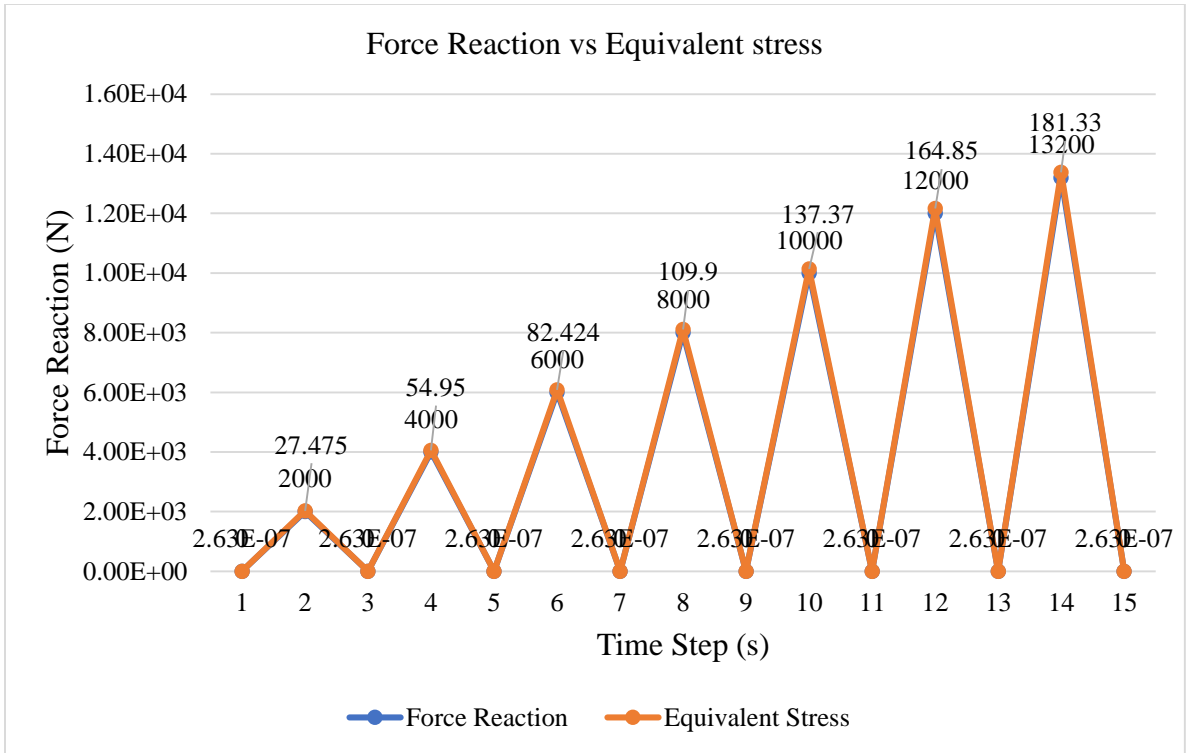


Figure 4. 6 Force Reaction versus Equivalent Stress of the pre-stressed railway bridge

The cyclic load is drawn versus the equivalent stress as indicated in Figure 4.7 below

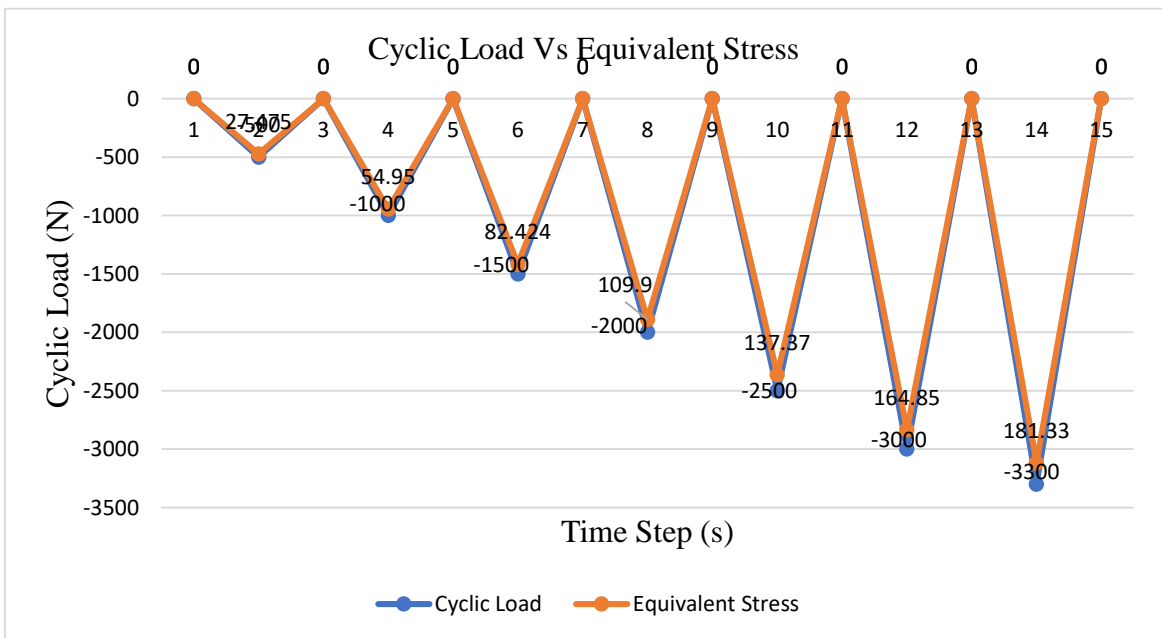


Figure 4. 7 Cyclic load Vs Equivalent Stress

Table 4. 4 Maximum and Minimum Values

Parameters	With 165 kN	
	Max	Min
Deformation	0.0086204 mm	0 mm
Equivalent stress	181.33 MPa	0 MPa
Fatigue life	1e ⁸ Cycle	0 Cycle

4.2.3 General Fatigue Results

Fatigue is a progressive process of micro-crack initiation and propagation toward the point at which failure occurs. The mechanical properties of the material will change under repeated cyclic loading, such as permanently increasing strain on the member, causing the stiffness to decrease. Cyclic loading may also cause a concentration of stress at the pre-stressed wires' surface, which can lead to sudden fracture. The fatigue performance of a material is commonly represented on graphs, with stress ranges plotted against the failure cycle number.

4.2.3.1 Fatigue Life

The pre-stressed railway bridge is loaded with an operational live load of 165 kN with 6 axles. The result contour plot shows the available or fatigue life for the fatigue analysis. Figure 4.3 below indicates that the available life of the new railway bridge. The minimum fatigue life obtained is 1e⁸ cycles. This number of cycles corresponds to about 114 years which is approximately above the design life of the railway bridge, implying some parts of the railway bridge do not fail before the design life of 100 years (175,200,000 cycles) is achieved. However, most parts of the bridge, especially the steel bearing can attain life greater than 1e¹⁰ cycles (infinite life). Moreover, the software output result shows that the failure occurs on the mid-section of the railway bridge of concrete section.

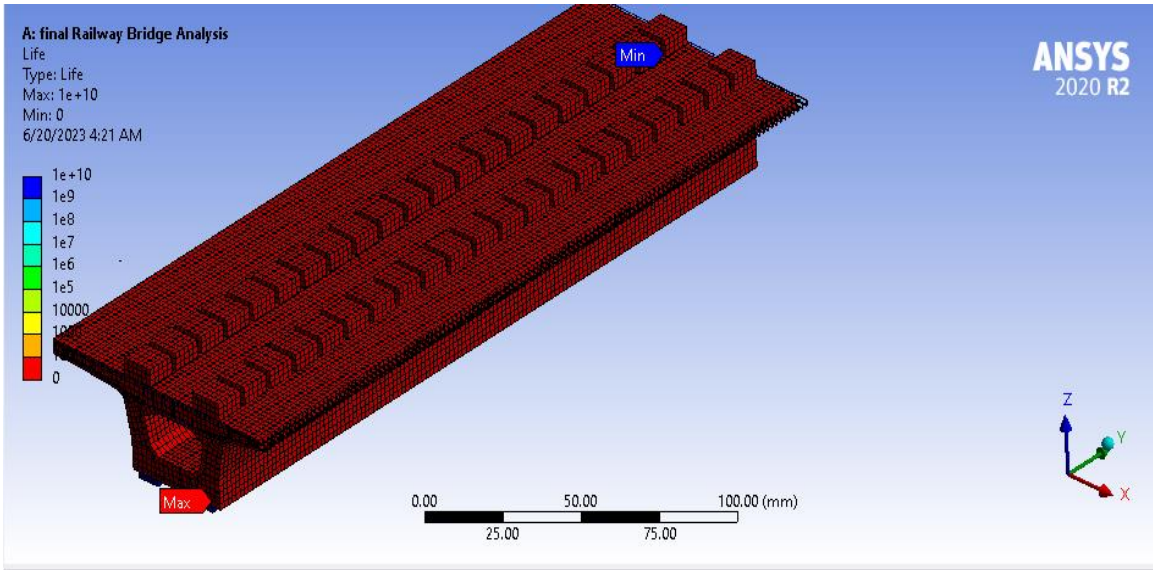


Figure 4. 8 Available Life for operational load

4.2.3.2 Fatigue Damage

Fatigue damage on the structure is the design life divided by available life and it is the contour plot of damage at a given service life. The minimum fatigue damage on the sleeper is 0.1 which is less than 1, an indication that the bridge will sustain for its design life. Values less than zero for fatigue damage imply the part is safe and does not fail before attaining its design life. The contour plot for fatigue damage is shown in Figure 4.9 below.

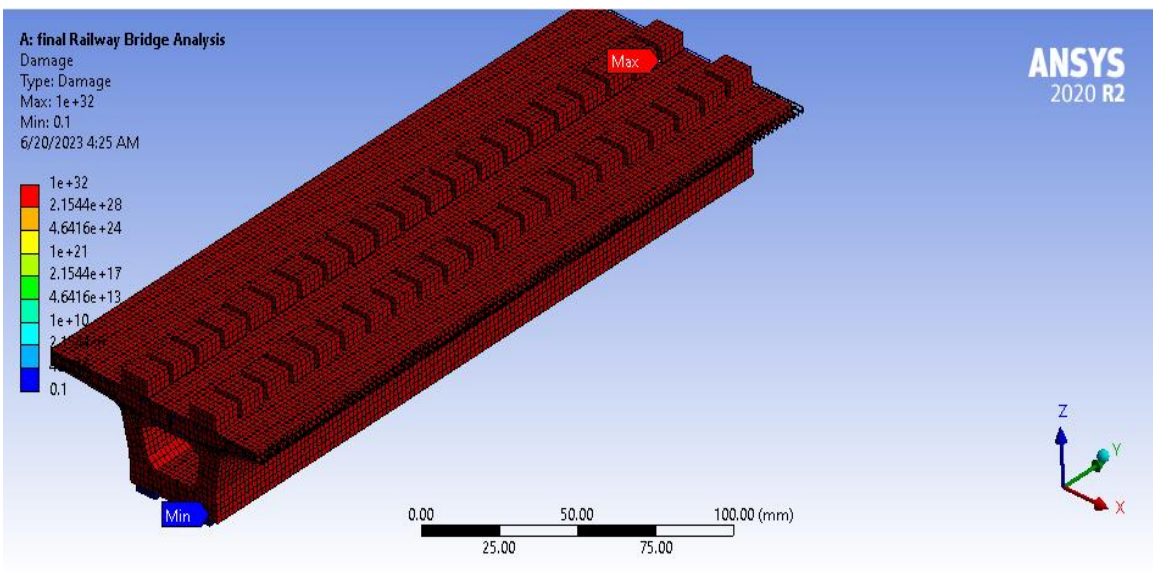


Figure 4. 9 Fatigue Damage

In the figure 4.9 above the maximum damage value is $1e^{32}$ MPa and minimum value of damage is 0.1.

4.2.3.3 Fatigue Safety Factor

Safety factor is the plot of the factor of safety versus fatigue failure at a given design life. From the software result the maximum value of factor of safety is displayed 15 while values less than one imply the part fails before its design life is attained. The minimum factor of safety obtained is 1 equal to 1, an indication that the railway bridge serves its intended design life. The maximum factor of safety is 15 and the minimum factor of safety is 1 as shown in the Figure 4.10 below.

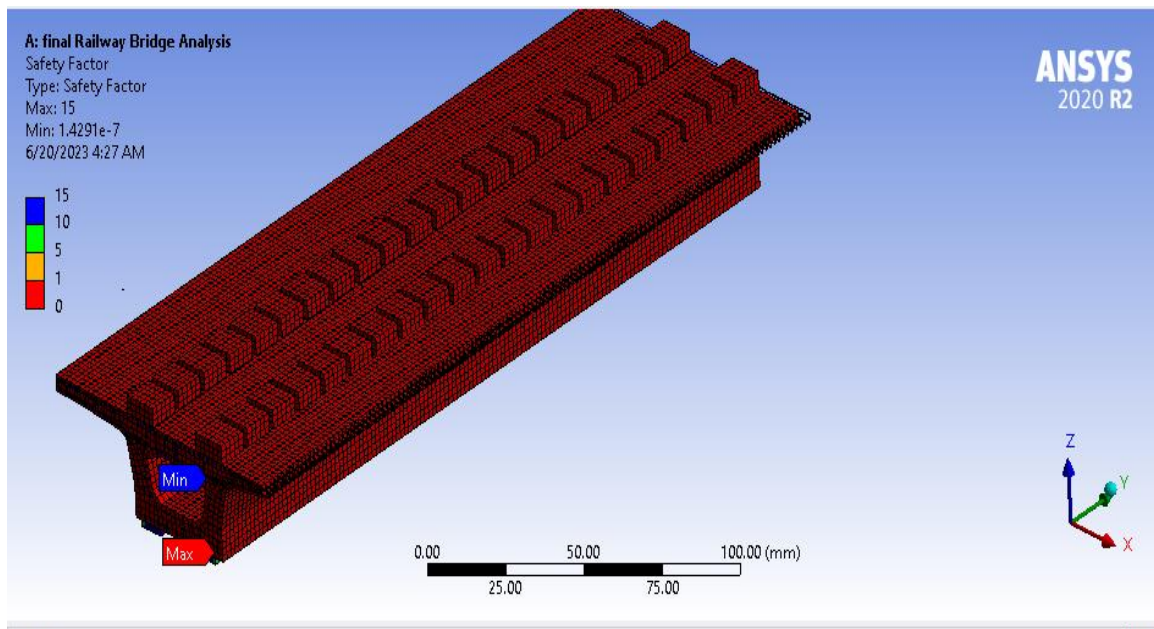


Figure 4. 10 Safety Factor

4.2.3.4 Equivalent Alternating Stress

It is the stress used to query the fatigue S-N curve after accounting for fatigue loading type, mean stress effects, multi-axial effects, and any other factors in the fatigue analysis. In a Stress Life fatigue analysis, the S-N curve needs to query and relate to the fatigue life. The maximum equivalent alternating stress shown in Figure 4.11 is 181.33 MPa.

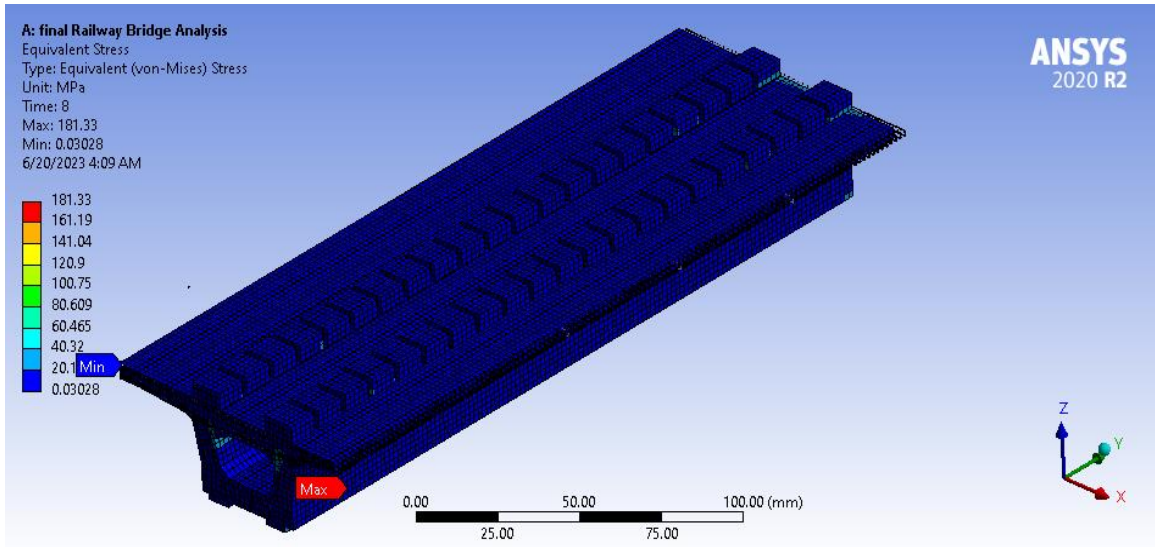


Figure 4. 11 Equivalent Alternating Stress

4.2.3.4 Fatigue Sensitivity

The fatigue sensitivity curve is used to show how the values of the fatigue results change as a function of loading at critical location on the model. This fatigue sensitivity may be scoped. It is possible to find fatigue sensitivity for life, damage and factor of safety. Figure 4.12 below shows how the fatigue changes with loading history on the railway bridge structure.

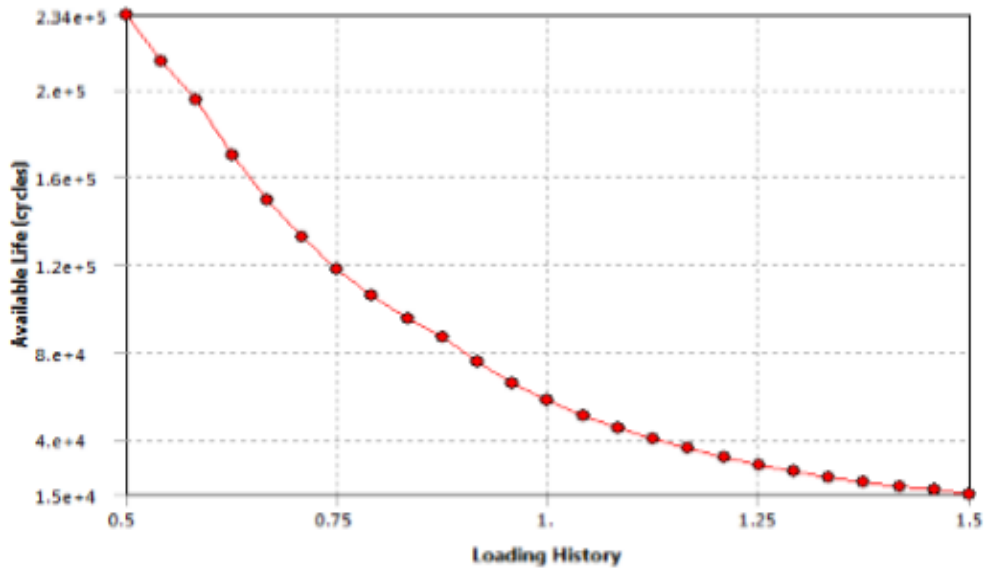


Figure 4. 12 Fatigue Sensitivity Curve.

CHAPTER FIVE CONCLUSION AND RECOMMENDATION

5.1 Conclusions

- In this thesis, the evaluation of the fatigue life of a railway bridge subjected to design and operational loadings were carried out to determine the remaining fatigue life of the railway bridge. Static and impact simulations were conducted on pre-stressed box girder railway bridges with single-track models. The material properties of the pre-stressed railway bridge were C-50 concrete, and pre-stressing wire with spacing of 30 mm and 40 mm on the horizontal and vertical respectively.
- IRC 24 (IRC 2001), has specified the minimum limit of the Total deflection shall be less than $L/600$ which is caused by the combination of dead load, live load and impact load. Concerning this, the total deformation of this railway bridge is 2.34 mm which is within the allowable deflection limit.
- The results from the static simulation revealed that the railway bridge will serve its design life of 100 years (175,200,000.00 cycles). For the operational live load considered in this simple model, the railway bridge fails after $1e^8$ cycles with a safety factor equal to one and fatigue damage less than one as the structure is newly constructed.

5.2 Recommendation

It can be seen from the study that the railway girder bridge is adequate in fatigue and serves well above the design life. The bridge develops cracks that are likely to limit the bridge's ability to hold the geometry of the line of the line and therefore fail in that criterion. It's therefore recommended that after estimating the remaining fatigue life appropriate maintenance measures shall be carried out before it is subjected to a sudden crash. In this thesis, the research is limited to fatigue life of pre-stressed concrete box girder railway bridges using ANSYS 2020 software due tooperational cyclic load. From this thesis, some recommedndation and sugestions are listed below for further works as a continuity of this paper.

- The laboratory/expermental fatigue test of pre-stress concrete railway bridge is necessary to plot S-N curve.
- More research shall be carried out in better ways in analysis of railway bridge in consideration of Shrinkage value from experimental test.

REFERENCES

- [1] C. Engineering, L. Supervisor, R. Artur, and G. Santos, ‘Structural Stress-Based Methodologies For Fatigue Assessment Of Welded Railway Bridges’, no. March, 2021.
- [2] S. Krishna, A. Paraitham, and W. Virginia, ‘Load rating analysis , field testing of steel railroad bridges - dailey branch bridges at mileposts 1 . 4 and 5 . 8 Load Rating Analysis , Field Testing of Steel Railroad Bridges – Dailey Branch Department of Civil and Environmental Engineering Copyright ’, 2016.
- [3] I. Ajibola, ‘Assessment of Reinforced Concrete Dapped End Beams Subjected to Cyclic Loading under Bond Deterioration and Retrofitting Approach’, 2021.
- [4] B. Lena, ‘*Dynamic Analysis of a Railway Bridge subjected to High Speed Trains*’, 2004.
- [5] S. R. et al. Matias, ‘Railway slab track systems : review and research potentials Railway slab track systems : review and research potentials’, *Structure and Infrastructure Engineering*, vol. 0, no. 0, pp. 1–19, 2020.
- [6] R. Kumppong and P. Herabat, ‘Finite-Element Analysis for Fatigue Evaluation of Reinforced Concrete Bridge Deck’, vol. 13, no. 6, pp. 1017–1031, 2010.
- [7] I. Abdoukader, ‘Economic Design Comparison of Pre-Stressed Concrete Slab & Box-Girder Railway Bridges’, no. June, 2017.
- [8] A. Pipinato, C. Pellegrino, and C. Modena, ‘Fatigue Damage Estimation in Existing Railway Steel Bridges by Detailed Loading History Analysis’, vol. 2012, 2012.
- [9] N. S. et al. Gulgec, ‘Structural sensing with deep learning : Strain estimation from acceleration data for fatigue assessment’, pp. 1–16, 2020.
- [10] L. Design, A. M. Rakoczy, D. Otter, and S. Dick, ‘Railroad bridge fatigue life estimation using the probabilistic method and new fatigue resistance for riveted details’, *Structure and Infrastructure Engineering*, vol. 0, no. 0, pp. 1–13, 2019.
- [11] H. Li and G. Wu, ‘applied sciences Fatigue Evaluation of Steel Bridge Details Integrating Multi-Scale Dynamic Analysis of Coupled Train-Track-Bridge System and Fracture Mechanics’, 2020.
- [12] T. Structures, C. Structures, and G. S. Index, ‘Manual for Railway Engineering’, vol. 2, 2010.

- [13] M. R. Drawings and D. Principle, ‘Addis Ababa Light Rail Transit Projects’, p. 2, 2015.
- [14] N. D. Adasooriya, ‘Case Studies in Structural Engineering Fatigue reliability assessment of ageing railway truss bridges : Rationality of probabilistic stress-life approach’, *Tissue and Cell*, vol. 6, pp. 1–10, 2016.
- [15] G. A. A. E. Abrham, *Ceng 6903*, vol. 2002. 2020.
- [16] S. Landge, U. Bhagat, S. Bhaisare, V. Prakash, and I. P. Khedikar, ‘Analysis and Design of Pre-stressed Concrete I-Girder Bridge’, 2018.
- [17] L. Elfgren, ‘Prestressed Concrete Bridges Condition Assessment and Future Challenges A State-of-Art Report’, 2018.
- [18] V. Ansnaes and H. Elgazzar, ‘Concrete Cracks in Composite’, 2012.
- [19] C. Cole, M. Spiryagin, and M. Dhanasekar, ‘VERTICAL DYNAMIC INTERACTION OF TRAINS AND RAIL’, vol. 13, no. 1, pp. 88–97, 2013.
- [20] M. Sergio Ruiz, ‘Dynamics of Prestressed Concrete Railway Bridges’, 2001.
- [21] P. Concrete, *DESIGN HANDBOOK*. .
- [22] P. Taylor, A. M. Chateauneuf, W. E. Raphael, R. J. B. M. Pitti, and I. Pascal, ‘Structure and Infrastructure Engineering : Maintenance , Management , Life-Cycle Design and Performance Reliability of prestressed concrete structures considering creep models’, no. February 2015, pp. 37–41.
- [23] P. Ameen and M. Szymanski, ‘Fatigue in Plain Concrete’, 2006.
- [24] Q. Pu, H. Wang, H. Gou, Y. Bao, and M. Yan, ‘applied sciences Fatigue Behavior of Prestressed Concrete Beam for Straddle-Type Monorail Tracks’.
- [25] Y. Lee, R. E. Kim, W. Suh, and K. Park, ‘Probabilistic Fatigue Life Updating for Railway Bridges Based on Local Inspection and Repair’.
- [26] P. Taylor, P. Moyo, and R. Tait, ‘Structure and Infrastructure Engineering : Maintenance , Management , Life-Cycle Design and Performance Structural performance assessment and fatigue analysis of a railway bridge’, no. January 2015, pp. 37–41.
- [27] C. et al. Wang *et al.*, ‘Fatigue assessment of a reinforced concrete railway bridge based on a coupled dynamic system’, *Structure and Infrastructure Engineering*, vol. 0, no. 0, pp. 1–19, 2019.
- [28] K. Olsson and J. Pettersson, ‘Fatigue Assessment Methods for Reinforced

- Concrete Bridges in Eurocode Comparative study of design methods for railway bridges’.
- [29] L. Shan, ‘Railway Sleeper Modelling with Deterministic and Non-deterministic Support Conditions’, 2012.
- [30] R. et al. You, ‘Fatigue Life Assessment Method for Prestressed Concrete Sleepers’, vol. 3, no. November, pp. 1–13, 2017.
- [31] B. R. Browell and A. Hancq, ‘Calculating and Displaying Fatigue Results The ANSYS Fatigue Module has a wide range of features for performing calculations and presenting analysis results . Table of Contents’, 2006.
- [32] S. Puerto, M. Mashayekhi, M. Sanayei, and E. Santini, ‘Multiaxial fatigue assessment of complex steel connections : A case study of a vertical-lift gussetless truss bridge’, *Engineering Structures*, vol. 235, no. June 2020, p. 111996, 2021.
- [33] Z. X. Li, T. H. T. Chan, and J. M. Ko, ‘Fatigue analysis and life prediction of bridges with structural health monitoring data - Part I : methodology and strategy’, vol. 23, pp. 45–53, 2001.
- [34] Ethiopian Railway Corporation, ‘49 Reference Drawing of Precast Tensioned Simply Supported Box-girder Span 25m (straight and curved line).pdf’. Addis Ababa, 2015.
- [35] C. L. P. C. Laboratory, ‘Ethiopia LRT project Reinforcement Test Report’, pp.1–111.
- [36] G. Rikard, “‘Static and dynamic finite element analysis of concrete sleepers.’” *Chalmers University of Technology, Göteborg, Sweden., Göteborg, Sweden, 2000.*
- [37] K. Chen, J. Song, and S. Zhang, ‘Simulation and Analysis for Externally Prestressed Concrete Bridge Based on ANSYS’, vol. 249, pp. 1737–1742, 2011.
- [38] A. W. Documentation, ‘ANSYS Workbench Documentation’.
- [39] E. Standard, ‘En 1992-1-1’, 2004.
- [40] C. Engineering, ‘Analysis Of Cyclic And Long-Term Effects In Continuous Precast Railway Bridge Decks’, no. May, 2012.
- [41] S. Walton and T. E. Bradberry, ‘Comparison of Methods of Estimating Prestress Losses for Bridge Girders’, no. 512, 2004.
- [42] T. Katarina and D. Jana, ‘Analysis of Creep Effects in a Concrete Beam Using Various Software’, vol. 738, pp. 79–88, 2017.

APPENDICES

Appendix A: Sleeper Type A9P Sketch used for Validation

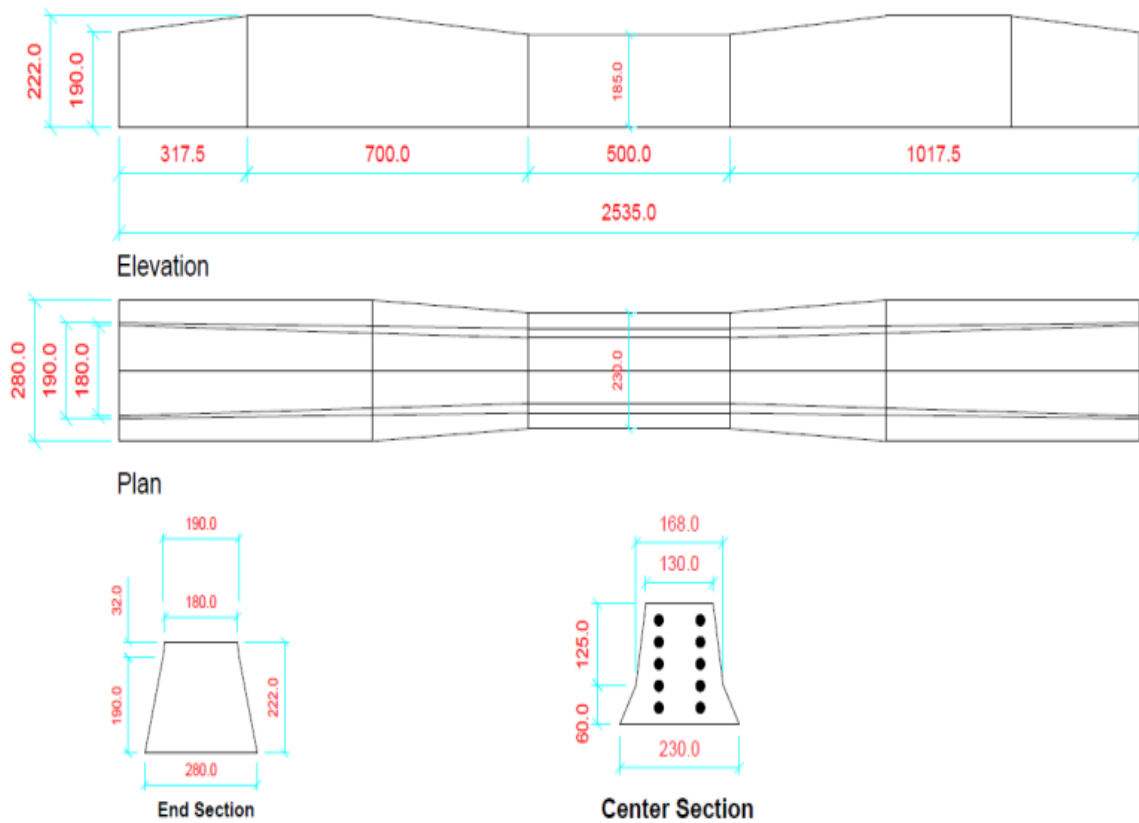


Figure A. 1: Sleeper type A9P used for validation from Rikard 2000

APPENDIX B: Life of Railway Bridge

Table B. 1: Number of load cycles in 100 years				
		Trains/day	Locomotives	Wagons
Passenger	No	100	1	1
	No of bogies		3	3
	No of axles per bogie		2	2
	Wheel per axle		2	2
	Total no of wheels		1200	1200
	Total		100	1200
Total No of wheels/day for two cars	2,400			
Total number of wheels in 100 years	175,200,000.00			
Number of cycles per rail seat in 100 years	87,600,000.00			

APPENDIX C: Static Analysis Numerical Results for Validation

From the railway bridge modelled in static structural analysis, numerical results of the railway bridge and Sleeper for validation are attached from figure C. 1 to C. 2.

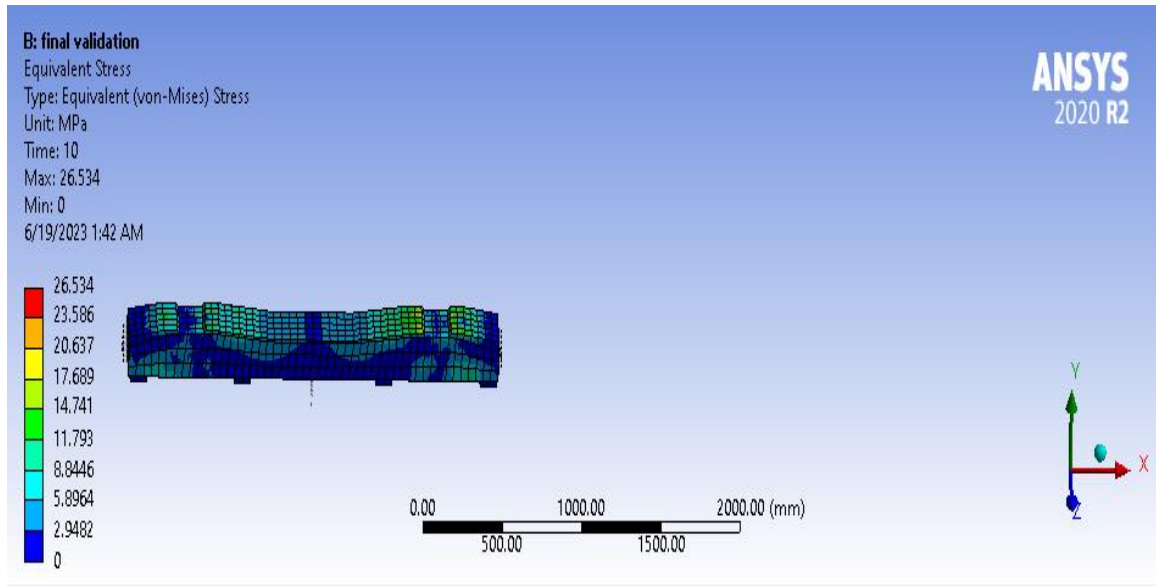


Figure C. 1: Contour plot for equivalent stress at 70 km/h and 25-ton axle load

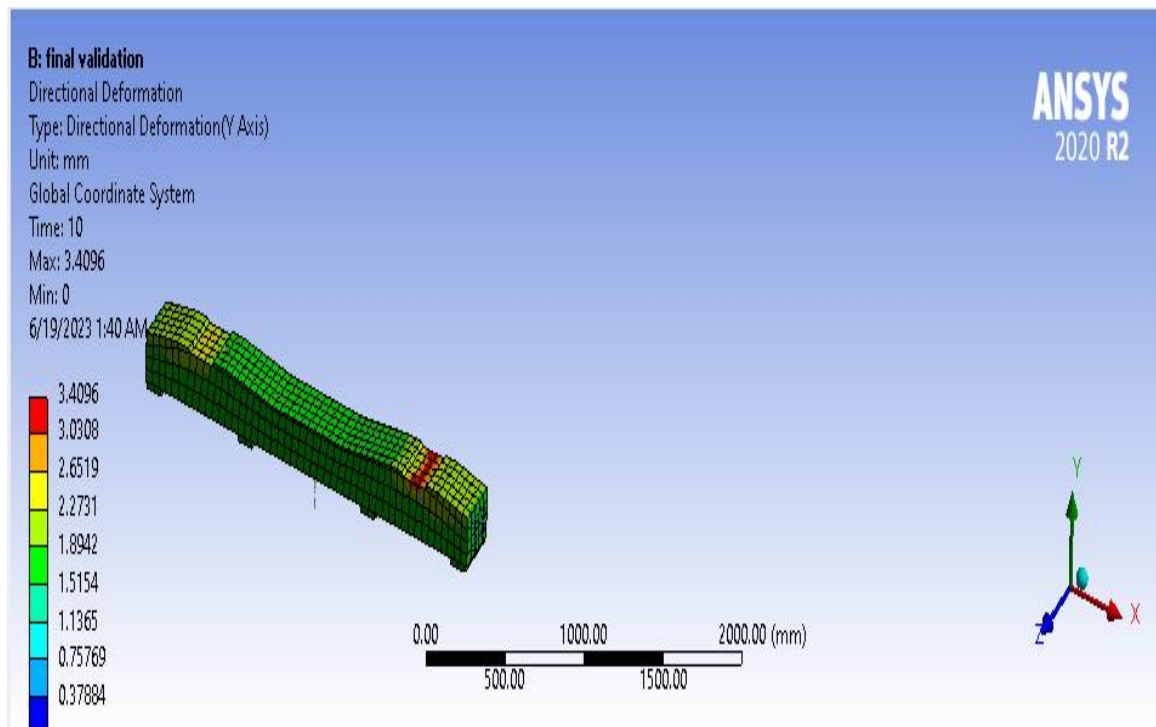


Figure C. 2: Directional deformation for sleeper

APPENDIX D: Static Analysis Modeling and Numerical Results for Pre-Stressed Concrete Railway Bridge

From the railway bridge modelled in static structural analysis, numerical results of the railway bridge are attached from figure D-1 to D-17.

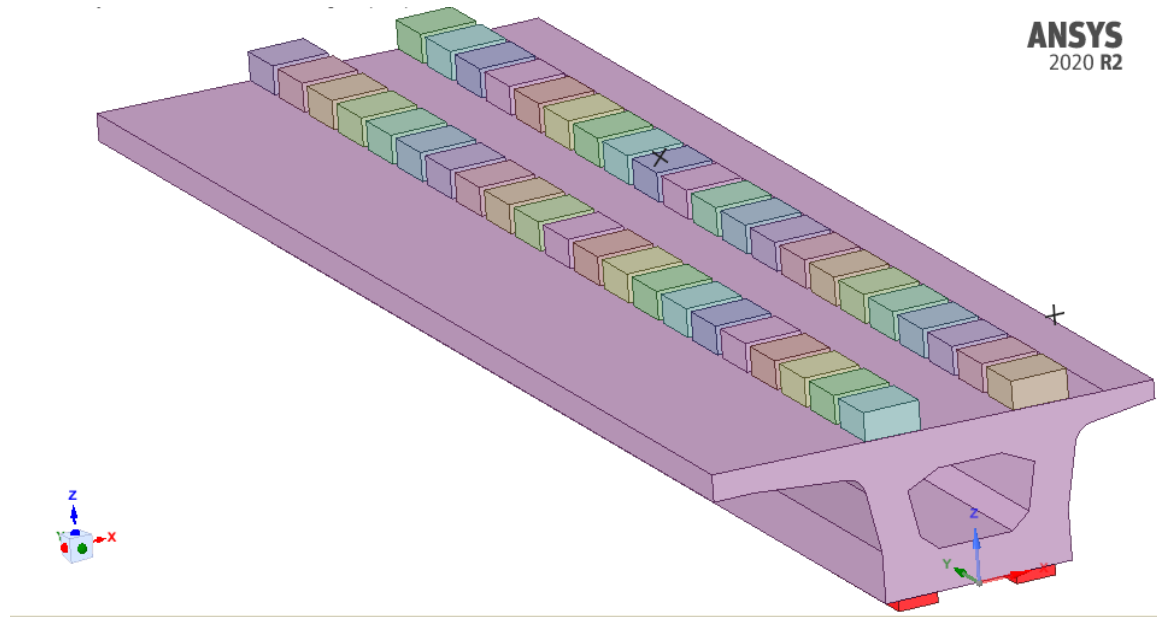


Figure D. 1: Pre-stressed Concrete Box Girder with Box Sleeper Modeling

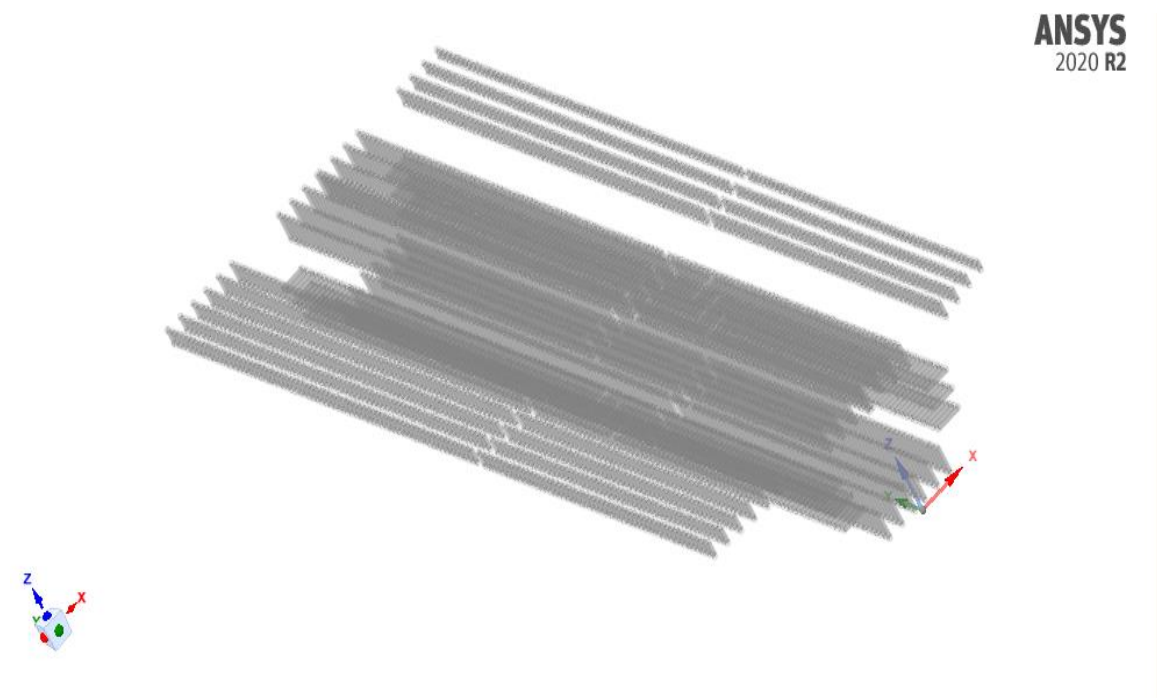


Figure D. 2: Diameter of 10 Reinforcement Modeling

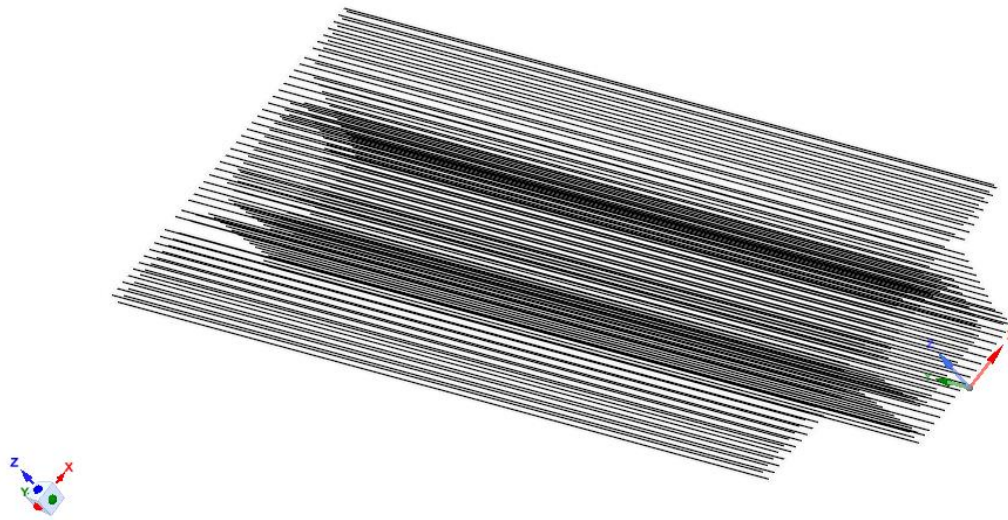


Figure D. 3: Diameter of 12 Reinforcement Modeling

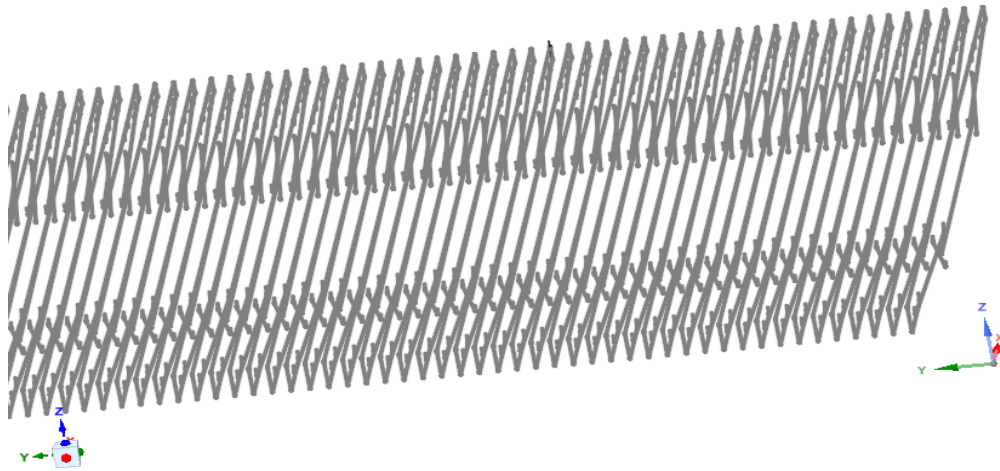


Figure D. 4: Diameter of 16 Reinforcement Modeling



Figure D. 5: Diameter of 16 Reinforcement Modeling

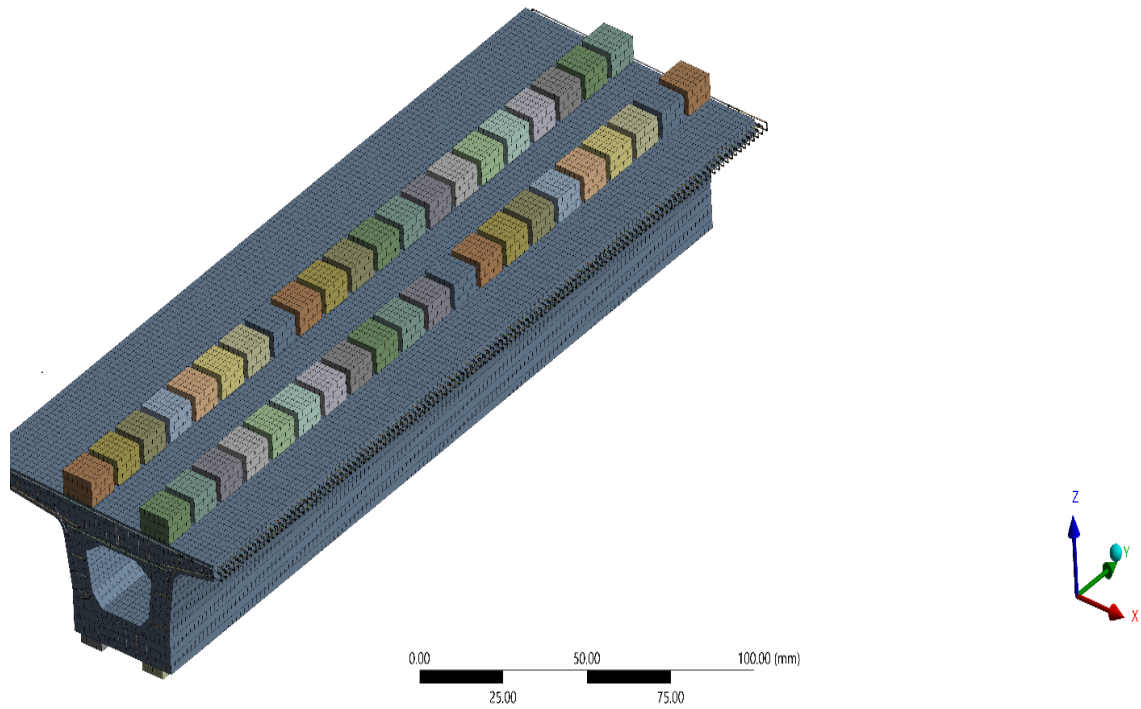


Figure D. 6: Mesh Size of Prestressed Concrete Box Girder Railway Bridge

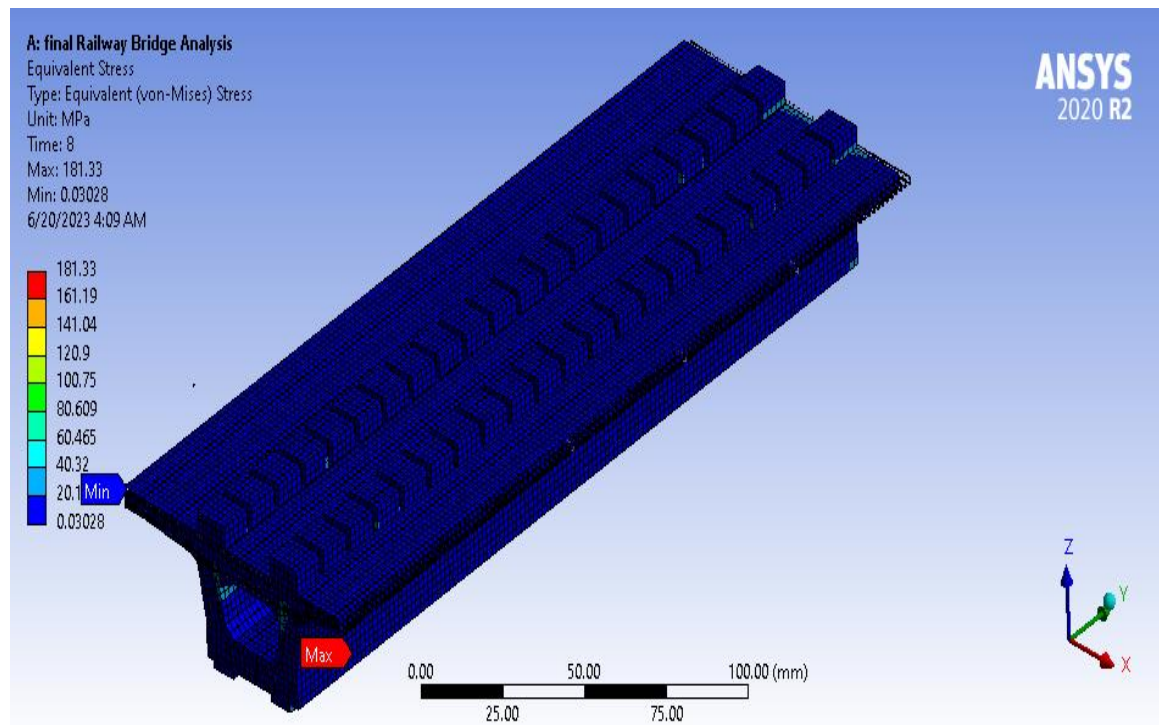


Figure D. 7: Contour plot for equivalent stress at 70 km/h and 165-kN axle load

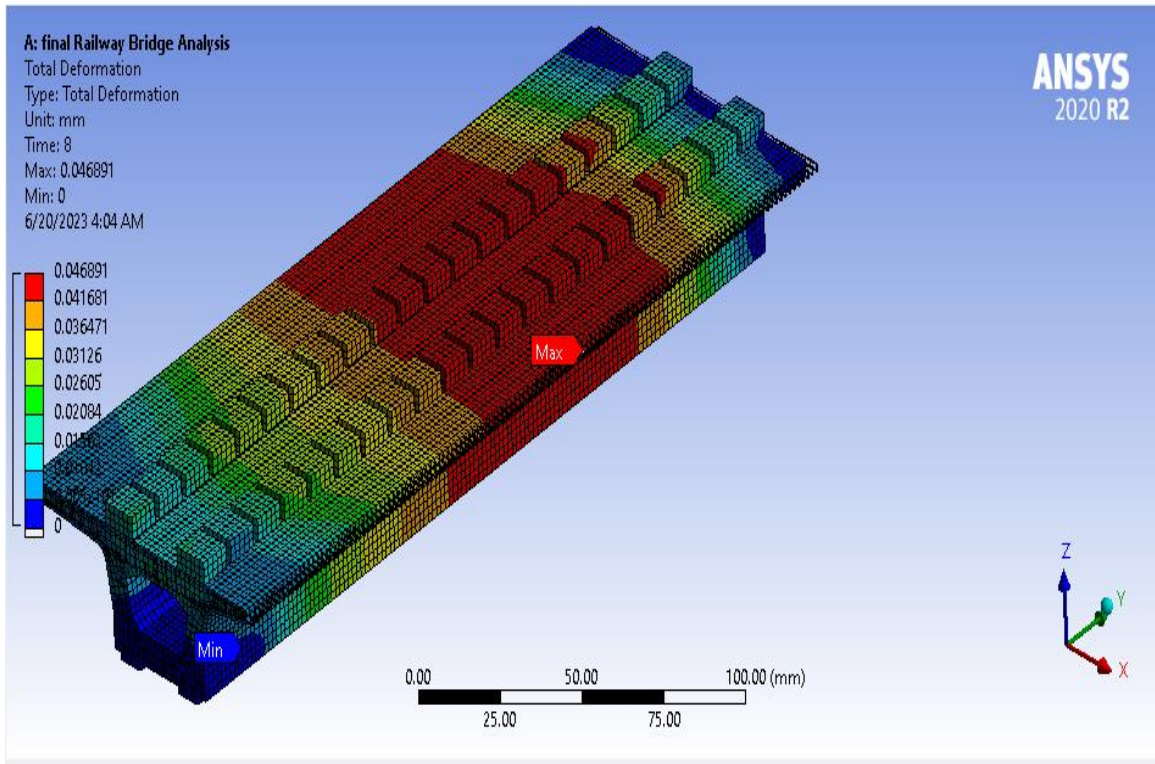


Figure D. 8: Total deformation for Railway Bridge

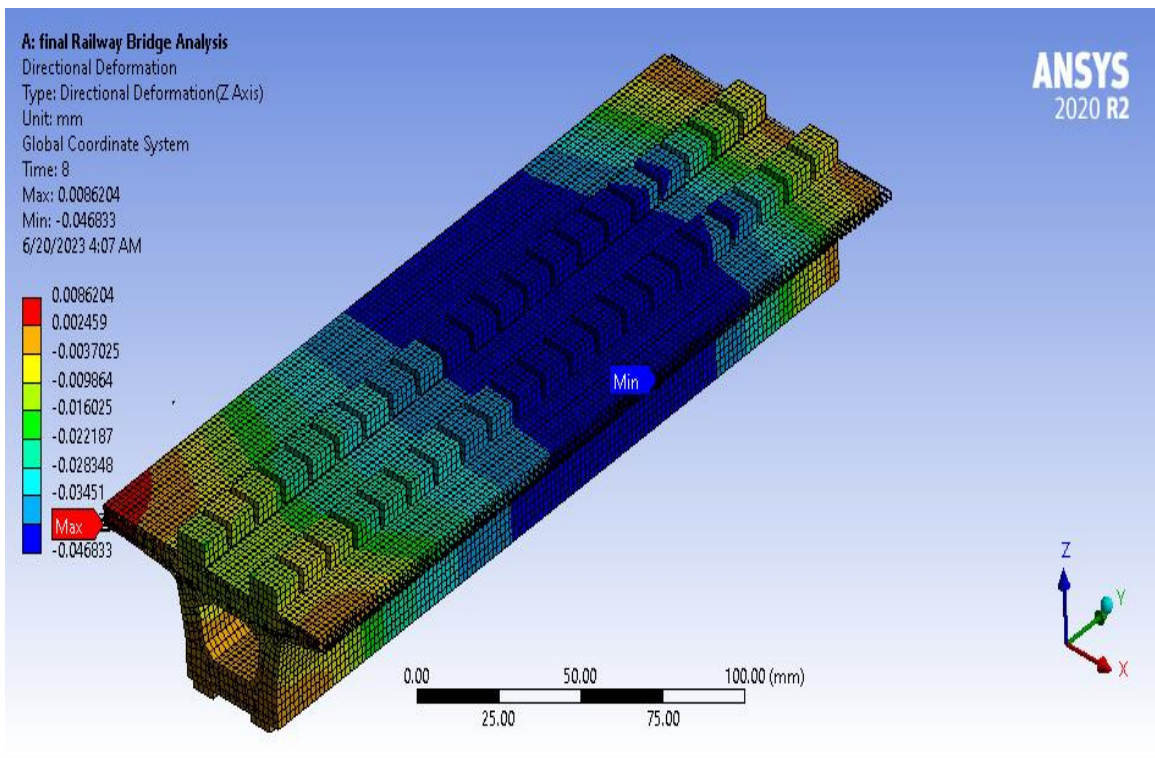


Figure D. 9: Directional deformation for Railway Bridge

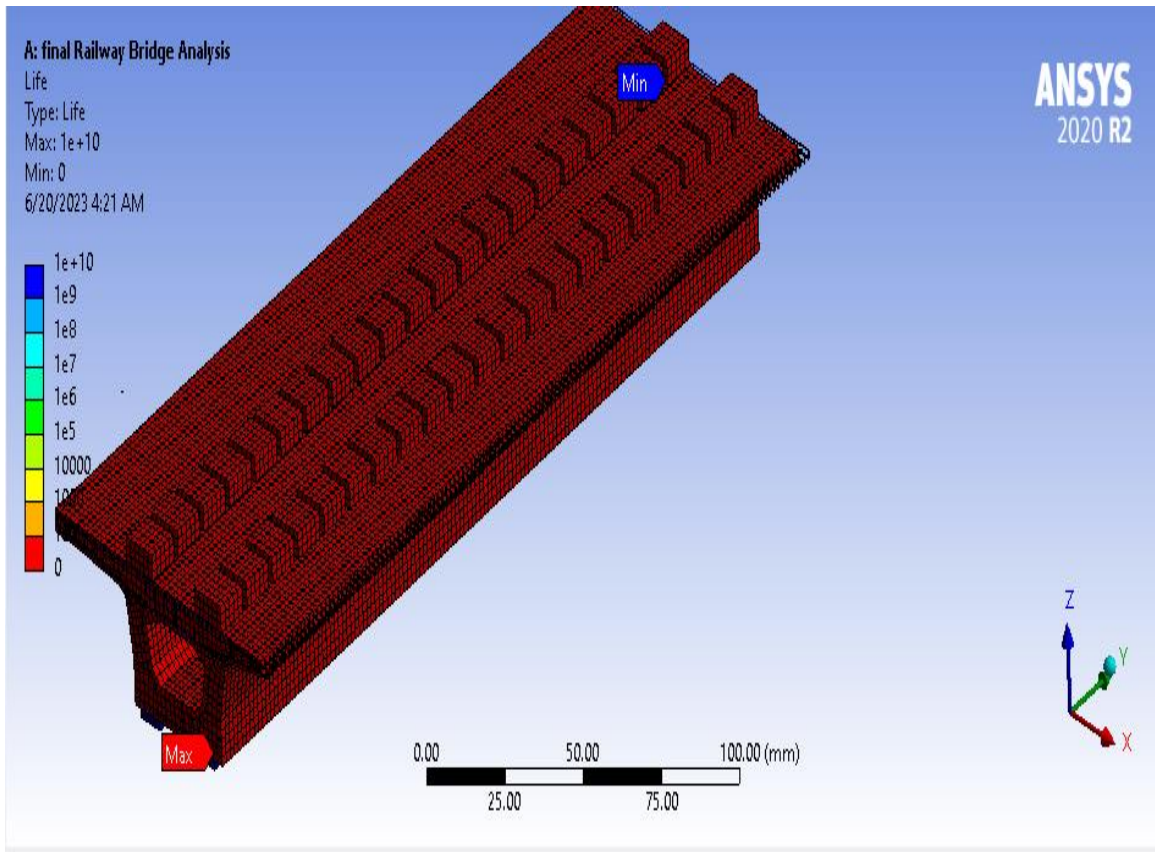


Figure D. 10: Maximum Fatigue life for Railway Bridge

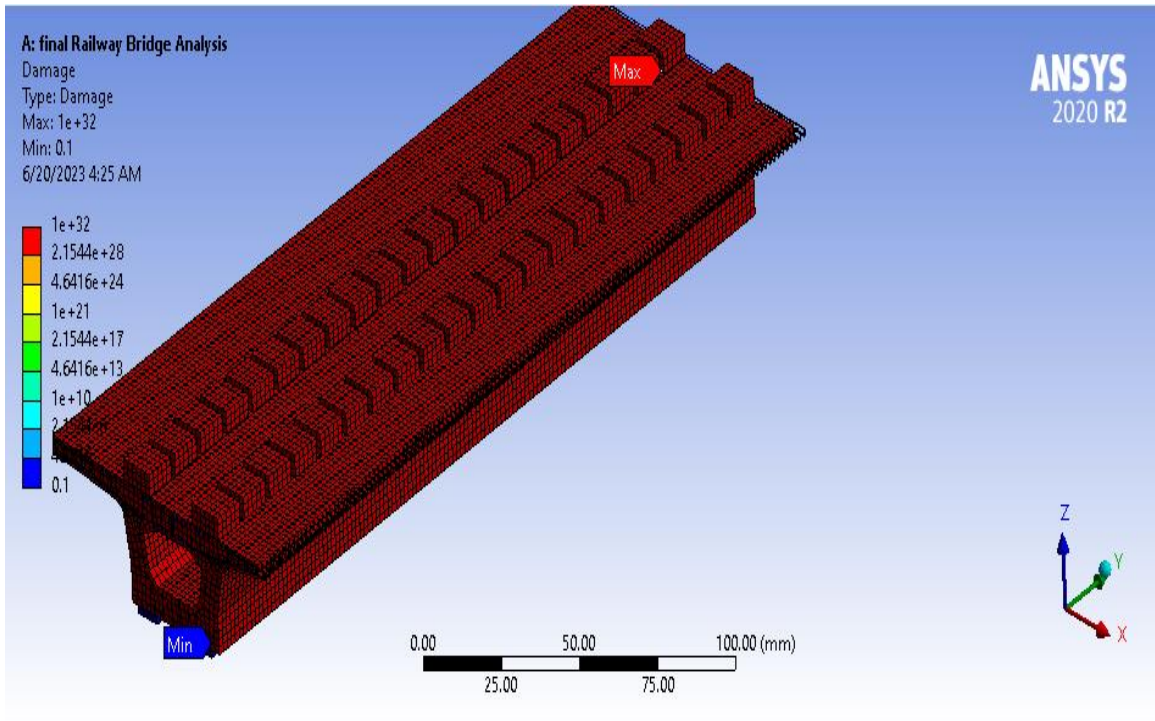


Figure D. 11: Minimum damage for Railway Bridge

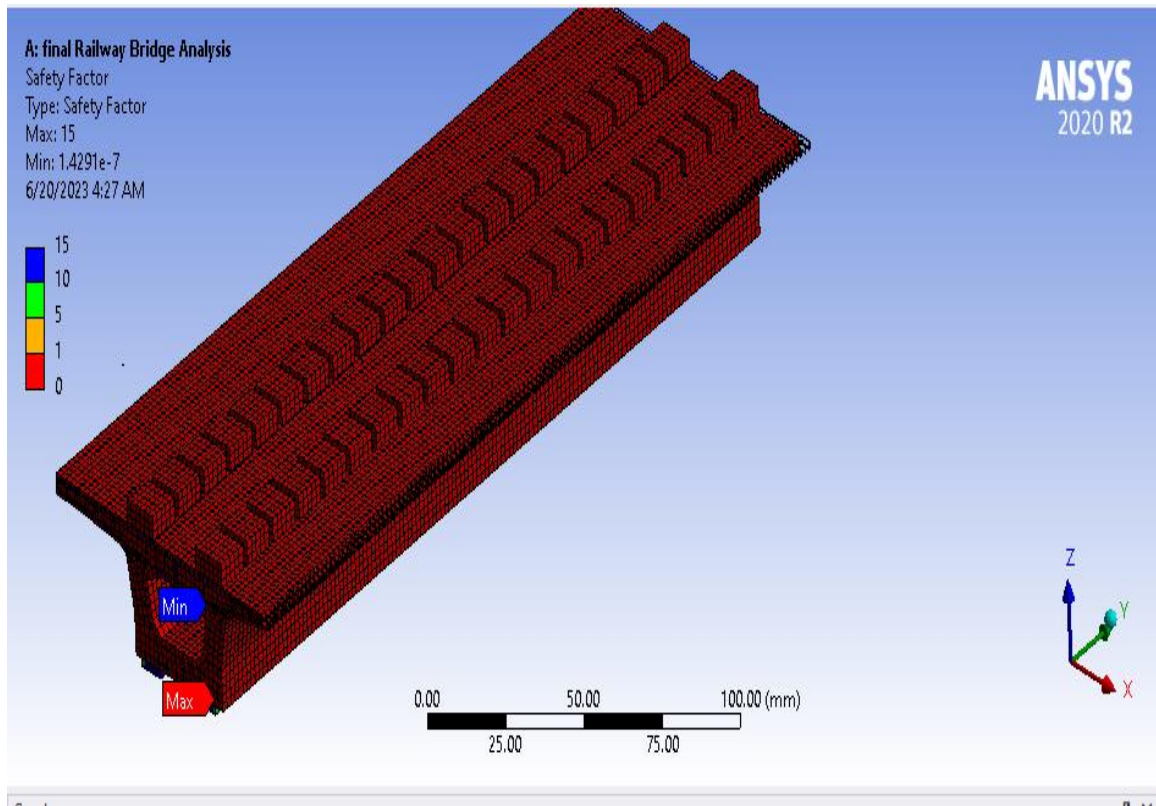


Figure D. 12: Safety Factor for Railway Bridge

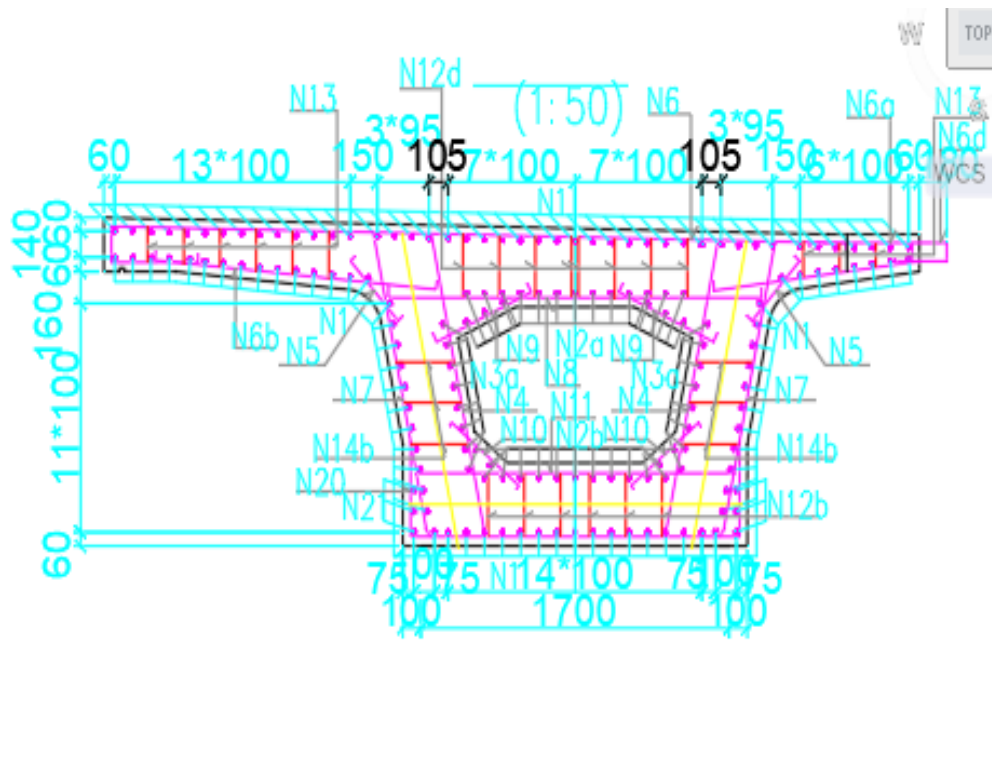


Figure D. 13: Reinforcement Detail for the railway bridge

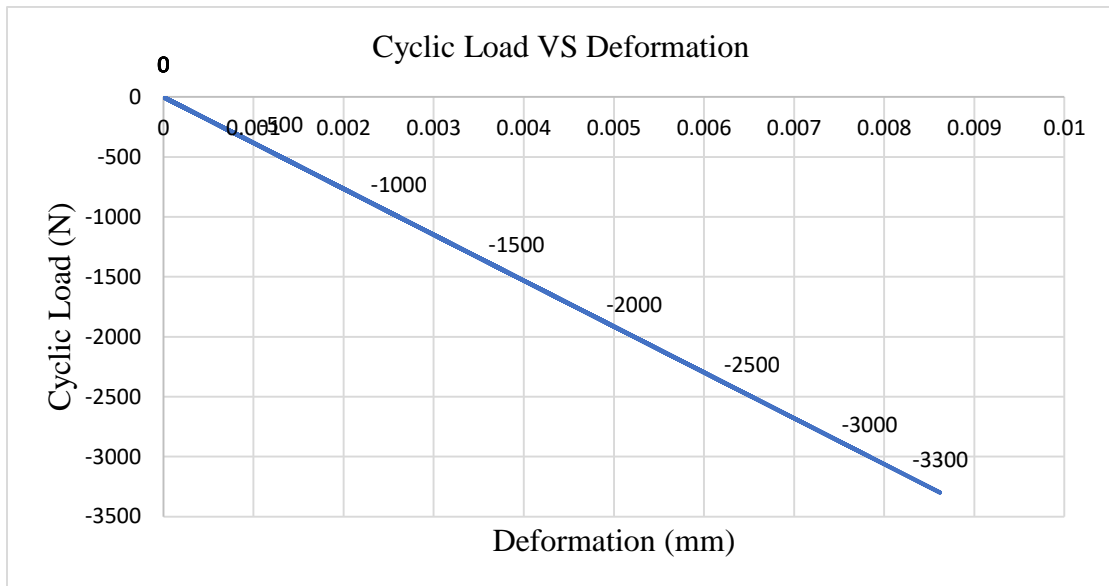


Figure D. 14: Cyclic Load versus Deformation

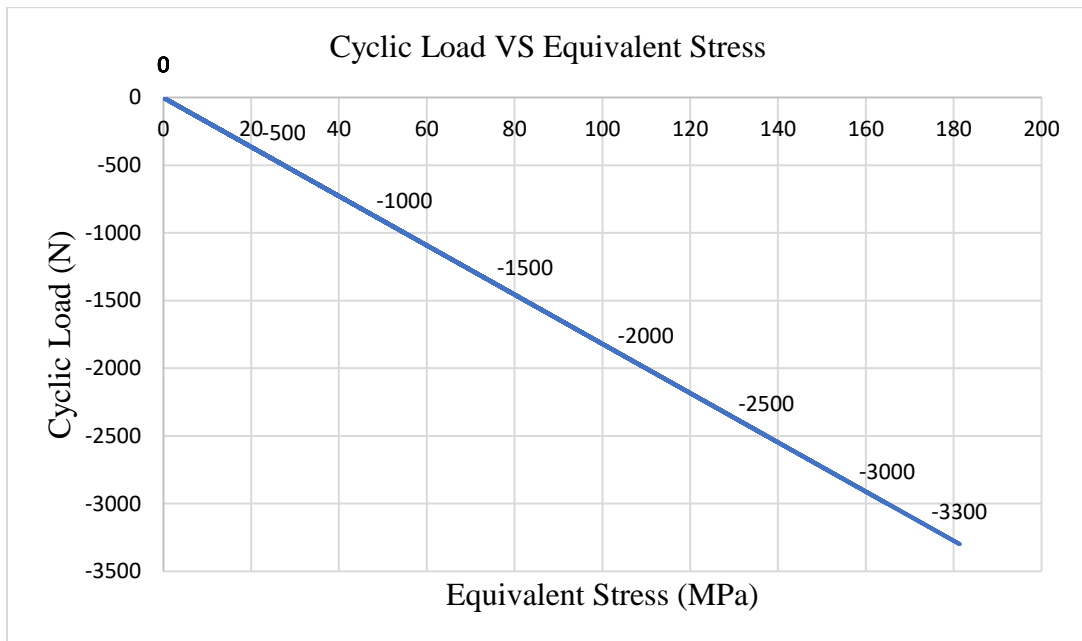


Figure D. 15: Cyclic Load versus Equivalent Stress

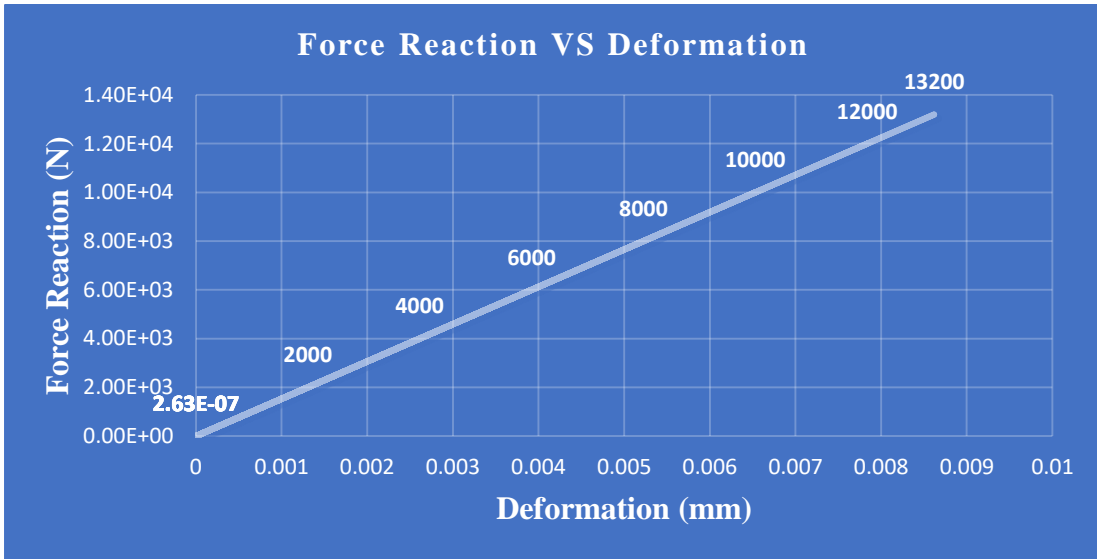


Figure D. 16: Force Reaction versus Deformation

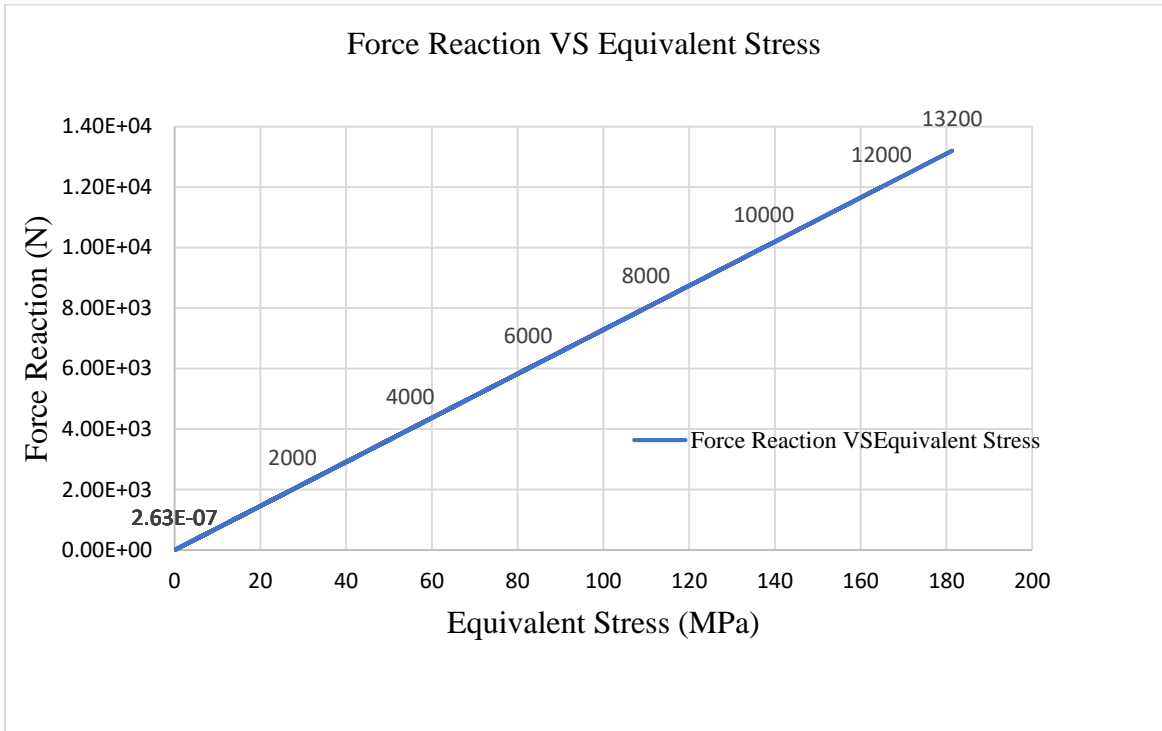


Figure D. 17: Force Reaction versus Equivalent Stress